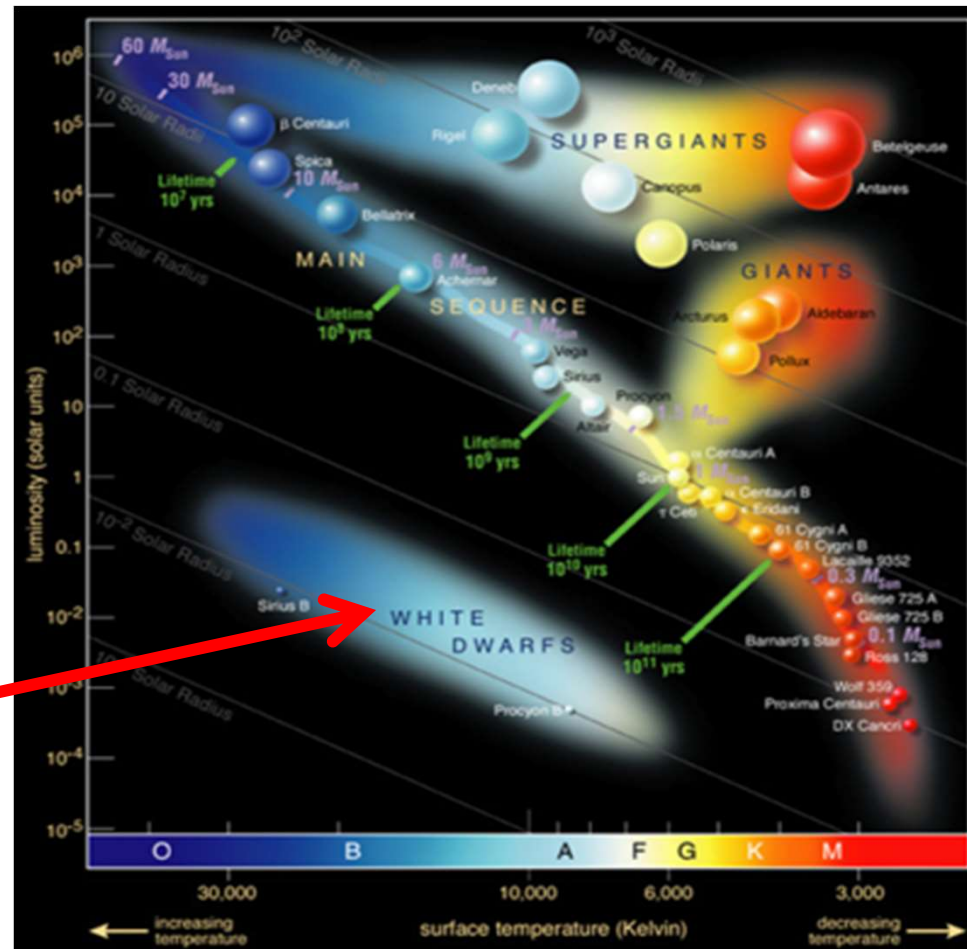


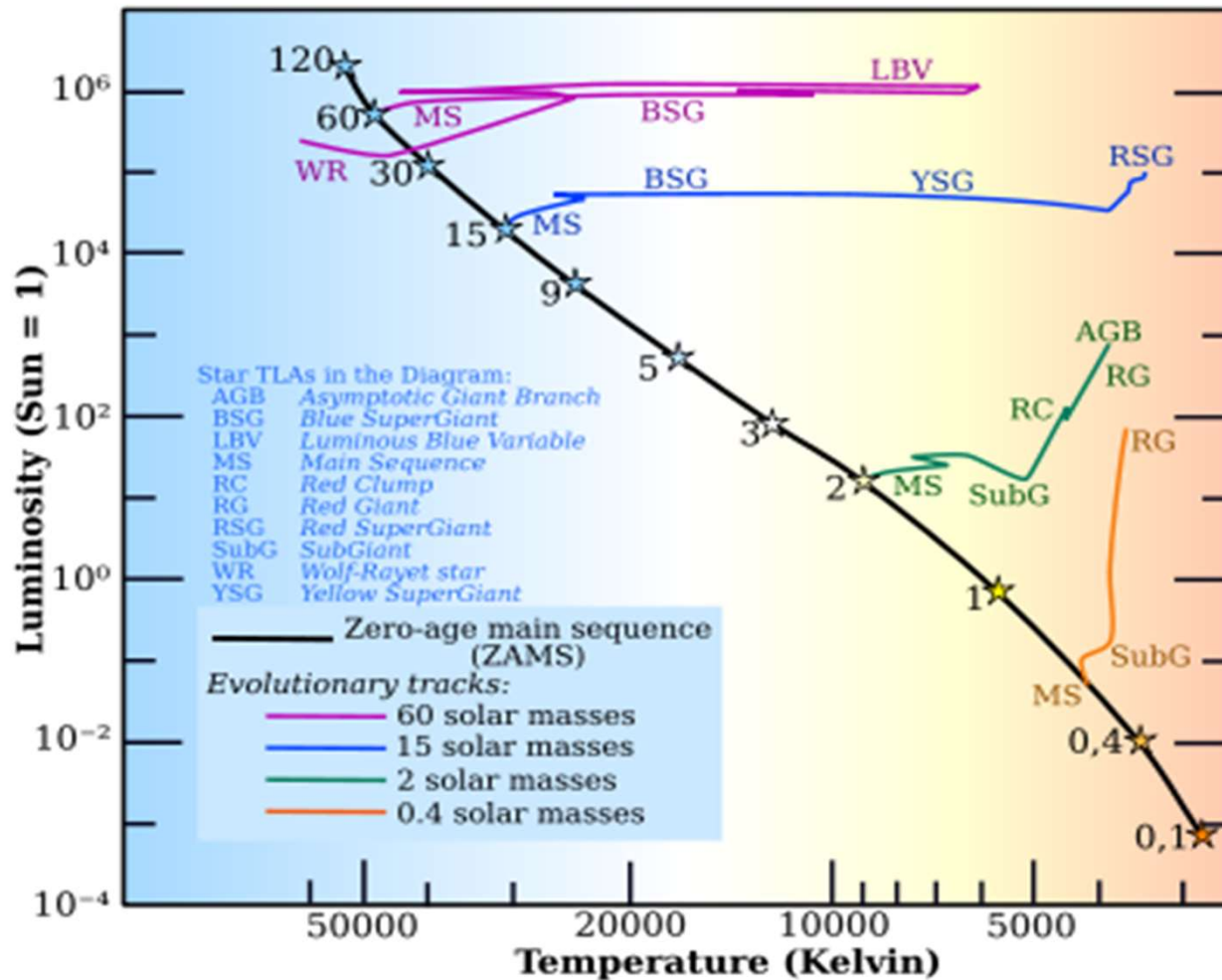
A tour de modeling and analysis of stellar atmospheres throughout the HRD



except for
white dwarfs

Some different types of stars...

Hot luminous stars:
 Massive,
 main-sequence (MS)
 or evolved, ~10 R_{sun}.
 Strong, fast stellar
 winds

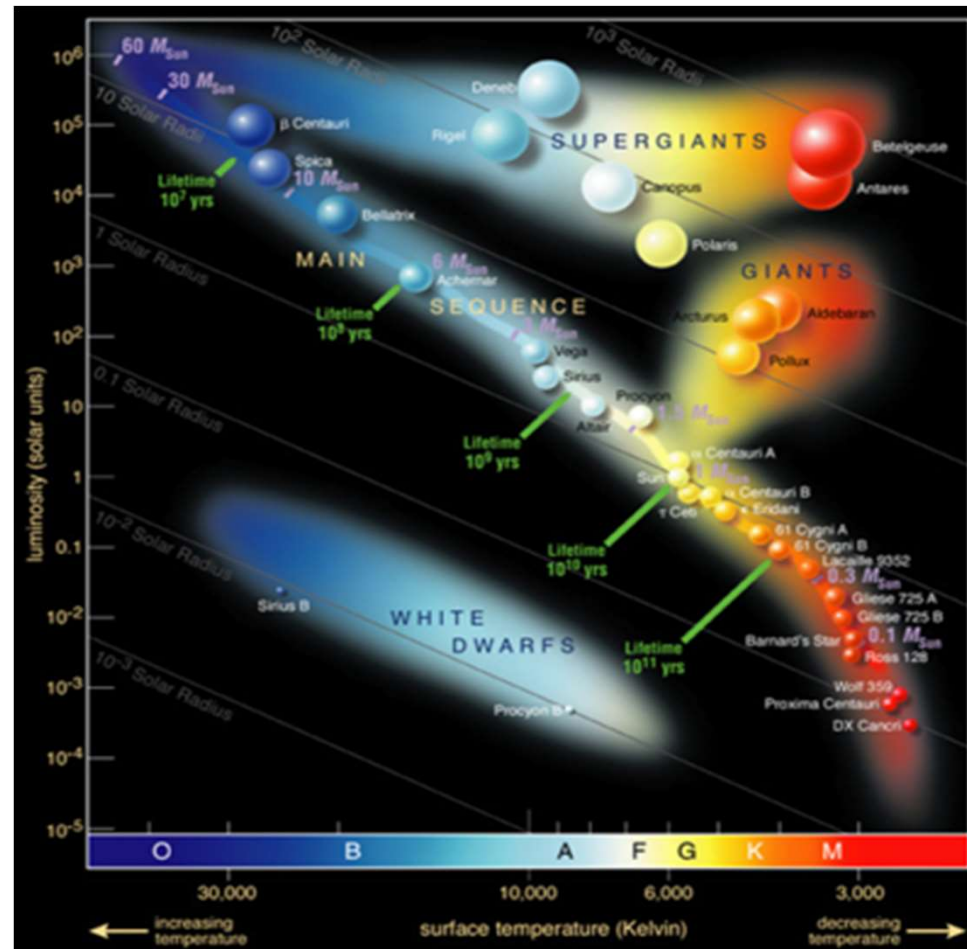


Cool, luminous stars
 (RSG, AGB):
 Massive or low/intermediate
 mass, evolved,
 several 100 (!) R_{sun}.
 Strong, slow stellar winds

Solar-type stars:
 Low-mass, on or near MS,
 hot surrounding coronae,
 weak stellar wind
 (e.g. solar wind)

A tour de modeling and analysis of stellar atmospheres throughout the HRD

Different regimes require different key input physics and assumptions

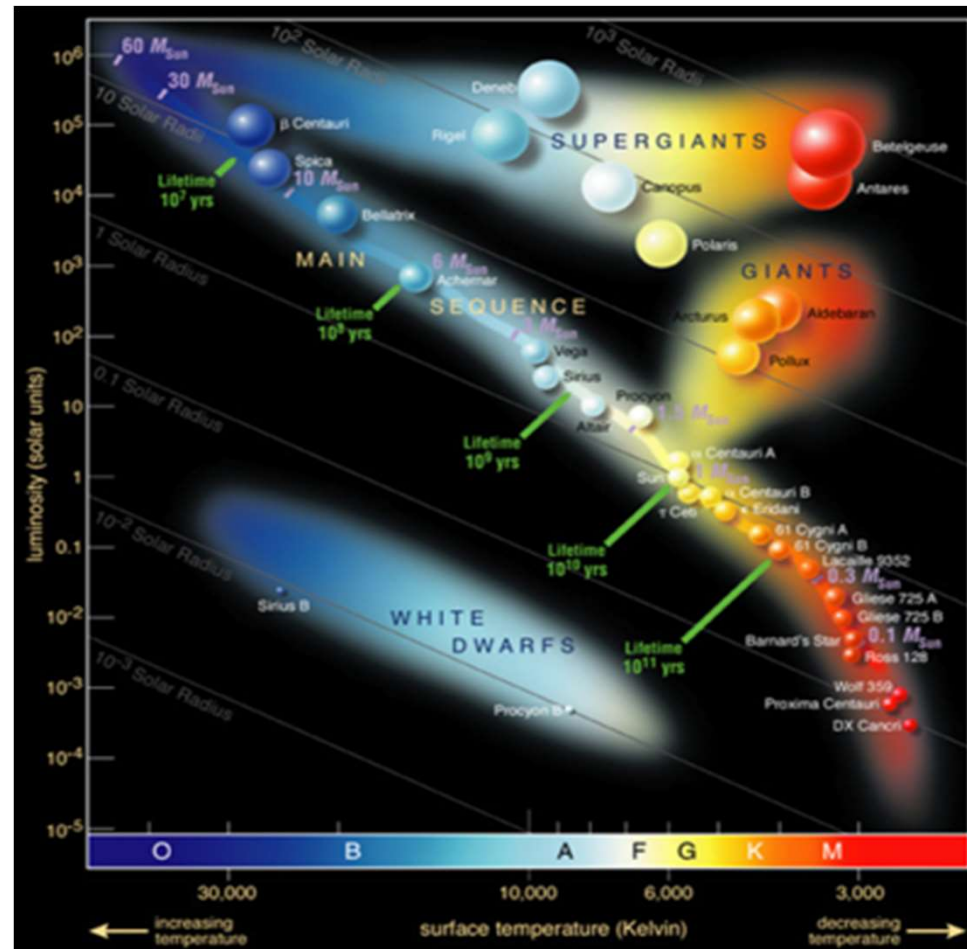


- LTE or NLTE
- Spectral line blocking/blanketing
- (sub-) Surface convection
- Geometry and dimensionality
- Velocity fields and outflows

Spectroscopy and Photometry

ALSO:
Analysis
of different
WAVELENGTH
BANDS
is different

(X-ray, UV,
optical, infra-
red...)



Depends on where in
atmosphere light
escapes from

Question: Why is this
“formation depth”
different for different
wavebands and
diagnostics?

Spectroscopy and Photometry (see Chap. 2)

...gives insight into and understanding of our cosmos

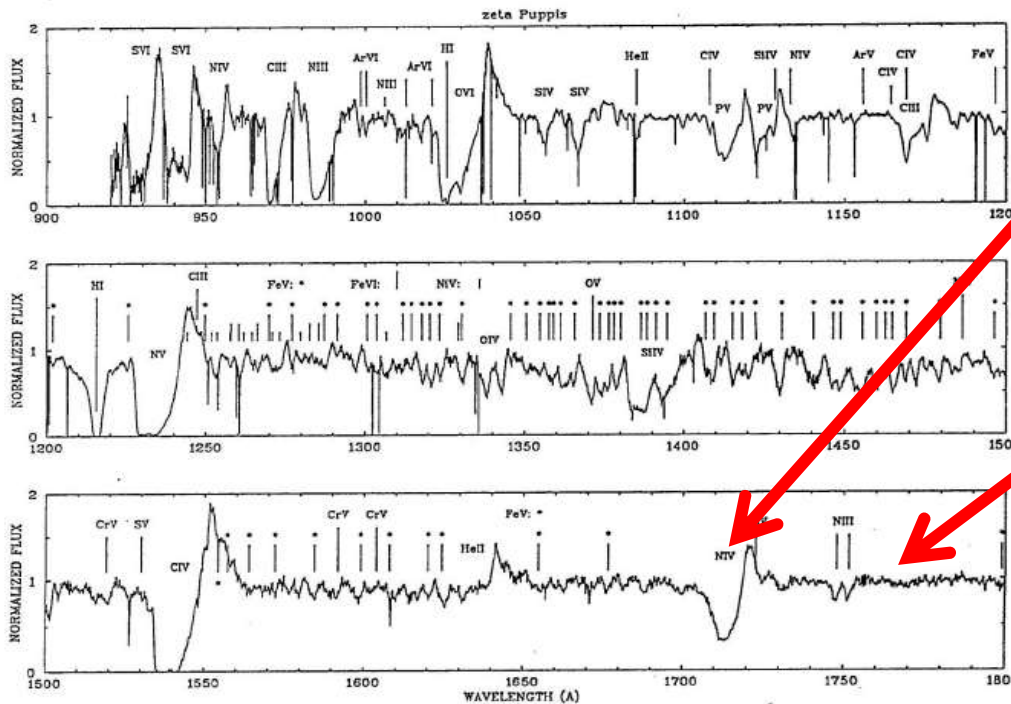
- ▶ provides
 - ▶ **stellar properties**, mass, radius, luminosity, energy production, chemical composition, properties of outflows
 - ▶ **properties of (inter) stellar plasmas**, temperature, density, excitation, chemical comp., magnetic fields

- ▶ INPUT for stellar, galactic and cosmologic **evolution** and for stellar and galactic structure

- ▶ requires
 - ▶ **plasma physics**, plasma is "normal" state of atmospheres and interstellar matter (plasma diagnostics, line broadening, influence of magnetic fields,...)
 - ▶ **atomic physics/ quantum mechanics**, interaction light/matter (micro quantities)
 - ▶ **radiative transfer**, interaction light/matter (macroscopic description)
 - ▶ **thermodynamics**, thermodynamic equilibria: TE, LTE (local), NLTE (non-local)
 - ▶ **hydrodynamics**, atmospheric structure, velocity fields, shockwaves,...

Spectroscopy (see Chap. 2)

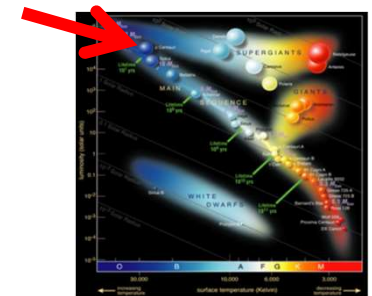
UV spectrum of the O4I(f) supergiant ζ Pup



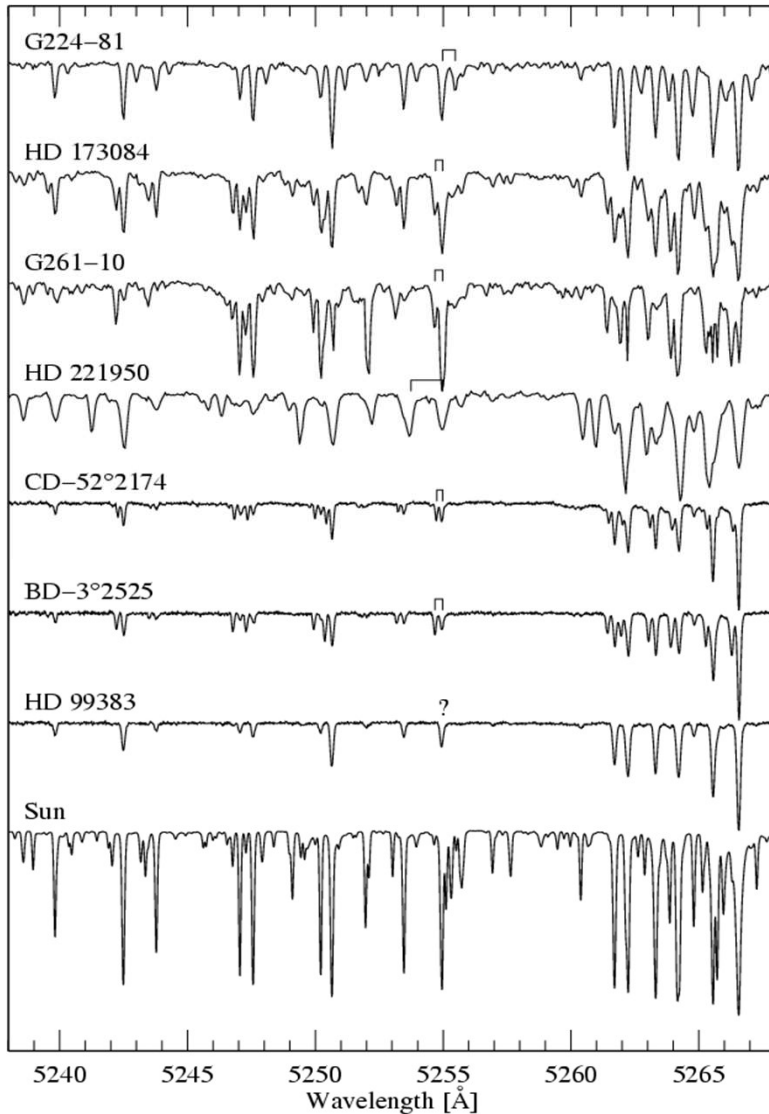
montage of **Copernicus** ($\lambda < 1500 \text{ \AA}$, high res. mode, $\Delta\lambda \approx 0.05 \text{ \AA}$, Morton & Underhill 1977) and **IUE** ($\Delta\lambda \approx 0.1 \text{ \AA}$) observations

UV “P-Cygni” lines formed in rapidly accelerating, hot stellar winds

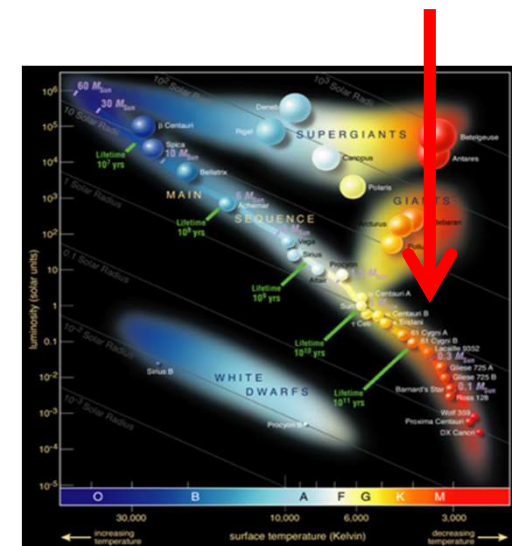
(quasi-) Continuum formed in (quasi-) hydrostatic photosphere



Spectroscopy



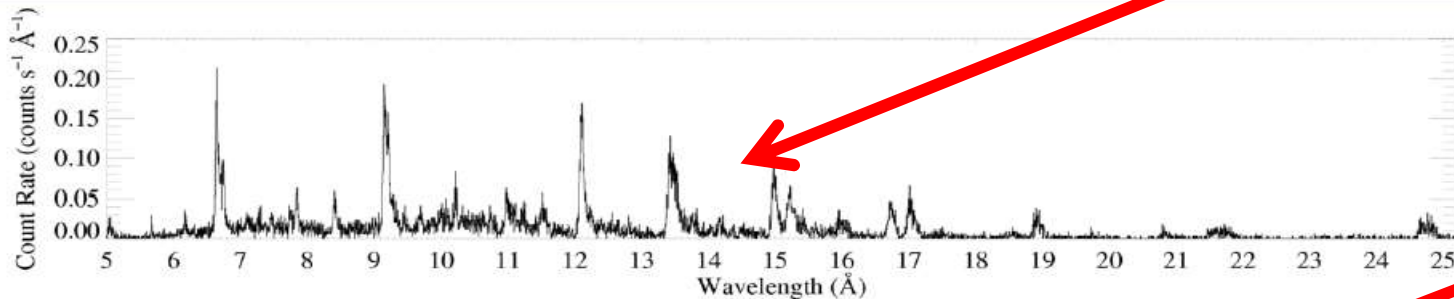
Lines and continuum in the **optical** around **5200 Å**, in cool solar-type stars, formed in the photosphere



Spectroscopy

Chandra grating (HETGS/MEG) spectra

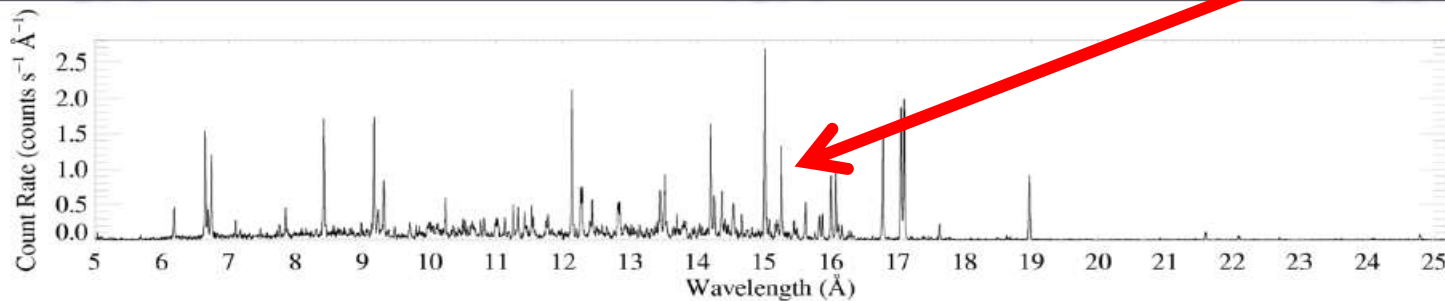
ζ Pup (O4 If)



5Å

15Å

25Å



Capella (G5 III)

X-rays from hot stars, formed in shocks in stellar wind

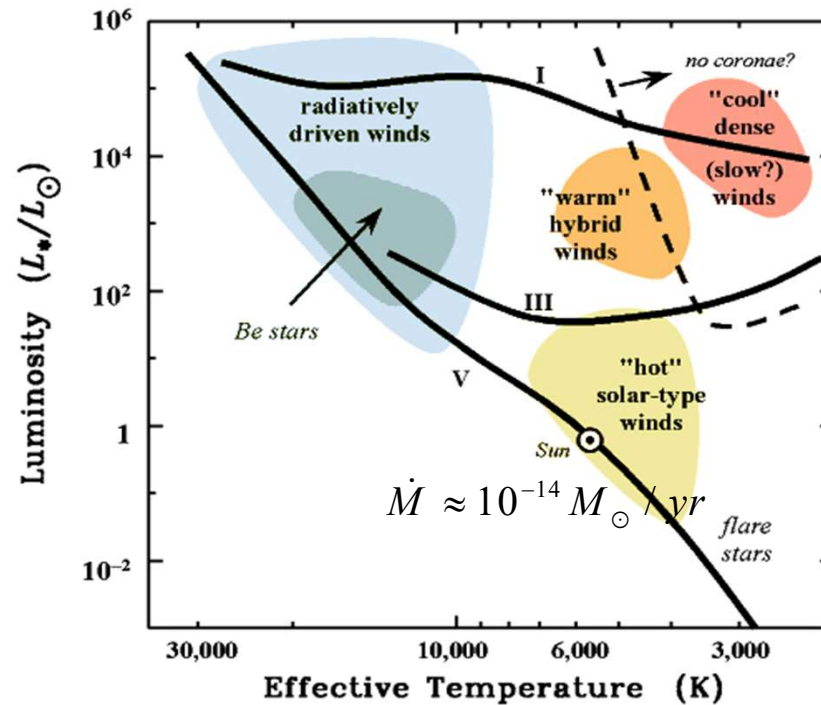
X-rays from cool stars, formed in hot corona

A tour de modeling and analysis of stellar atmospheres throughout the HRD

Stellar Winds (see Chap. 8/9)

KEY QUESTION: What provides the force able to overcome gravity?

$$\dot{M} \approx 10^{-4} \dots 10^{-8} M_{\odot} / yr$$



- LTE or NLTE
- Spectral line blocking/blanketing
- (sub-) Surface convection
- Geometry and dimensionality
- Velocity fields and outflows

A tour de modeling and analysis of stellar atmospheres throughout the HRD

KEY QUESTION: What provides the force able to overcome gravity?

Pressure gradient

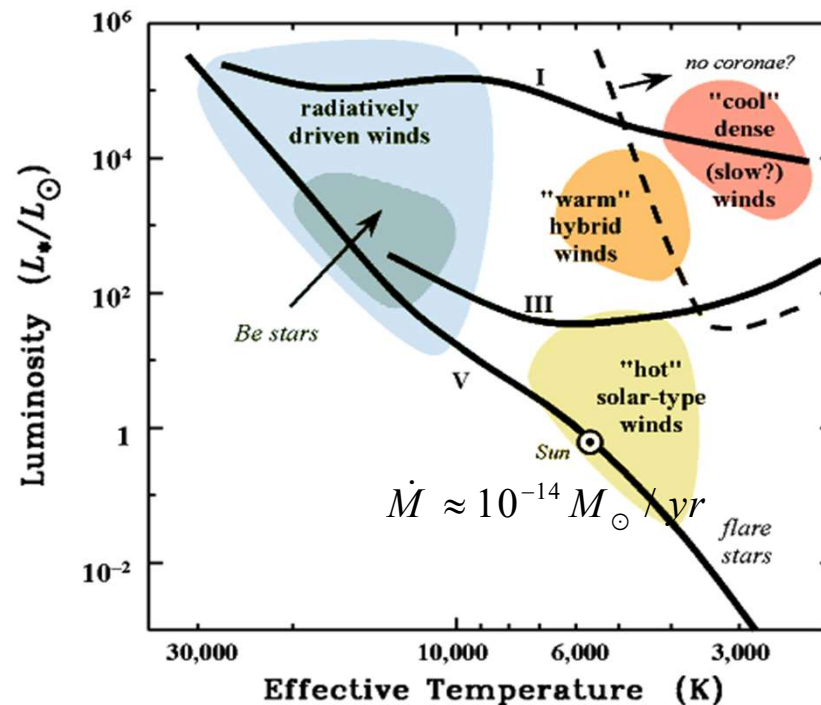
in hot coronae of solar-type stars

Radiation force:

Dust scattering (in pulsation-levitated material, see Chap. 8) in cool AGB stars (S. Höfner and colleagues)

Same mechanism in cool RSGs?

$$\dot{M} \approx 10^{-4} \dots 10^{-8} M_{\odot} / yr$$



- LTE or NLTE
- Spectral line blocking/blanketing
- (sub-) Surface convection
- Geometry and dimensionality
- **Velocity fields and outflows**

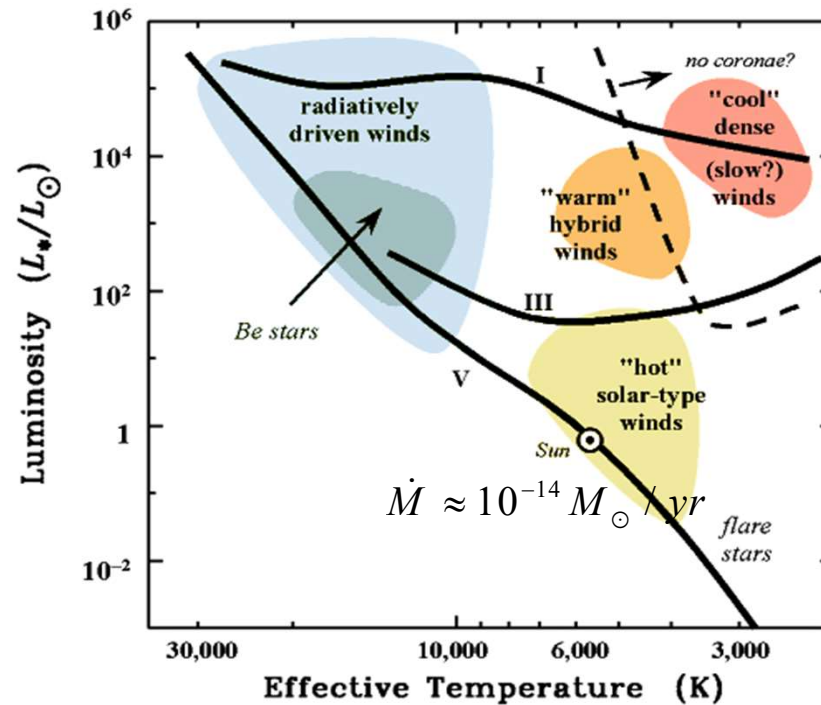
A tour de modeling and analysis of stellar atmospheres throughout the HRD

KEY QUESTION: What provides the force able to overcome gravity?

Radiation force:

line scattering in hot, luminous stars
 → done at USM, more to follow in Chap. 8/9

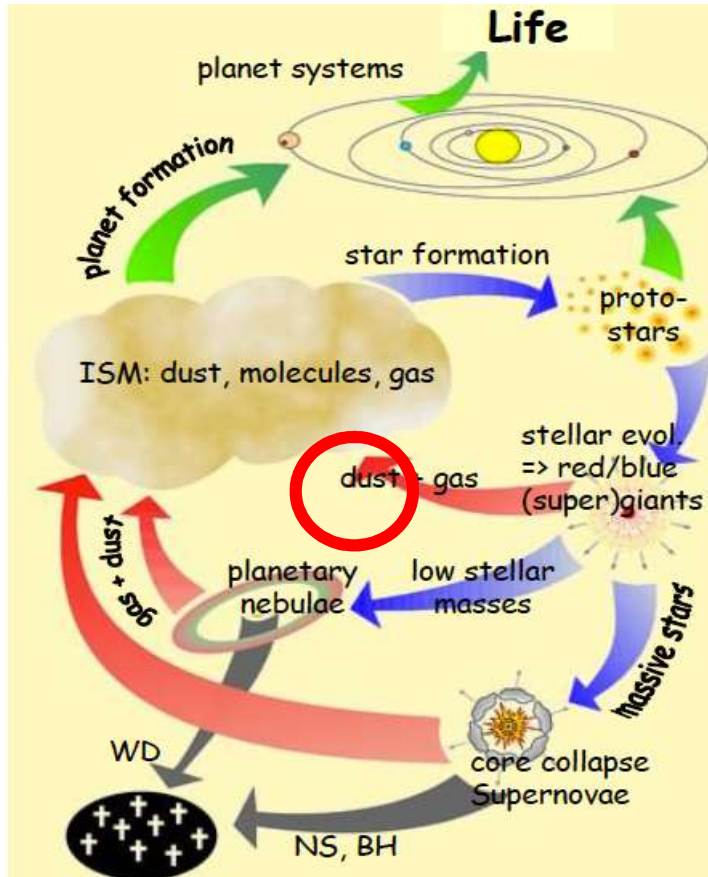
$$\dot{M} \approx 10^{-4} \dots 10^{-8} M_{\odot} / yr$$



- LTE or NLTE
- Spectral line blocking/blanketing
- (sub-) Surface convection
- Geometry and dimensionality
- **Velocity fields and outflows**

Question: How do you think the high mass loss of stars with high luminosities affects the evolution of the star and its surroundings?


from introductory slides ...



Feedback

- massive stars determine energy (kinetic and radiation) and momentum budget of surrounding ISM
- kinetic energy and momentum budget via winds (of different strengths, in dependence of evolutionary status)
- massive stars enrich environment with metals, via winds and SNe, determine chemo-dynamical evolution of Galaxies (exclusively before onset of SNe Ia)
 - in particular: first chemical enrichment of Universe by First (VMS) Stars

→“FEEDBACK”



Bubble Nebula (NGC 7635) in Cassiopeia

wind-blown bubble around BD+602522 (O6.5III_f)

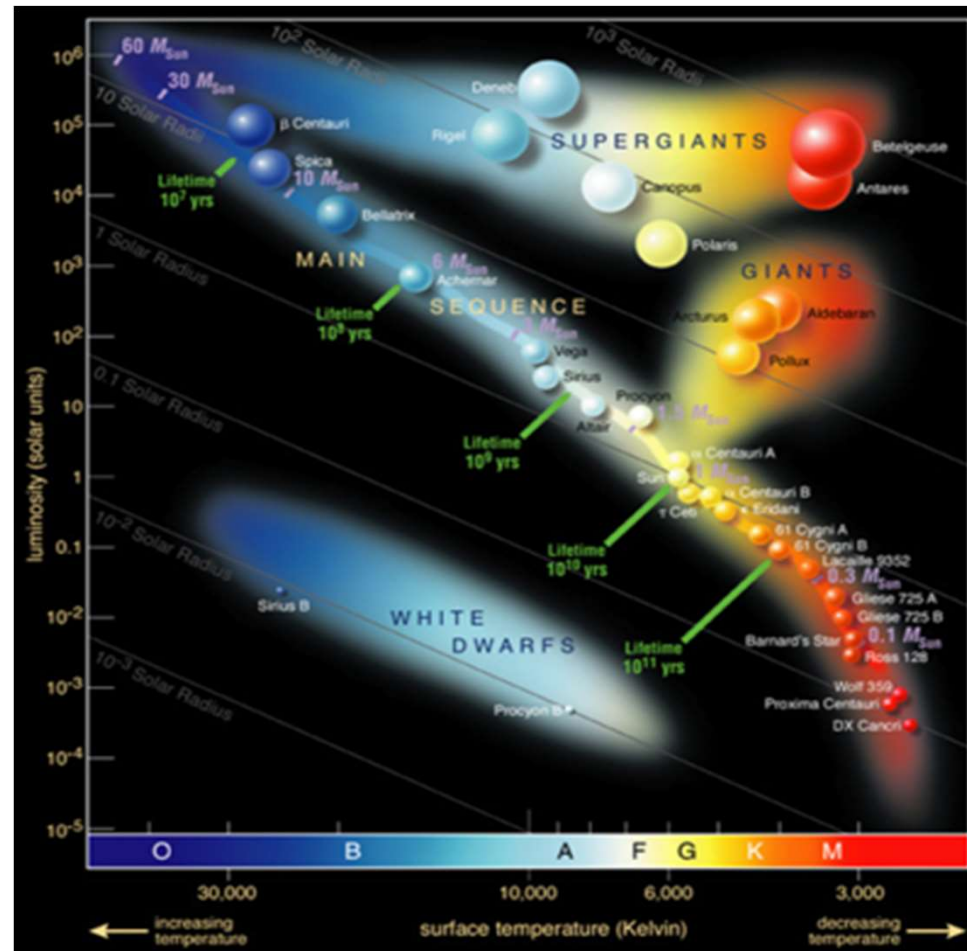
IMPRS advanced course - Radiative transfer, stellar atmospheres and winds

31

Stellar Winds from hot/evolved cool stars control evolution/late evolution, and feed the ISM with nuclear processed material

A tour de modeling and analysis of stellar atmospheres throughout the HRD

In the following,
we focus on stellar
photospheres



From Chap. 6 Summary: stellar atmospheres - the solution principle

THUS problem of stellar atmospheres solved (in principle, without convection, p-p geometry, static)

Given $\log g_*$, T_{eff} , abundances

(A) hydrostatic equilibrium

$$\frac{dp_{\text{gas}}}{dz} = -g(g_* - g_{\text{rad}}); \quad g_{\text{rad}} = \frac{4\pi}{c} \int_0^\infty \chi_\nu H_\nu d\nu = \frac{4\pi}{c} \left(\sigma^{\text{TH}} H(z) + \int_0^\infty \chi_\nu^{\text{rest}} H_\nu d\nu \right)$$

$$\Rightarrow \frac{dp_{\text{gas}}}{dz} = -g g_* + \sigma^{\text{TH}} \frac{\sigma_B T_{\text{eff}}^4}{c} + \frac{4\pi}{c} \int_0^\infty \chi_\nu^{\text{rest}} H_\nu d\nu \quad H = \frac{1}{4\pi} \sigma_B T_{\text{eff}}^4 \quad (= \frac{1}{4\pi} F)$$

(B) equation of rad. transfer

$$\mu \frac{dI_\nu}{dz} = \chi_\nu (S_\nu - I_\nu) \quad \forall \nu, \mu \Rightarrow J_\nu = \frac{1}{2} \int_{-1}^{+1} I_\nu(\mu) d\mu; \quad H_\nu = \frac{1}{2} \int_{-1}^{+1} I_\nu(\mu) \mu d\mu$$

(C) a) radiative equilibrium

$$\int_0^\infty (\chi_\nu - \chi_\nu^{\text{rest}}) J_\nu d\nu = \int_0^\infty \left\{ \sigma^{\text{TH}} J_\nu + \chi_\nu^{\text{rest}} S_\nu^{\text{rest}} - (\sigma^{\text{TH}} + \chi_\nu^{\text{rest}}) J_\nu \right\} d\nu = \int_0^\infty \chi_\nu^{\text{rest}} (S_\nu^{\text{rest}} - J_\nu) d\nu \stackrel{?}{=} 0$$

scattering terms cancel, since conservative

b) flux-conservation: $4\pi \int_0^\infty H_\nu(z) d\nu = 4\pi H(z) \stackrel{?}{=} \sigma_B T_{\text{eff}}^4 \Rightarrow \Delta T(z) \rightarrow \Delta \chi_\nu(z) \text{ etc}$

(D) equation of state $p_{\text{gas}}(z) = \frac{k_B}{\mu m_H} \rho(z) T(z)$ solution by iteration!

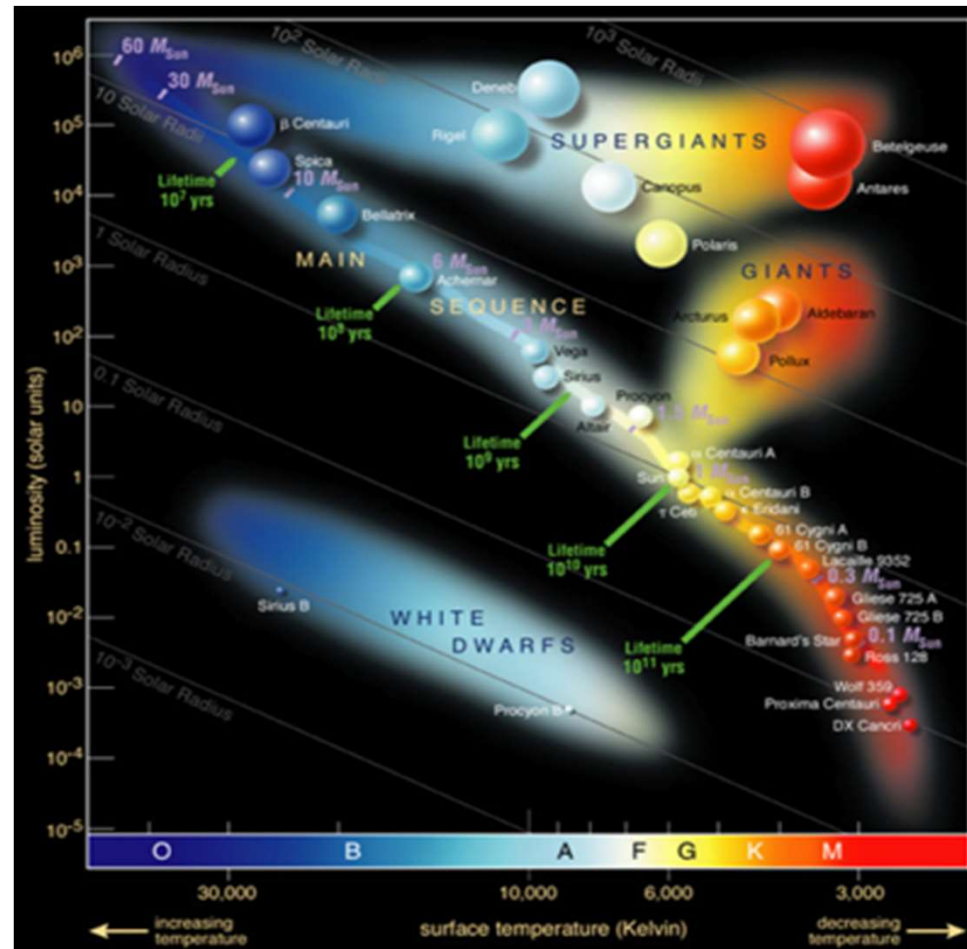
OBSERVATIONS!!

Solution of differential equations A and B by **discretization differential operators** => finite differences
all quantities have to be evaluated on suitable grid

Eq. of radiative transfer (B) usually solved by the so-called Feautrier and/or Rybicki scheme

Stellar Atmospheres in practice

A tour de modeling and analysis of stellar atmospheres throughout the HRD



- LTE or NLTE
- Spectral line blocking/blanketing
- (sub-) Surface convection
- Geometry and dimensionality
- Velocity fields and outflows

LTE or NLTE? (see part 1)

When is LTE valid???

roughly: electron collisions
 $\propto n_e T^{3/2}$

>> photoabsorption rates
 $\propto I_\nu(T) \propto T^x, x \geq 1$

LTE: T low, n_e high
 NLTE: T high, n_e low

dwarfs (giants), late B and cooler
 all supergiants + rest

however:
 NLTE-effects also
 in cooler stars, e.g..
 iron in sun

HOT STARS:

Complete model atmosphere and synthetic spectrum must be calculated in NLTE

NLTE calculations for various applications
 (including Supernovae remnants) within the
 expertise of USM

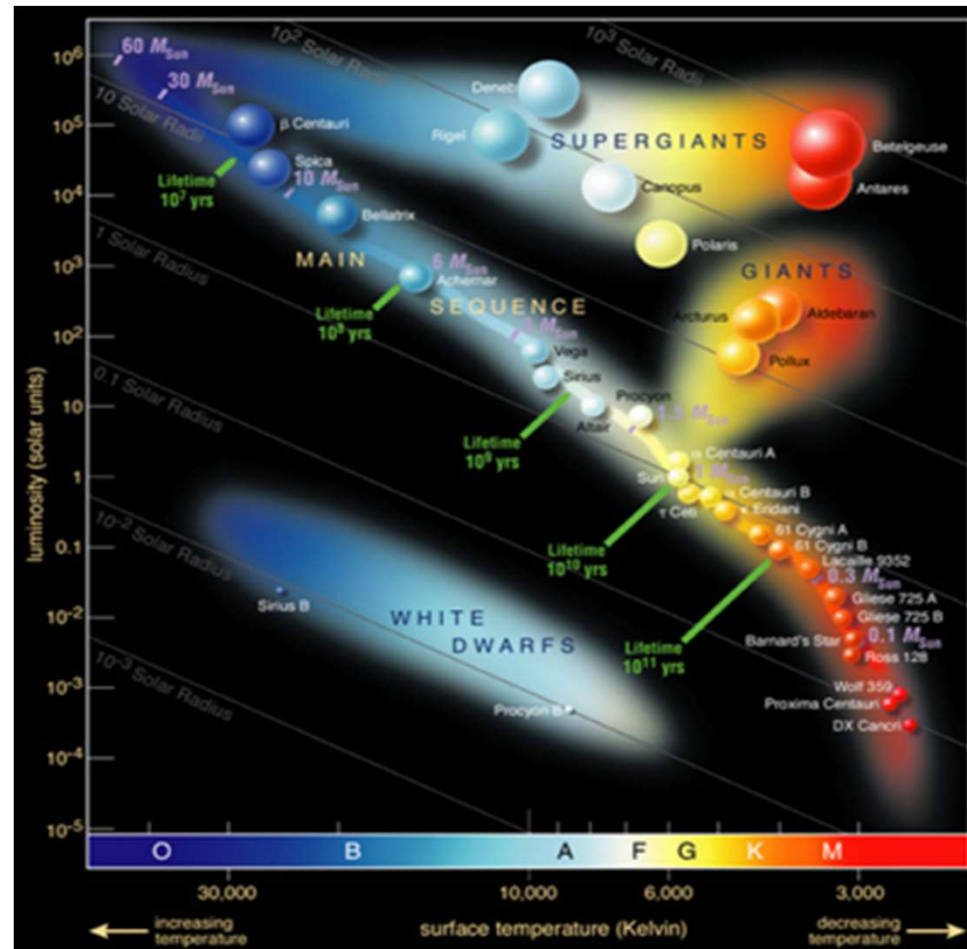
COOL STARS:

Standard to neglect NLTE-effects on atmospheric structure, might be included when calculating line spectra for individual "trace" elements (typically used for chemical abundance determinations)

BUT: See work by Phoenix-team (Hauschildt et al.)
 ALSO: RSGs still somewhat open question

Stellar Atmospheres in practice

A tour de modeling and analysis of stellar atmospheres throughout the HRD



- LTE or NLTE
- Spectral line blocking/blanketing
- (sub-) Surface convection
- Geometry and dimensionality
- Velocity fields and outflows

Spectral line blocking/blanketing

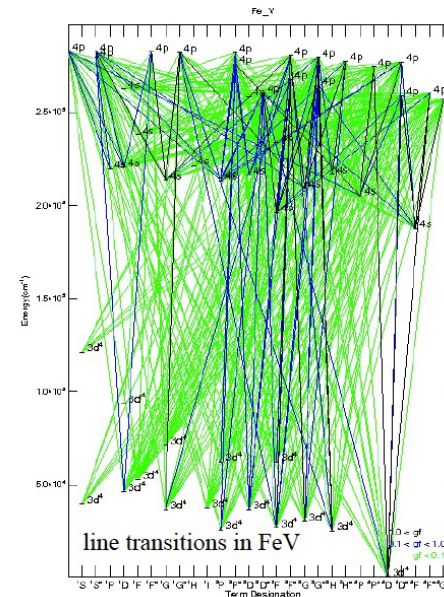
- Effects of numerous -- literally millions -- of (primarily metal) spectral lines upon the atmospheric structure and flux distribution
- Q: Why is this tricky business?

Spectral line blocking/blanketing

- Effects of numerous -- literally millions -- of (primarily metal) spectral lines upon the atmospheric structure and flux distribution
- **Q: Why is this tricky business?**
 - Lots of atomic data required (thus atomic physics and/or experiments)
 - LTE or NLTE?
 - What lines are relevant?
(i.e., what ionization stages? Are there molecules present?)

Techniques:

Opacity Distribution Functions
 Opacity-Sampling
 Direct line by line calculations



Spectral line blocking/blanketing

Back-warming (and surface-cooling)

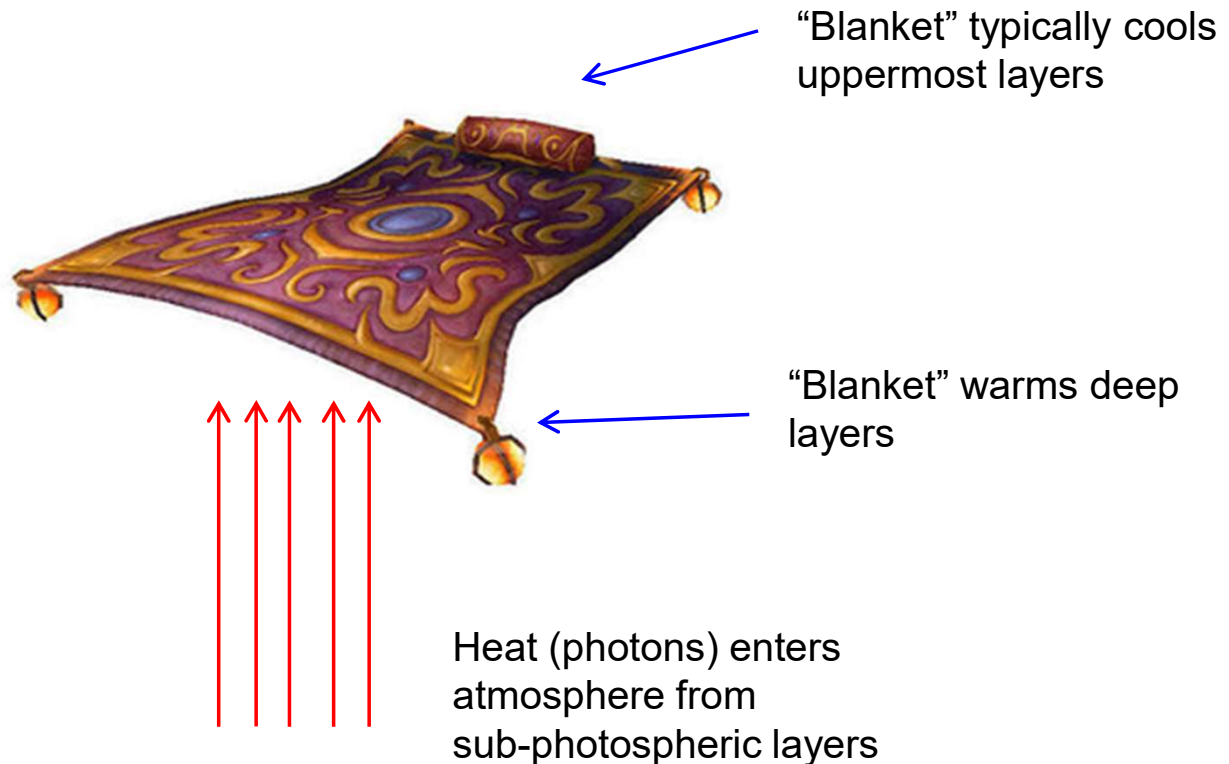
Numerous absorption lines

“block” (E)UV radiation flux

Total flux conservation

demands these photons be emitted elsewhere → redistributed to optical/infra-red

Lines act as “blanket”, whereby back-scattered line photons are (partly) thermalized and thus heat up deeper layers



Spectral line blocking/blanketing

Back-warming and flux redistribution

...occur in stars of all spectral types

$$\Delta T = T_{\text{no lines}} - T_{\text{with lines}}$$

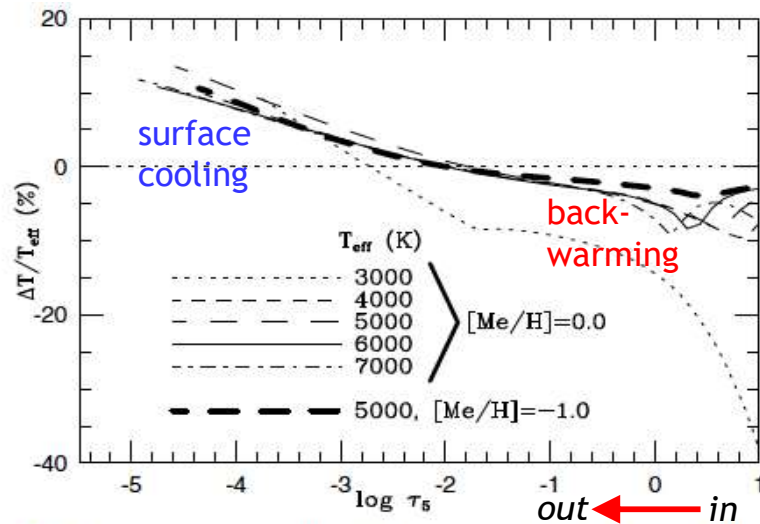


Fig. 4. The effects of switching off line absorption on the temperature structure of a sequence of models with $\log g = 3.0$ and solar metallicity. Note that $\Delta T \equiv T(\text{no lines}) - T(\text{lines})$. It is seen that the blanketing effects are fairly independent of effective temperature for models with $T_{\text{eff}} \geq 4000$.

Back warming in cool stars
(from Gustafsson et al. 2008)

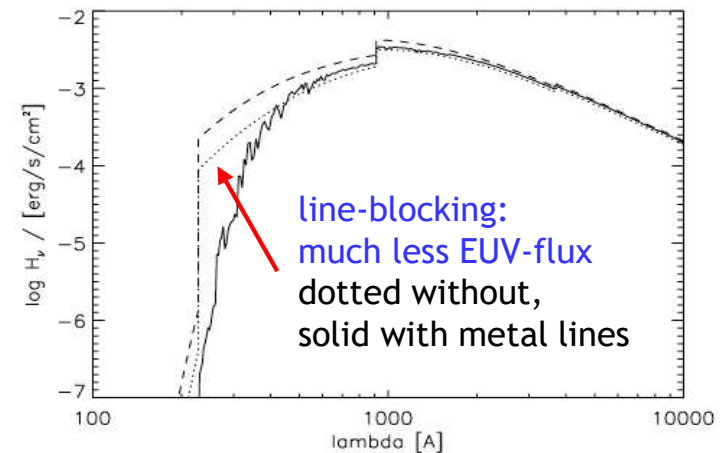


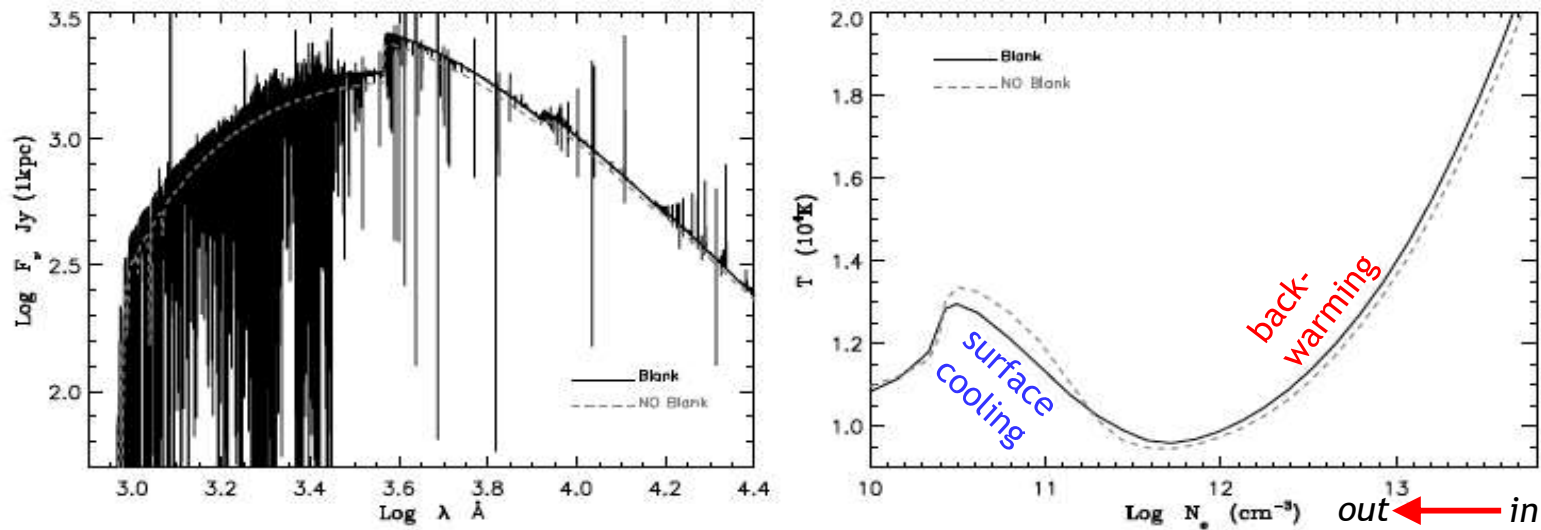
Fig. 10. Emergent Eddington flux H_ν as function of wavelength. Solid line: Current model of HD 15629 (O5V((f)) with parameters from Table 1 ($T_{\text{eff}} = 40\,500$ K, $\log g = 3.7$, "model 1"). Dotted: Pure H/He model without line-blocking/blanketing and negligible wind, at same T_{eff} and $\log g$ ("model 2"). Dashed: Pure H/He model, but with $T_{\text{eff}} = 45\,000$ K and $\log g = 3.9$ ("model 3").

UV to optical flux redistribution in hot stars
(from Repolust, Puls & Hererro 2004)

Spectral line blocking/blanketing

Back-warming and flux redistribution

...occur in stars of all spectral types



From Puls et al. 2008

Fig. 9 Effects of line blanketing (solid) vs. unblanketed models (dashed) on the flux distribution ($\log F_\nu$ (Jansky) vs. $\log \lambda$ (Å), left panel) and temperature structure (T (10^4 K) vs. $\log n_e$, right panel) in the atmosphere of a late B-hypergiant. Blanketing blocks flux in the UV, redistributes it towards longer wavelengths and causes back-warming.

Spectral line blocking/blanketing

in line/continuum forming regions, blanketed models at a certain T_{eff} have a plasma temperature corresponding to an unblanketed model with higher T'_{eff}

Back-warming – effect on effective temperature

RECALL: T_{eff} -- or total flux (plane-parallel) -- fundamental input parameter in model atmosphere!

From Gustafsson et al. 2008: Estimate effect by assuming a blanketed model with T_{eff} such that the deeper layers correspond to an unblanketed model with effective temperature $T'_{\text{eff}} > T_{\text{eff}}$

$$F = \sigma_B T_{\text{eff}}^4$$

T_{eff} in cool stars derived, e.g., by optical photometry

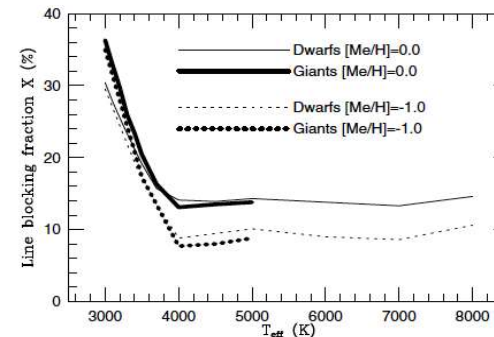


Fig. 3. The blocking fraction X in percent for models in the grid with two different metallicities. The dwarf models all have $\log g = 4.5$ while the giant models have $\log g$ values increasing with temperature, from $\log g = 0.0$ at $T_{\text{eff}} = 3000$ K to $\log g = 3.0$ at $T_{\text{eff}} = 5000$ K.

Question: Why does the line blocking fraction increase for very cool stars?

$$T'_{\text{eff}} = (1 - X)^{-\frac{1}{4}} \cdot T_{\text{eff}}, \quad (35)$$

where X is the fraction of the integrated continuous flux blocked out by spectral lines,

$$X = \frac{\int_0^{\infty} (F_{\text{cont}} - F_{\lambda}) d\lambda}{\int_0^{\infty} F_{\text{cont}} d\lambda}. \quad (36)$$

Spectral line blocking/blanketing

Back-warming – effect on effective temperature

RECALL: T_{eff} -- or total flux (plane-parallel) -- fundamental input parameter in model atmosphere!

Previous slide were LTE models. In hot stars, everything has to be done in NLTE...

$$F = \sigma_{\text{B}} T_{\text{eff}}^4$$

Question: Why is optical photometry generally NOT well suited to derive T_{eff} in hot stars?

Spectral line blocking/blanketing

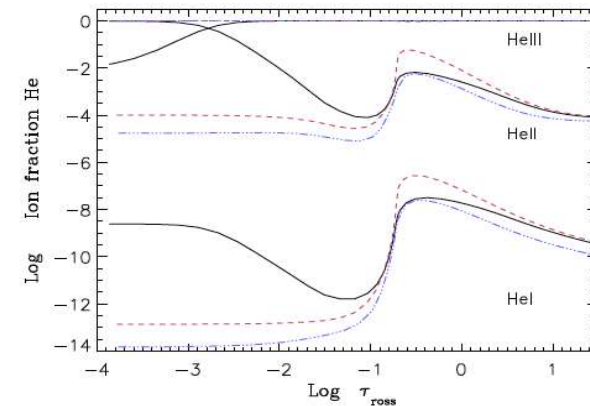
Instead, He ionization-balance is typically used
(or N for the very hottest stars, or, e.g., Si for B-stars)

HeI4387 HeI4922 HeI6678 HeI6683 HeI4471 HeI4713 HeII4200 HeII4541 HeII6404



Simultaneous fits to observed HeI and HeII lines
— from Repolust, Puls, Hererro (2004)

- Back-warming shifts ionization balance toward more completely ionized Helium in blanketed models
- thus fitting the same observed spectrum requires **lower** T_{eff} than in unblanketed models



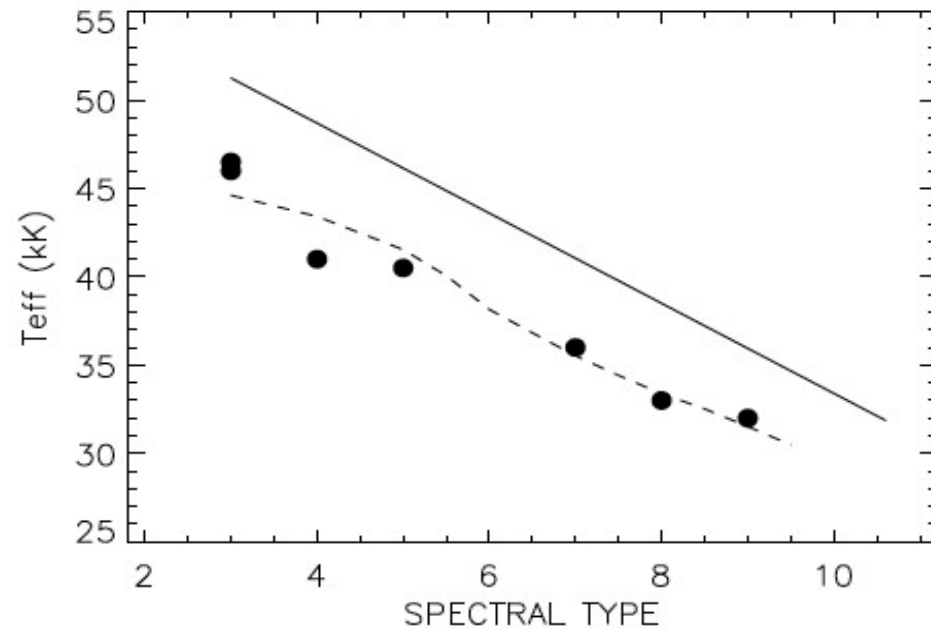
- black – blanketed $T_{\text{eff}}=45$ kK
- red – unblanketed $T_{\text{eff}}=45$ kK
- blue – unblanketed $T_{\text{eff}}=50$ kK

black and blue have similar (low) HeI/II ionization fractions in weak-line forming region, thus similar line profiles

Spectral line blocking/blanketing

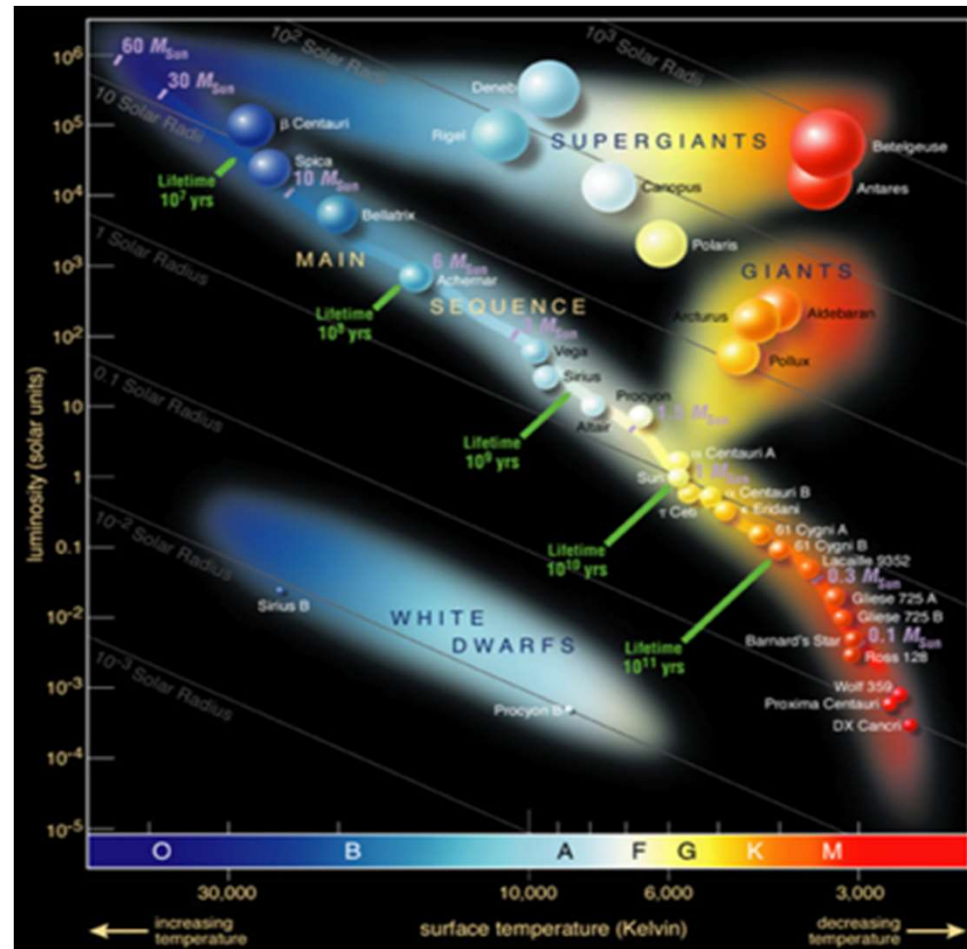
Instead, He ionization-balance is typically used
(or N for the very hottest stars, or, e.g., Si for B-stars)

Result: In hot O-stars with $T_{\text{eff}} \sim 40,000$ K, back-warming can lower the derived T_{eff} as compared to unblanketed models by several thousand degrees!
(~ 10 %)



New T_{eff} scale for O-dwarf stars. Solid line – unblanketed models. Dashed – blanketed calibration, dots – observed blanketed values (from Puls et al. 2008)

A tour de modeling and analysis of stellar atmospheres throughout the HRD



- LTE or NLTE
- Spectral line blocking/blanketing
- (sub-) Surface convection
- Geometry and dimensionality
- Velocity fields and outflows

Surface Convection

from part 1

Convection

energy transport not only by radiation,
however also by

- waves
- heat conduction
- convection

} not efficient in typical stellar atmospheres, but
... coronae, chromospheres
white dwarfs

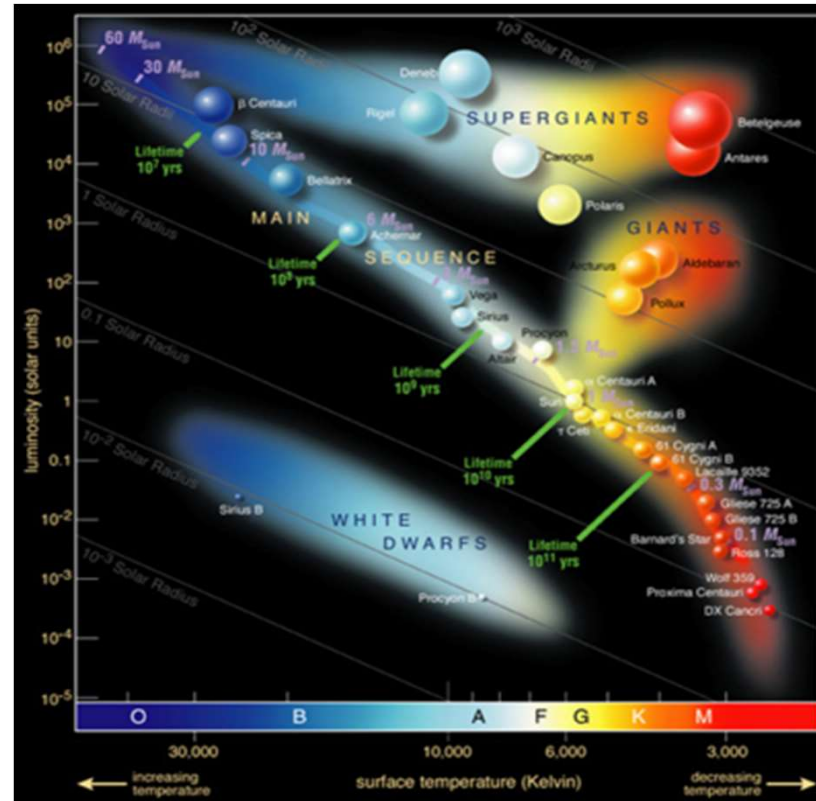
Thus

total flux = const

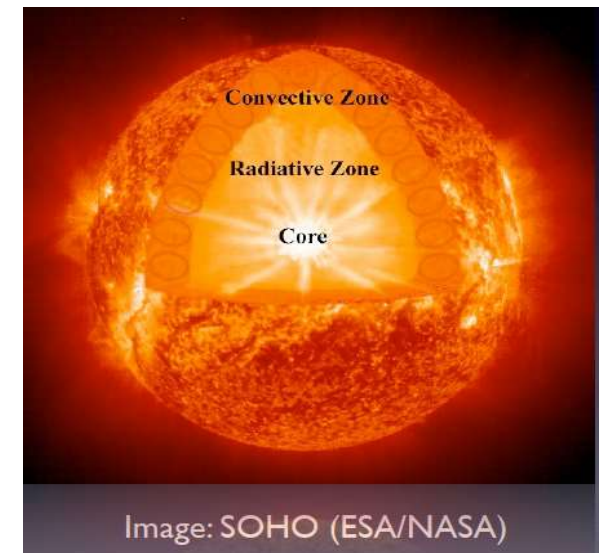
$$\nabla \cdot (\underline{F}^{\text{rad}} + \underline{F}^{\text{conv}}) \stackrel{\downarrow}{=} 0 \quad (\text{in quasi-hydrostatic atmospheres})$$

Surface Convection

OBSERVATIONS:
 “Sub-surface”
 convection in layers
 $T \sim 160,000$ K (due to
 iron-opacity peak)
 currently discussed
 also in hot stars



- H/He recombines in atmospheres of cool stars
- Provides MUCH opacity
- Convective Energy transport



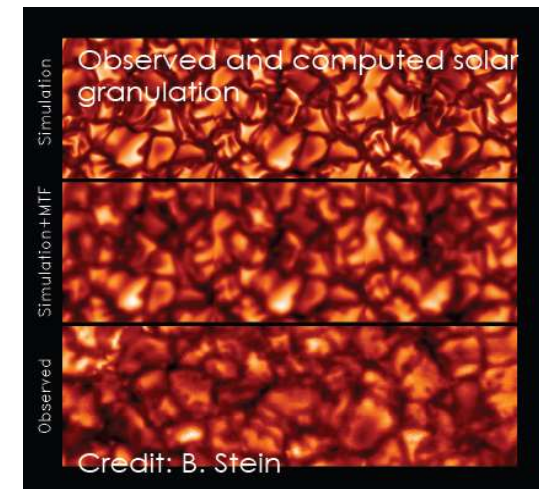
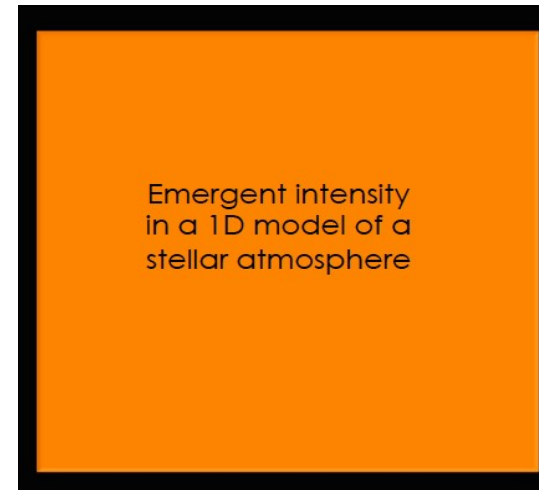
Surface Convection

Traditionally accounted for by rudimentary “mixing-length theory” (see Chap. 6) in 1-D atmosphere codes

BUT:

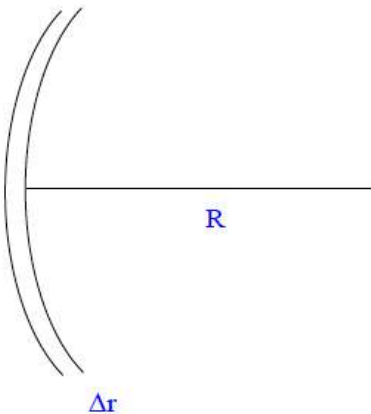
- Solar observations show very dynamic structure
- Granulation and lateral inhomogeneity

→ Need for full 3-D radiation-hydrodynamics simulations in which convective motions occur spontaneously if required conditions fulfilled (all physics of convection ‘naturally’ included)



Surface Convection

Solar-type stars:
 Photospheric extent \ll stellar radius
 Small granulation patterns



example: the sun

$R_{\text{sun}} \approx 700,000 \text{ km}$
 $\Delta r (\text{photo}) \approx 300 \text{ km}$

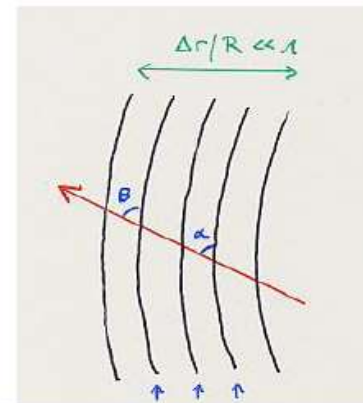
$\Rightarrow \Delta r / R \approx 4 \cdot 10^{-4}$

BUT corona

$\Delta r / R (\text{corona}) \approx 3$

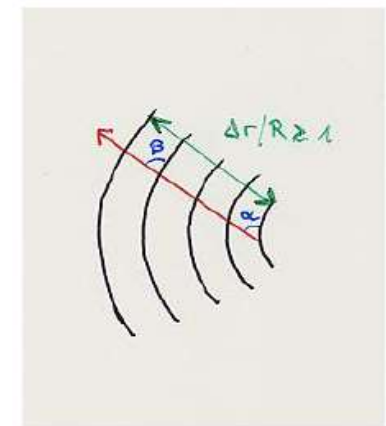
as long as $\Delta r / R \ll 1 \Rightarrow$ plane-parallel symmetry

light ray through atmosphere



lines of constant temperature and density (isocontours)

curvature of atmosphere insignificant for photons' path : $\alpha = \beta$



significant curvature : $\alpha \neq \beta$, spherical symmetry

solar photosphere / cromosphere
 atmospheres of
 main sequence stars
 white dwarfs
 giants (partly)

examples

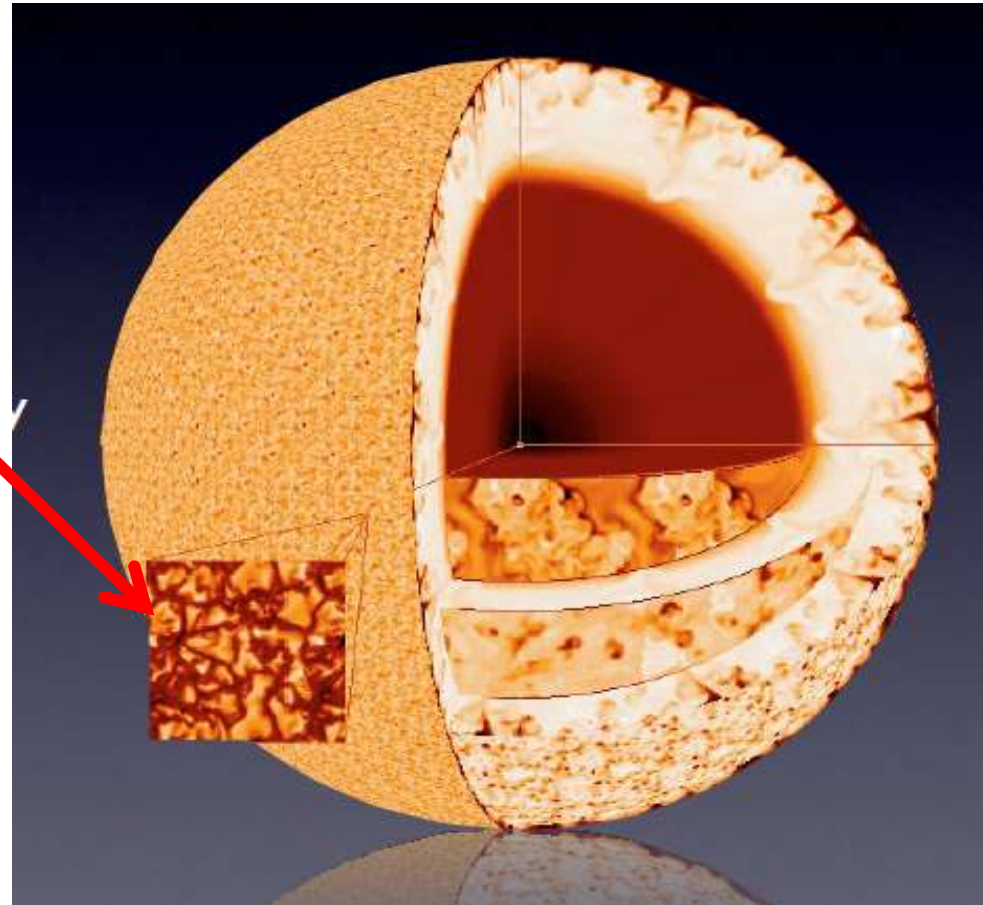
solar corona
 atmospheres of
 supergiants
 expanding envelopes (stellar winds)
 of OBA stars, M-giants and supergiants

Surface Convection

Solar-type stars:
Atmospheric extent \ll stellar radius
Small granulation patterns

→
**Box-in-a-star
Simulations**

(cmp. plane-parallel approximation)



From Wolfgang Hayek

Surface Convection

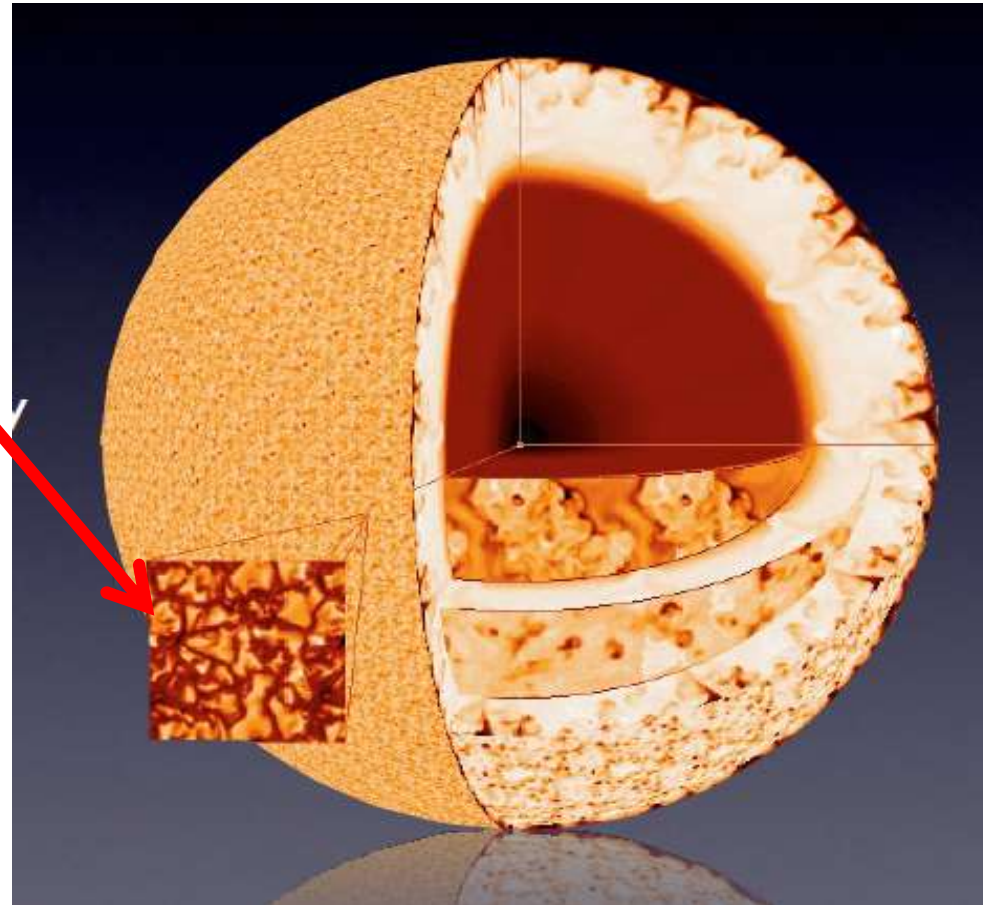
Approach
(teams by Nordlund, Steffen):

Solve radiation-hydrodynamical conservation equations of mass, momentum, and energy (closed by equation of state).

3-D radiative transfer included to calculate net radiative heating/cooling q_{rad} in energy equation, typically assuming LTE and a very simplified treatment of line-blanketing

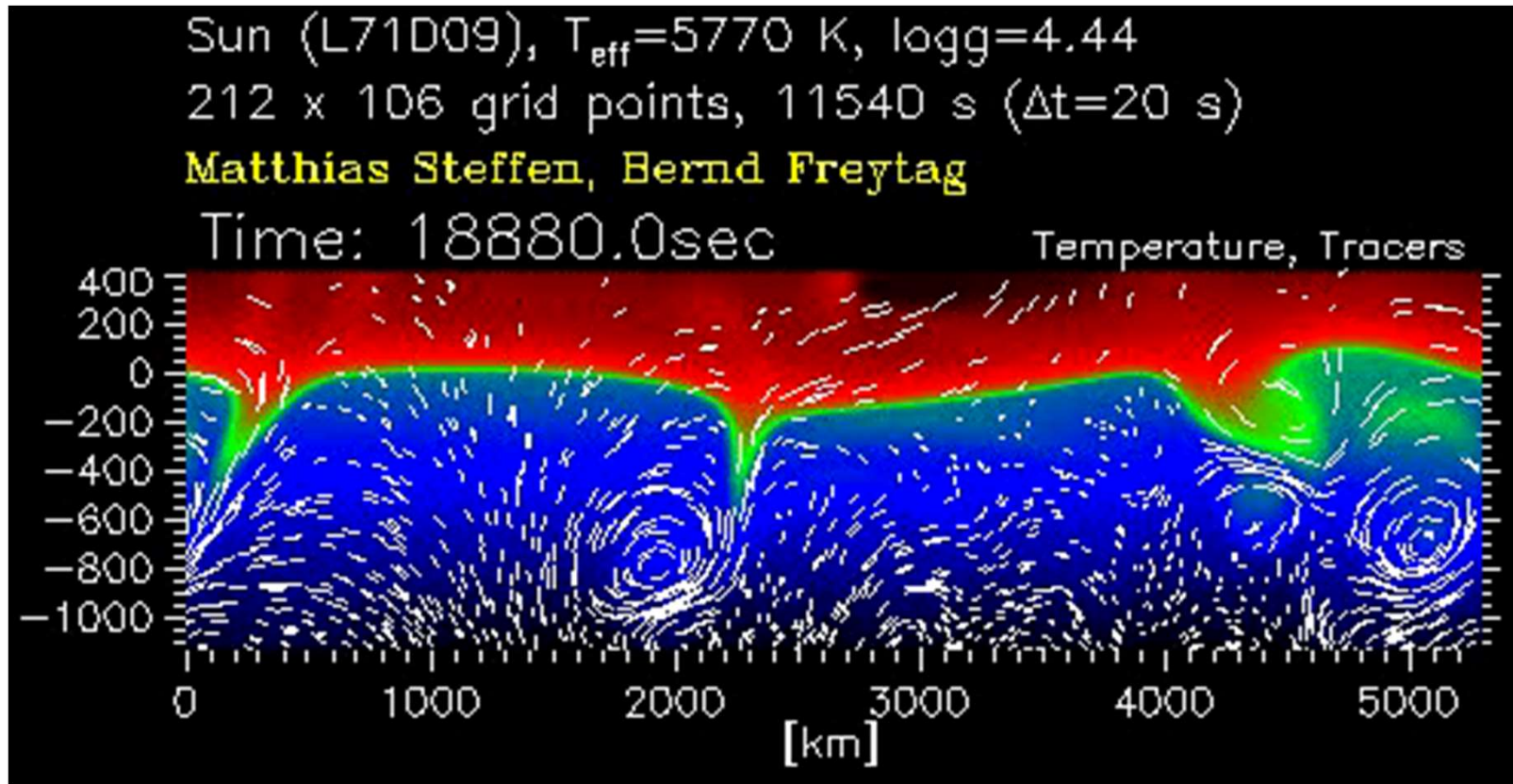
$$q_{\text{rad}} = 4\pi\rho \int_{\lambda} \kappa_{\lambda} (J_{\lambda} - S_{\lambda}) d\lambda,$$

(= 0 in case of radiative equilibrium)



From Wolfgang Hayek

Surface Convection



From Berndt Freytag's homepage:

<http://www.astro.uu.se/~bf/>

Surface Convection

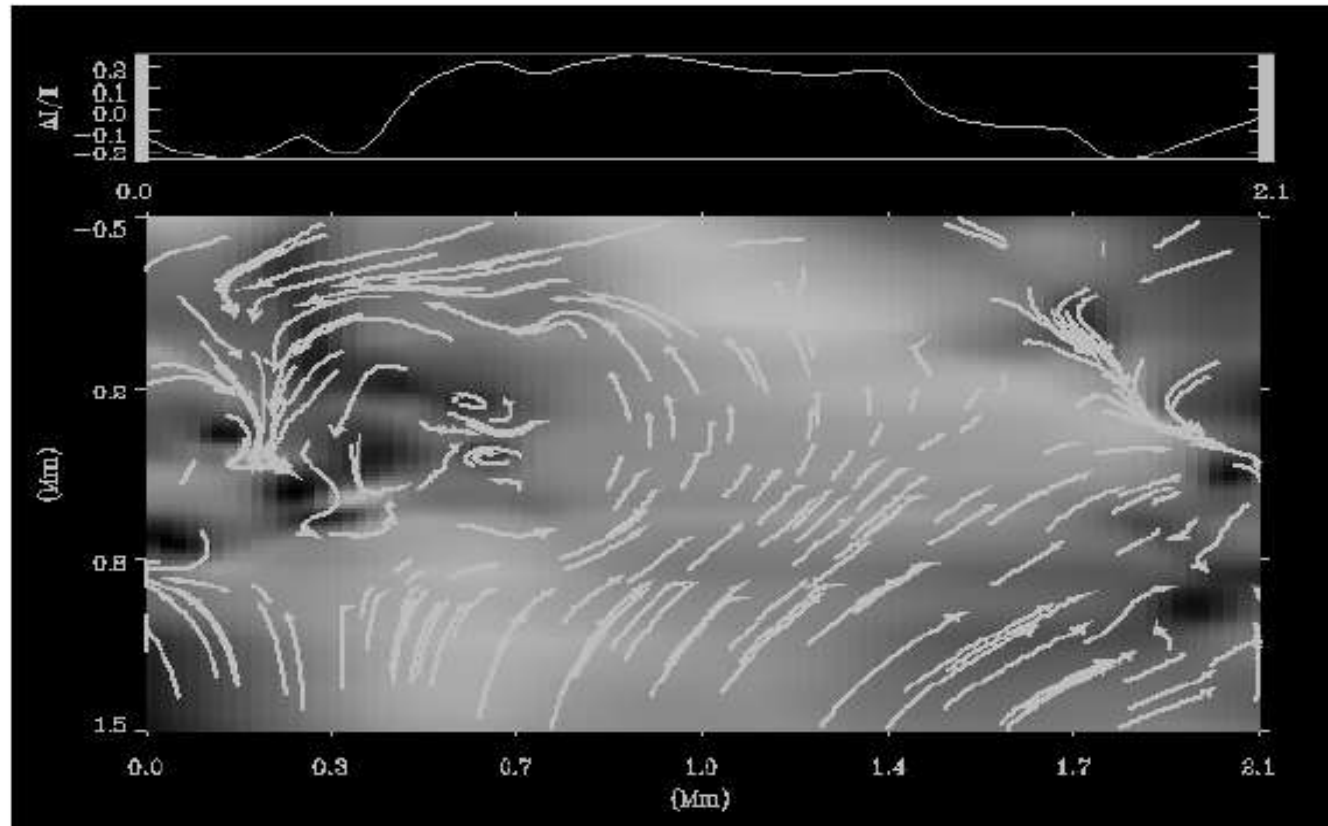


FIG. 4.—Pressure fluctuations about the mean hydrostatic equilibrium and the velocity field in an xz slice through a granule. The pressure is high above the centers of granules, which decelerates the warm upflowing fluid and diverts it horizontally. High pressure also occurs in the intergranular lanes where the horizontal motions are halted and gravity pulls the now cool, dense fluid down into the intergranular lanes. Horizontal rolls of high vorticity occur at the edges of the intergranular lanes. The emergent intensity profile across the slice is shown at the top.

From Stein & Nordlund (1998)

Surface Convection

Some key features:

Slow, broad upward motions, and
faster, thinner downward
motions

Non-thermal velocity fields

Overshooting from zone where
convection is efficient
according to stability criteria
(see Chap. 6)

Energy balance in upper layers not
only controlled by radiative
heating/cooling, but also by
cooling from adiabatic
expansion

See Stein & Nordlund (1998);
Collet et al. (2006), etc.

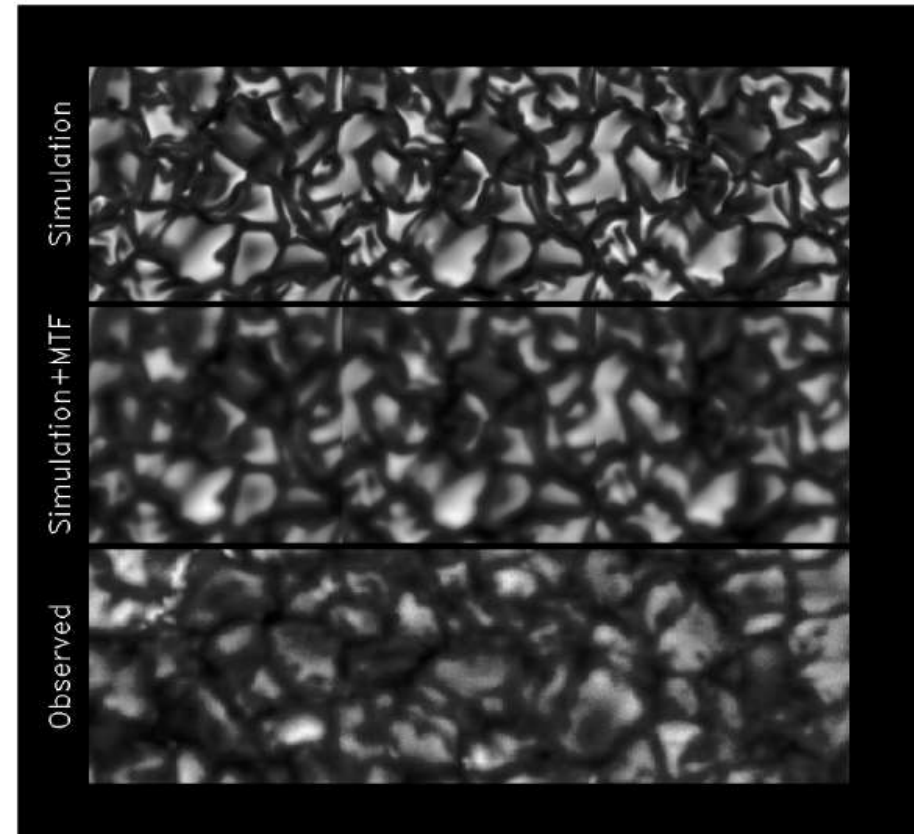


FIG. 19.—Comparison of granulation as seen in the emergent intensity from the simulations and as observed by the Swedish Vacuum Solar Telescope on La Palma. The top row shows three simulation images at 1 minute intervals, which together make a composite image 18×6 Mm in extent. The middle row shows this image smoothed by an Airy plus exponential point-spread function. The bottom row shows an 18×6 Mm white-light image from La Palma. Note the similar appearance of the smoothed simulation image and the observed granulation. The common edge brightening in the simulation is reduced when smoothed. Images by (Title 1996, private communication) taken in the CH G-band have much more contrast than white light and clearly reveal the edge brightening of granules.

Question: This does not look much like the traditional 1-D models we've discussed during the previous lecture! – Do you think we should throw them in the garbage?

Surface Convection

blue: mean temperature from 3D hydro-model (scatter = dashed)

red: from 1D semi-empirical model (Holweger & Müller, see Chap. 5)

green: from 1D theoretical model atmospheres (MARCS)

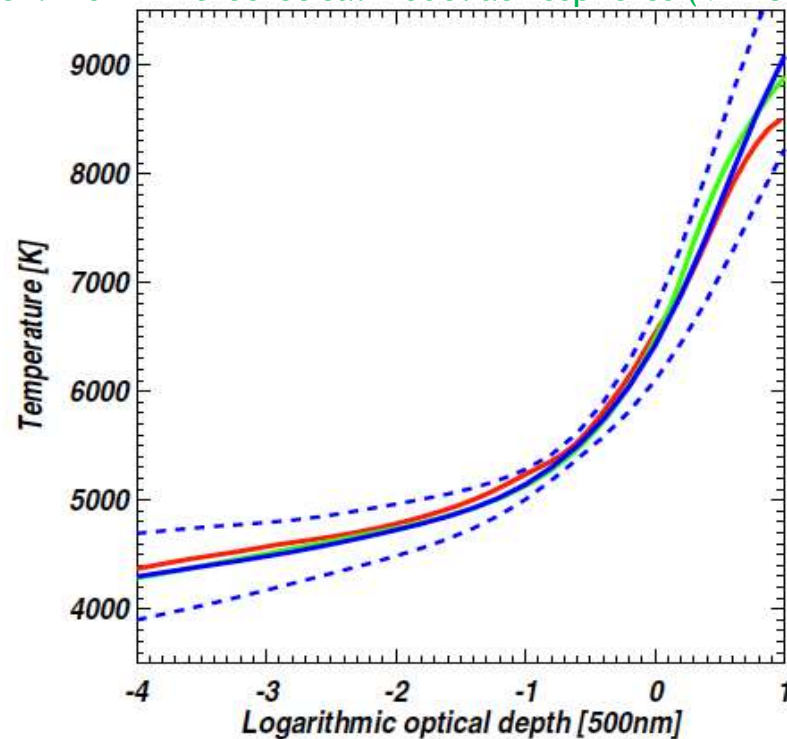


Figure 1: The mean temperature structure of the 3D hydrodynamical model of Trampedach et al. (2009) is shown as a function of optical depth at 500 nm (blue solid line). The blue dashed lines correspond to the spatial and temporal rms variations of the 3D model, while the red and green variations curves denote the 1D semi-empirical Holweger & Müller (1974) and the 1D theoretical MARCS (Gustafsson et al. 2008) model atmospheres, respectively.

In many (though not all) cases, AVERAGE properties still quite OK:

Convection in energy balance approximated by “mixing-length theory”

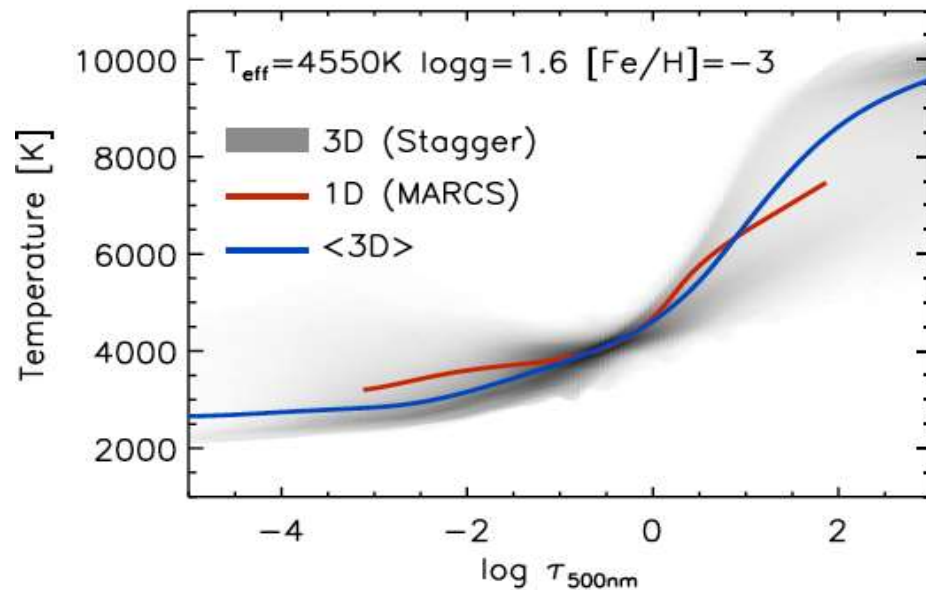
Non-thermal velocity fields due to convective motions included by means of so-called “micro-” and “macro-turbulence”

BUT quantitatively we always need to ask:

To what extent can average properties be modeled by traditional 1-D codes?

Unfortunately, a general answer very difficult to give, need to be considered case by case

Surface Convection



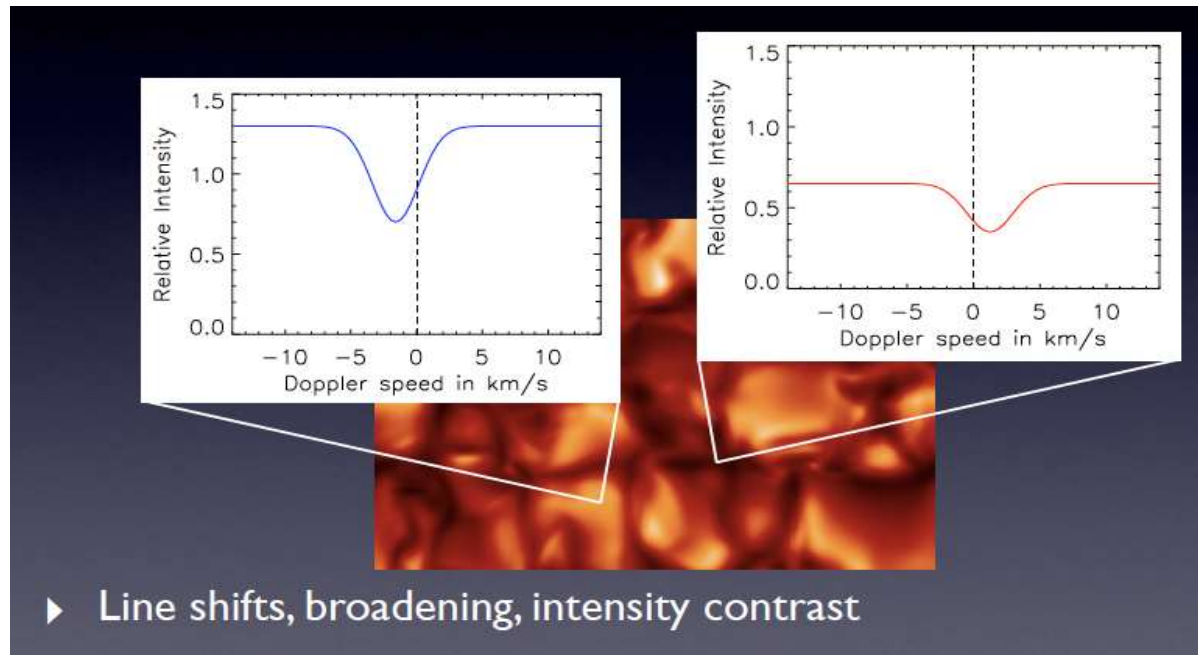
Metal-poor red giant, simulation by Remo Collet,
figure from talk by M. Bergemann

For example:

In metal-poor cool stars spectral lines are scarce
(Question: Why?),
and energy balance in upper photosphere controlled to
a higher degree by adiabatic expansion of convectively
overshot material.

In classical 1-D models though, these layers are
convectively stable, and energy balance controlled only
by radiation (radiative equilibrium, see part1).

Surface Convection



From talk by Hayek

3-D radiation-hydro models successful in reproducing many solar features (see overview in Asplund et al. 2009), e.g:

- Center-to-limb intensity variation
- Line profiles and their shifts and variations (without micro/macroturbulence)
- Observed granulation patterns

Surface Convection

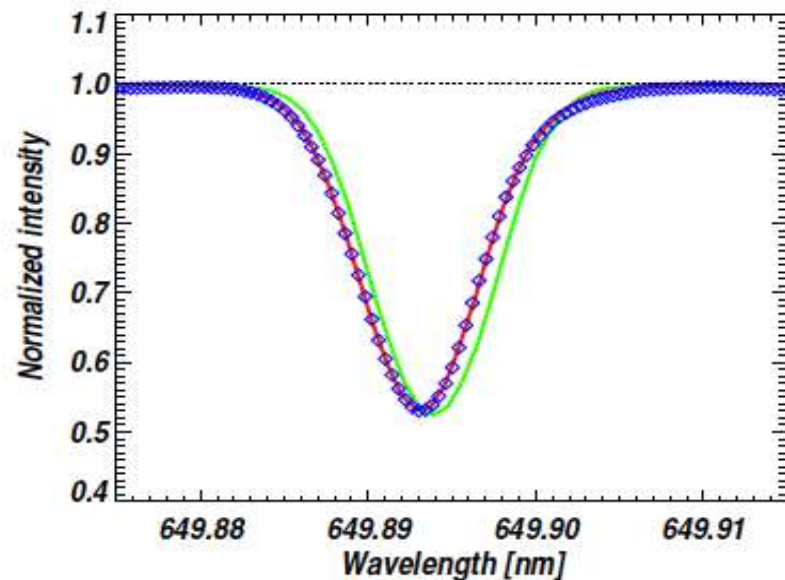


Figure 3: The predicted spectral line profile of a typical Fe I line from the 3D hydrodynamical solar model (red solid line) compared with the observations (blue rhombs). The agreement is clearly very satisfactory, which is the result of the Doppler shifts arising from the self-consistently computed convective motions that broaden, shift and skew the theoretical profile. For comparison purposes also the predicted profile from a 1D model atmosphere (here Holweger & Müller 1974) is shown; the 1D profile has been computed with a microturbulence of 1 km s^{-1} and a tuned macroturbulence to obtain the right overall linewidth. Note that even with these two free parameters the 1D profile can neither predict the shift nor the asymmetry of the line.

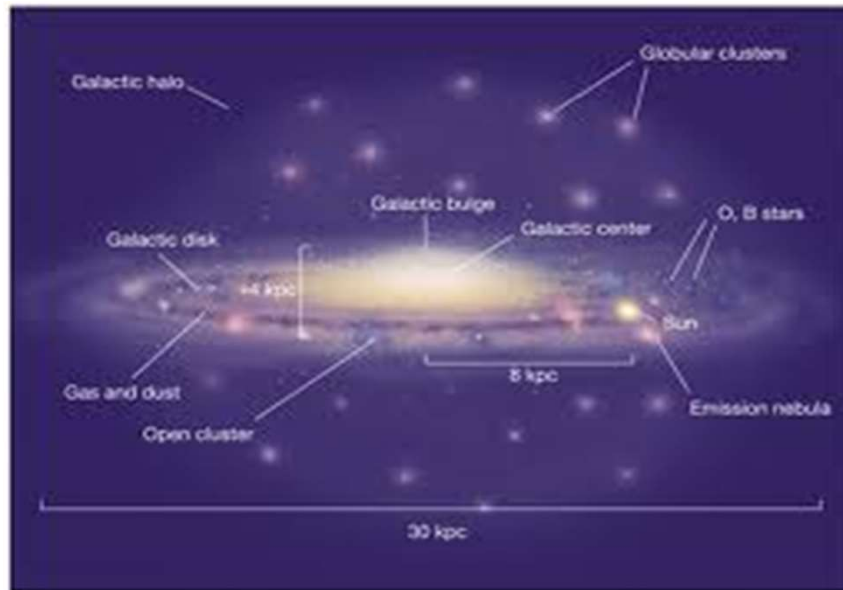
affects chemical abundance
(determined by means of line profile fitting to observations)

One MAJOR result:
Effects on line formation has led to a downward revision of the CNO solar abundances and the solar metallicity, and thus to a revision of the *standard cosmic chemical abundance scale*

Fig. from Asplund et al. (2009) – “The Chemical Composition of the Sun”

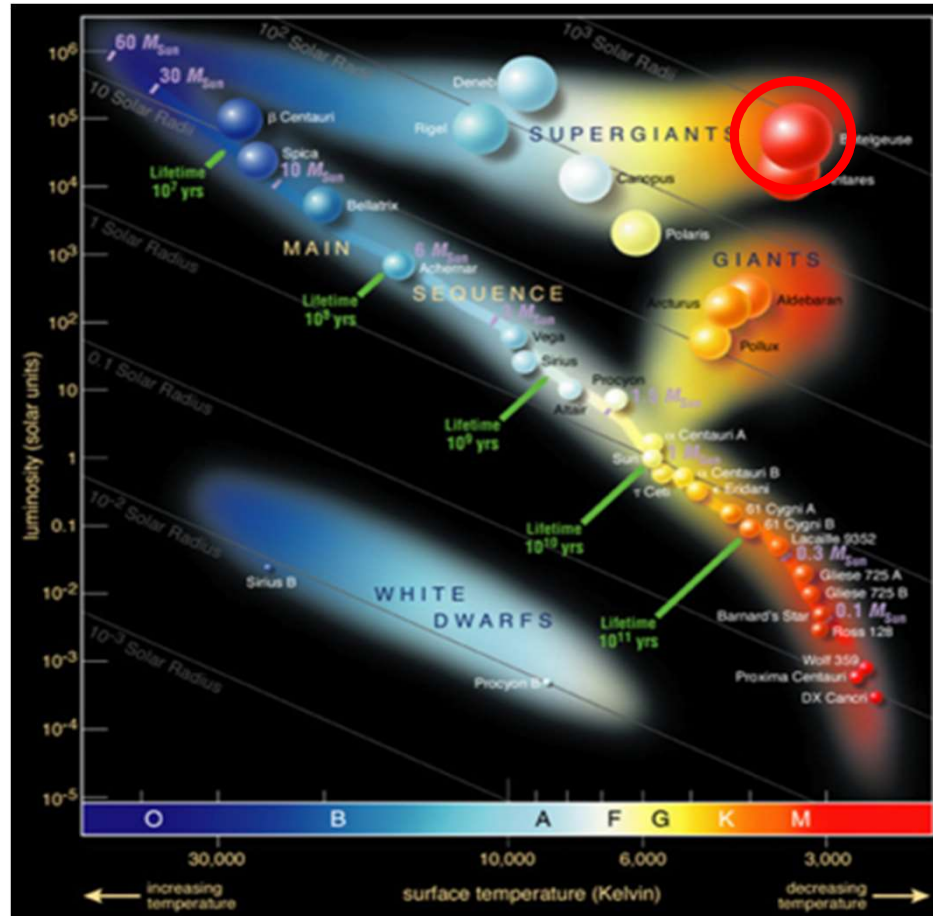
Surface Convection

Also potentially critical for **Galactic archeology...**



...which traces the chemical evolution of the Universe by analyzing VERY old, metal-poor Globular Cluster stars -- relics from the early epochs (e.g. Anna Frebel and collaborators)

Surface Convection



- Giant Convection Cells in the low-gravity, extended atmospheres of Red Supergiants
- Question: Why extended?

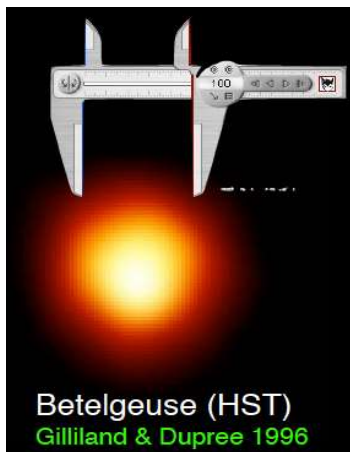
$$H = a^2 / g \quad (\text{with } a = v_s \text{ the isothermal speed of sound})$$

$$a^2_{\text{RSG}} / a^2_{\text{sun}} \approx T_{\text{RSG}} / T_{\text{sun}} = 0.5 \dots 0.6$$

$$g_{\text{RSG}} / g_{\text{sun}} \approx 10^{-4} !$$

(see Chap. 6)

Out to Jupiter...

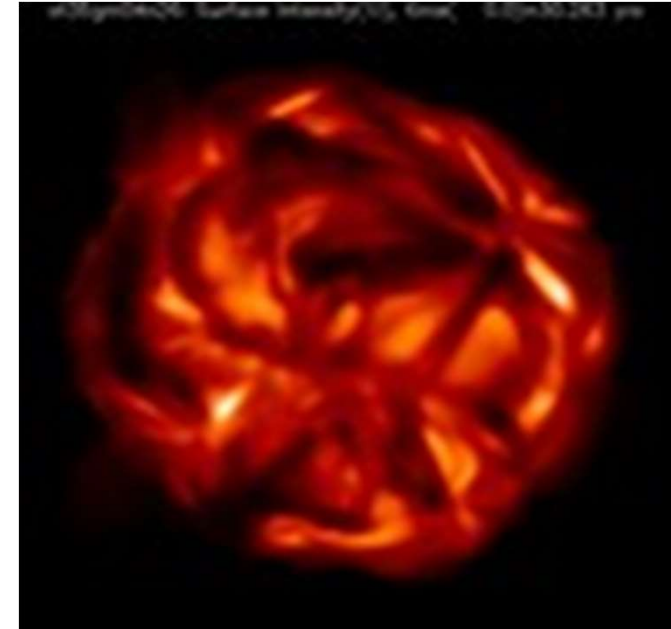


Surface Convection

Supergiants (or models including a stellar wind):
Atmospheric extent > stellar radius:

Box-in-a-star → Star-in-a-box

(1D: Plane-parallel → Spherical symmetry,
see Chap. 3)



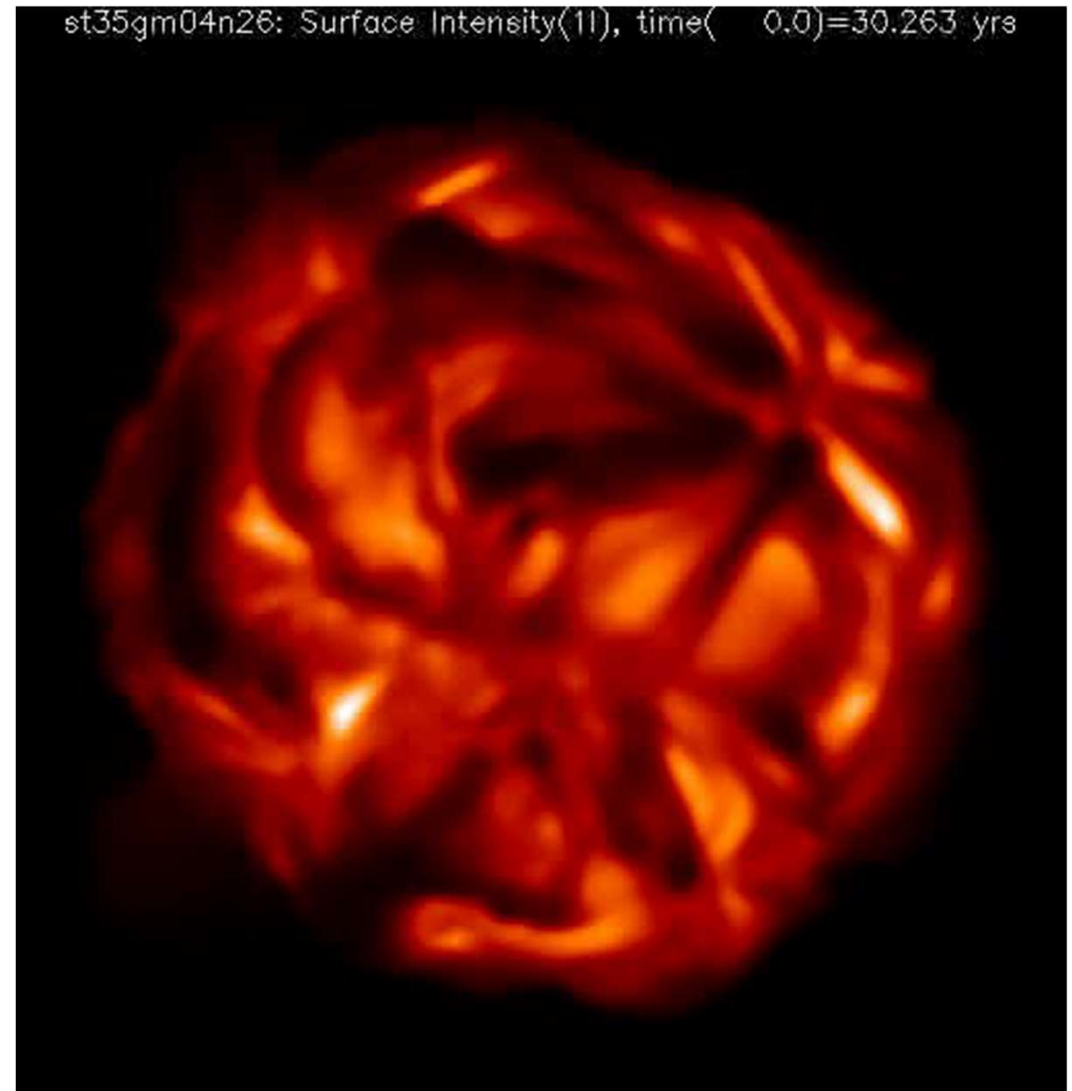
Star to model: Betelgeuse
Mass: 5 solar masses
Radius: 600 R_{sun}
Luminosity: 41400 L_{sun}
Grid: Cartesian cubical grid with 171^3 points
Edge length of box 1674 solar radii

Model by Berndt Freytag, note the **HUGE** convective cells visible in the emergent intensity map!!

Surface Convection

Star to model: Betelgeuse
Mass: 5 solar masses
Radius: 600 R_{sun}
Luminosity: 41400 L_{sun}
Grid: Cartesian cubical grid with 171^3 points
Edge length of box 1674 solar radii
Movie time span: 7.5 years

[http://www.astro.uu.se/~bf/movie/dst35gm04n26/
movie.html](http://www.astro.uu.se/~bf/movie/dst35gm04n26/movie.html)

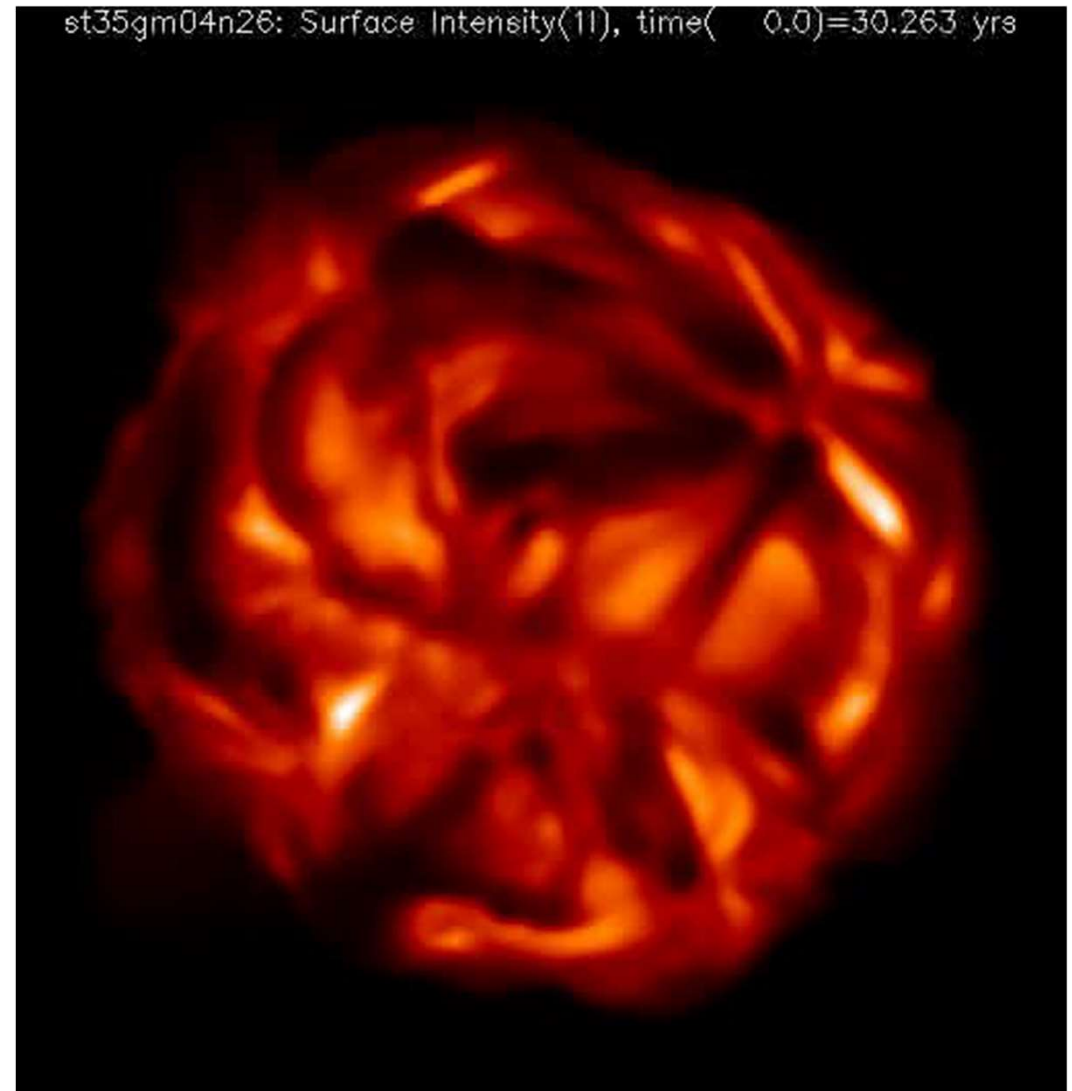


Surface Convection

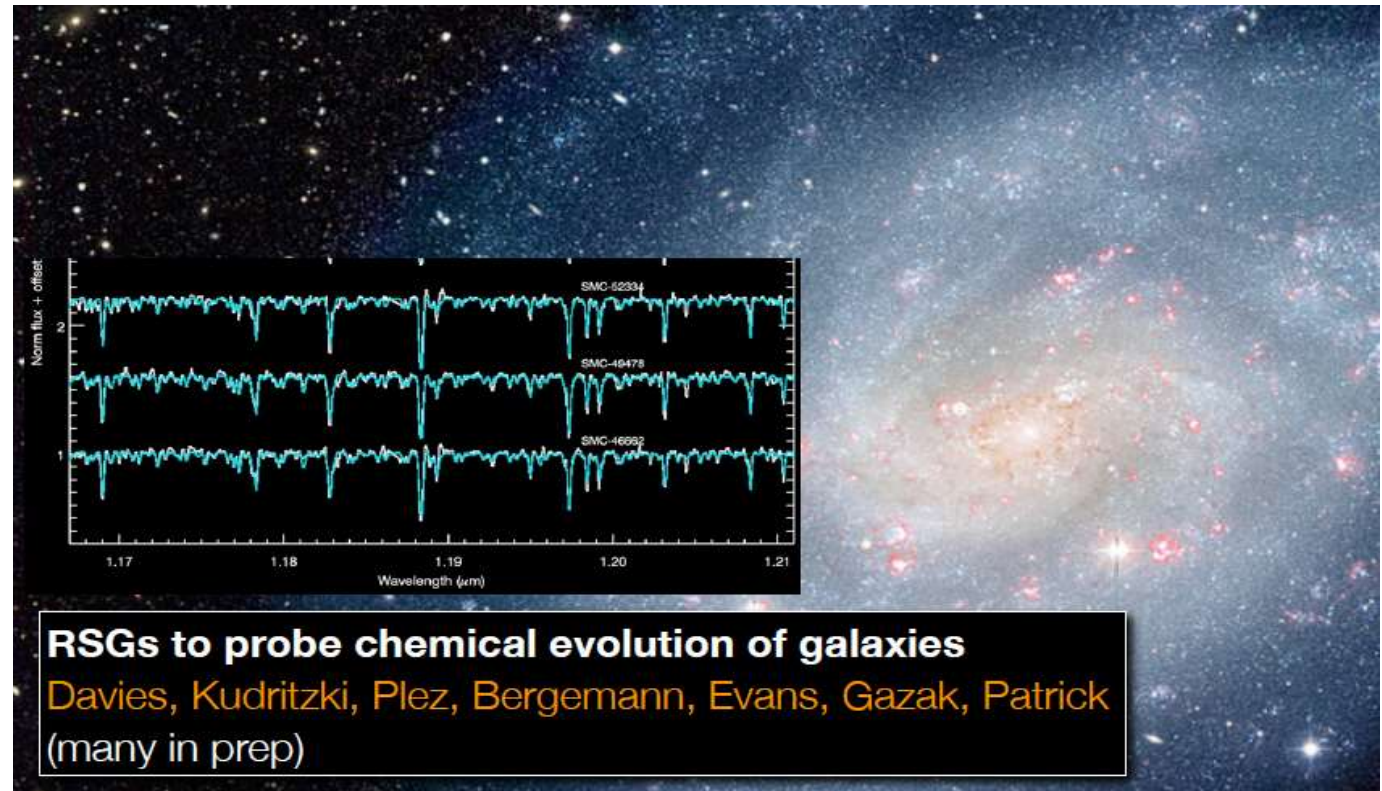
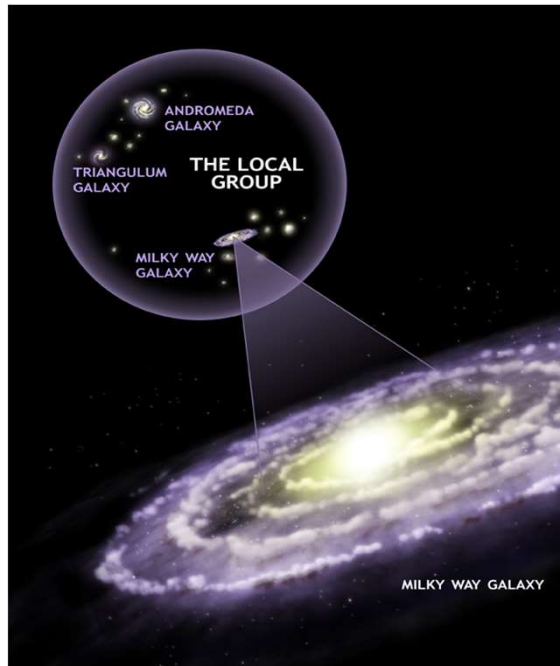
Extremely challenging,
models still in their infancies.
LOTS of exciting physics to explore, like

Pulsations
Convection
Numerical radiation-hydrodynamics
Role of magnetic fields
Stellar wind mechanisms

Also, to what extent can main effects be
captured by 1-D models?
For quantitative applications like....



Stellar Atmospheres in practice



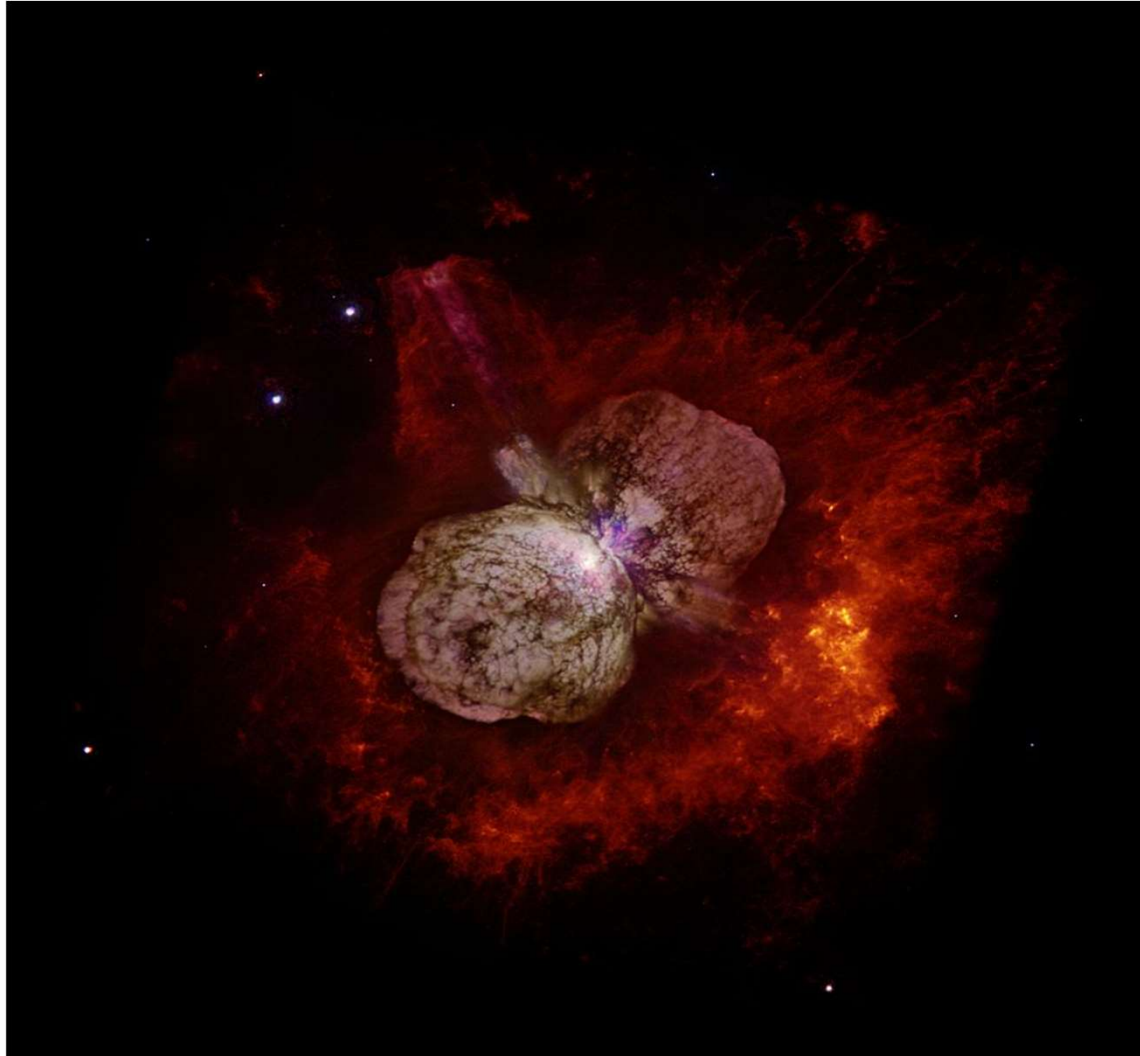
Question: Why are RSGs ideal for observational extragalactic stellar astrophysics, particularly in the near future?

important codes and their features

Codes	FASTWIND CMFGEN PoWR	WM-basic	TLUSTY Detail/Surface	Phoenix	MARCS Atlas	CO ⁵ BOLD* STAGGER
geometry	1-D spherical	1-D spherical	1-D plane-parallel	1-D/3-D spherical/ plane-parallel	1-D plane-parallel (MARCS also spherical)	3-D Cartesian
LTE/NLTE	NLTE	NLTE	NLTE	NLTE/LTE	LTE	LTE simplified
dynamics	quasi-static photosphere + prescribed supersonic outflow	time-independent hydrodynamics	hydrostatic	hydrostatic or allowing for supersonic outflows	hydrostatic	hydrodynamic
stellar wind	yes	yes	no	yes	no	no
major application	hot stars with winds	hot stars with dense winds, ion. fluxes, SNRs	hot stars with negligible winds	cool stars, brown dwarfs, SNRs	cool stars	cool stars
comments	CMFGEN also for SNRs; FASTWIND using approx. line- blocking	line-transfer in Sobolev approx. (see part 2)	Detail/Surface with LTE- blanketing	convection via mixing-length theory	convection via mixing-length theory	very long execution times, but model grids start to emerge

* Conservative CODE for the COmputation of COmpressible COnvection

And then there are, e.g.,



- Luminous Blue Variables (LBVs) like Eta Carina,
- Wolf-Rayet Stars (WRs)
- Planetary Nebulae (and their Central Stars)
- Be-stars with disks
- Brown Dwarfs
- Pre main-sequence T-Tauri and Herbig stars

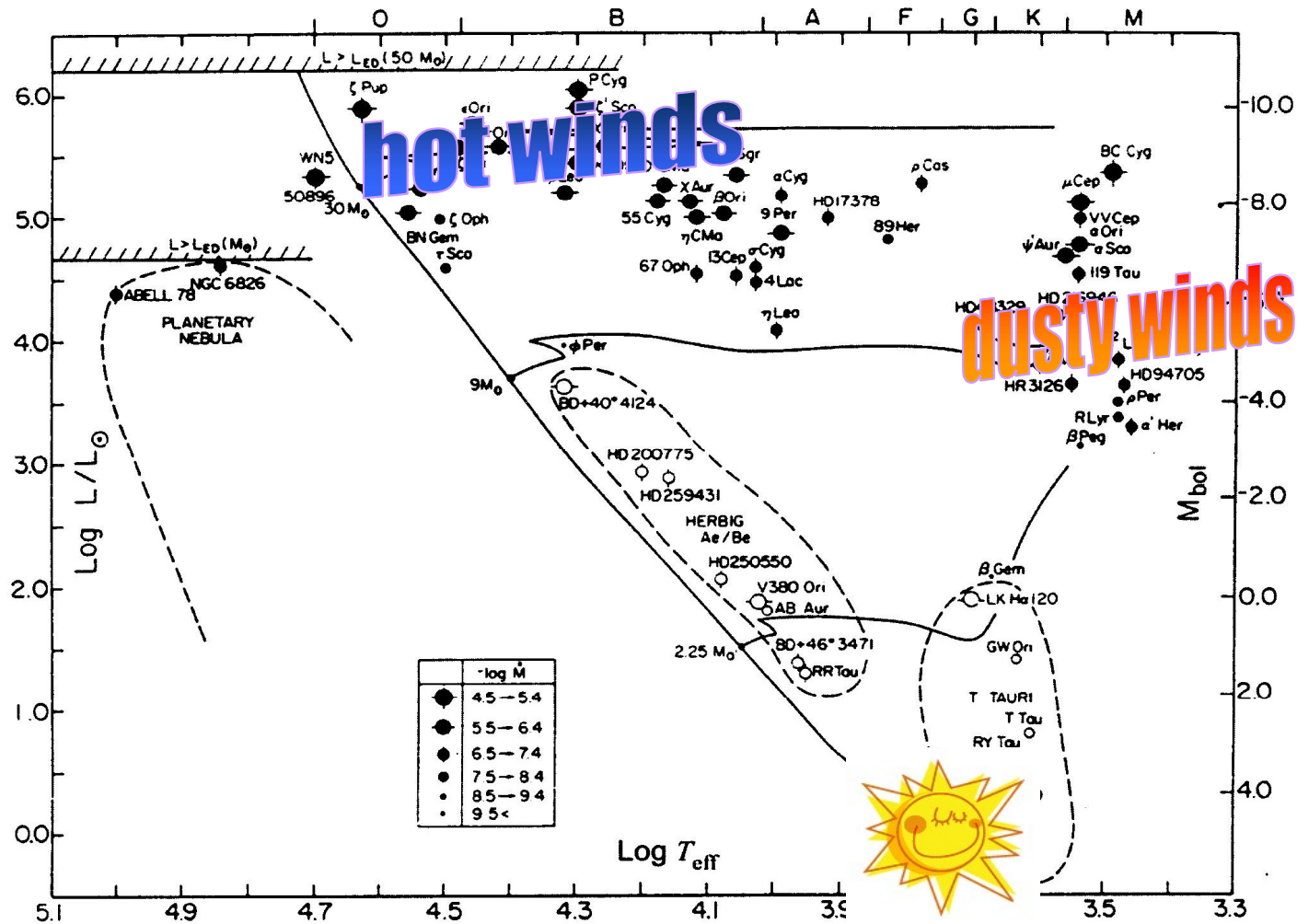
...and many other interesting objects

Stellar astronomy alive and kicking! Very rich in both

Physics

Observational applications

Chap. 8 – Stellar winds: an overview

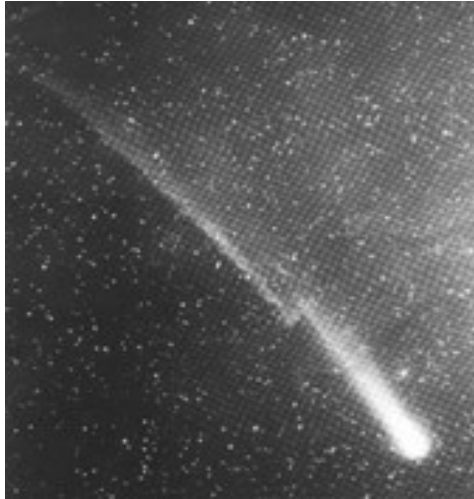


ubiquitous phenomenon

- solar type stars (incl. the sun)
- red supergiants/AGB-stars ("normal" + Mira Variables)
- hot stars (OBA supergiants, Luminous Blue Variables, OB-dwarfs, Central Stars of PN, sdO, sdB, Wolf-Rayet stars)
- T-Tauri stars
- and many more

The solar wind – a suspicion

comet Halley,
with „kink“ in
tail



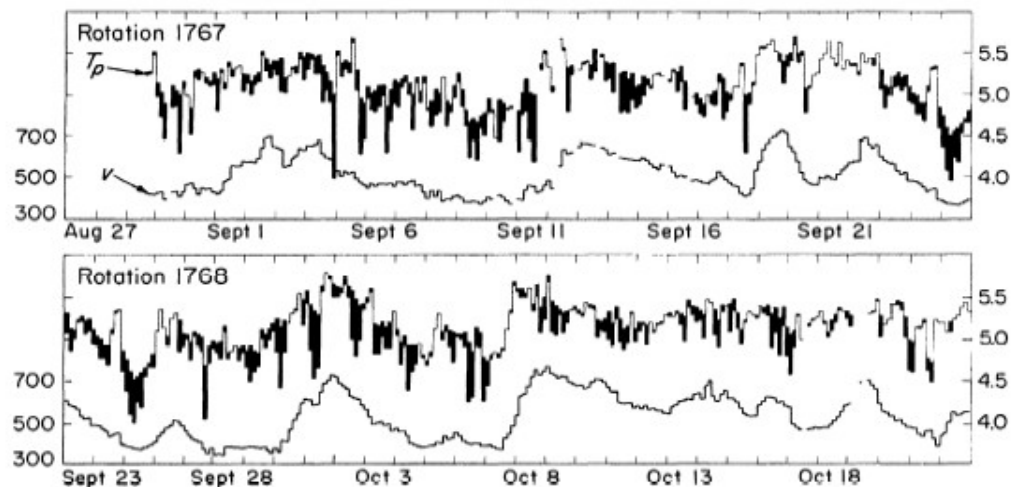
comet Hale-Bopp
with dust and
plasma tail (blue)



- comet tails *directed away from the sun*
- **Kepler**: influence of solar radiation pressure (-> radiation driven winds)
- *Ionic tail*: emits own radiation, sometimes different direction
- **Hoffmeister** (1943, subsequently Biermann): *solar particle radiation* different direction, since v (particle) comparable to v (comet)

The solar wind – the discovery

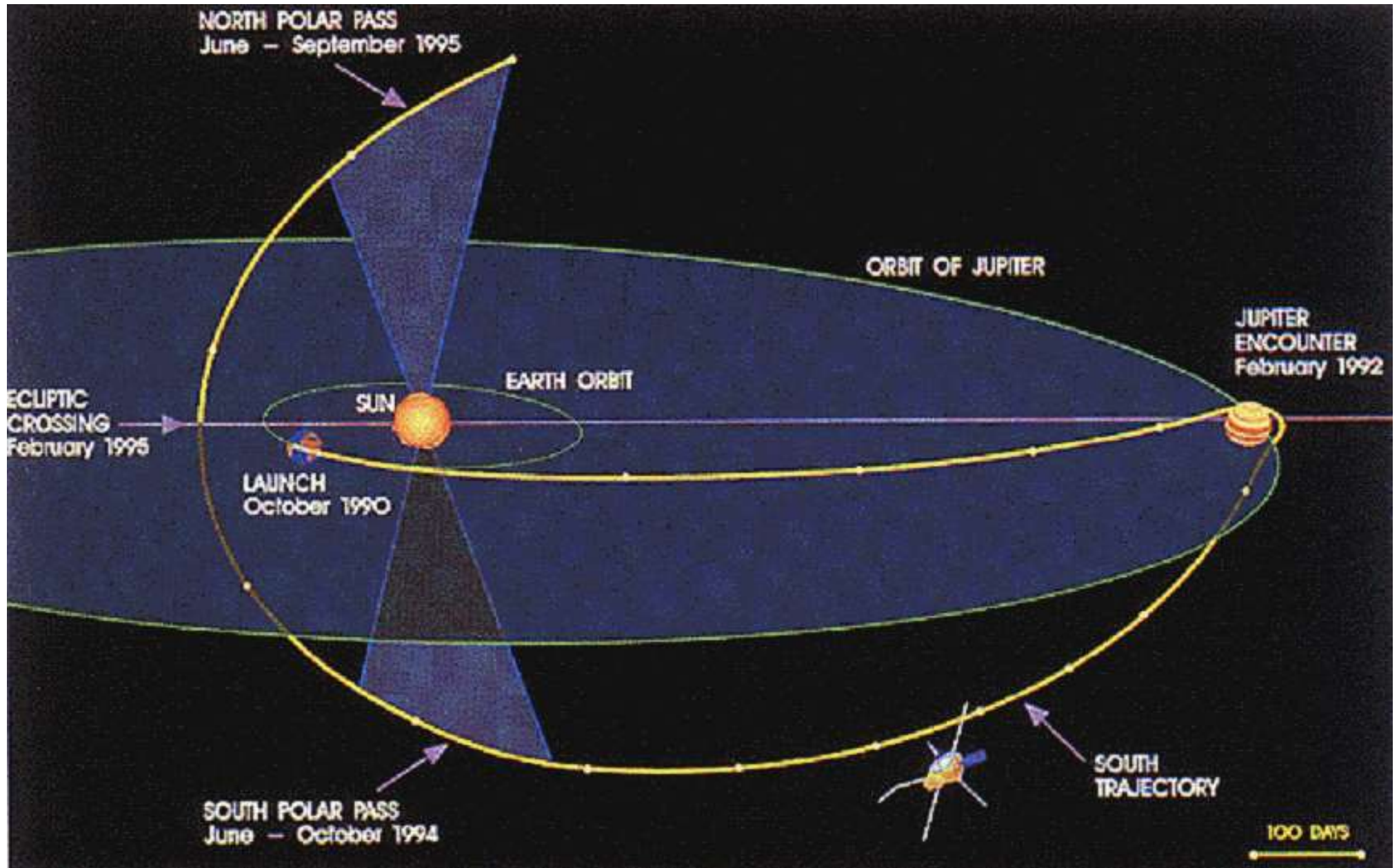
- **Eugene Parker (1958):** theoretical(!) investigation of coronal equilibrium: high temperature leads to (solar) wind (more detailed later on)
- **confirmed by**
 - Soviet measurements (Lunik2/3) with “ion-traps” (1959)
 - Explorer 10 (1961)
 - Mariner II (1962): measurement of fast and slow flows (27 day cycle -> co-rotating, related “coronal holes” and sun spots)



The solar wind – Ulysses ...



... surveying the polar regions



ULYSSES/SWOOPS

Los Alamos
Space and Atmosphere

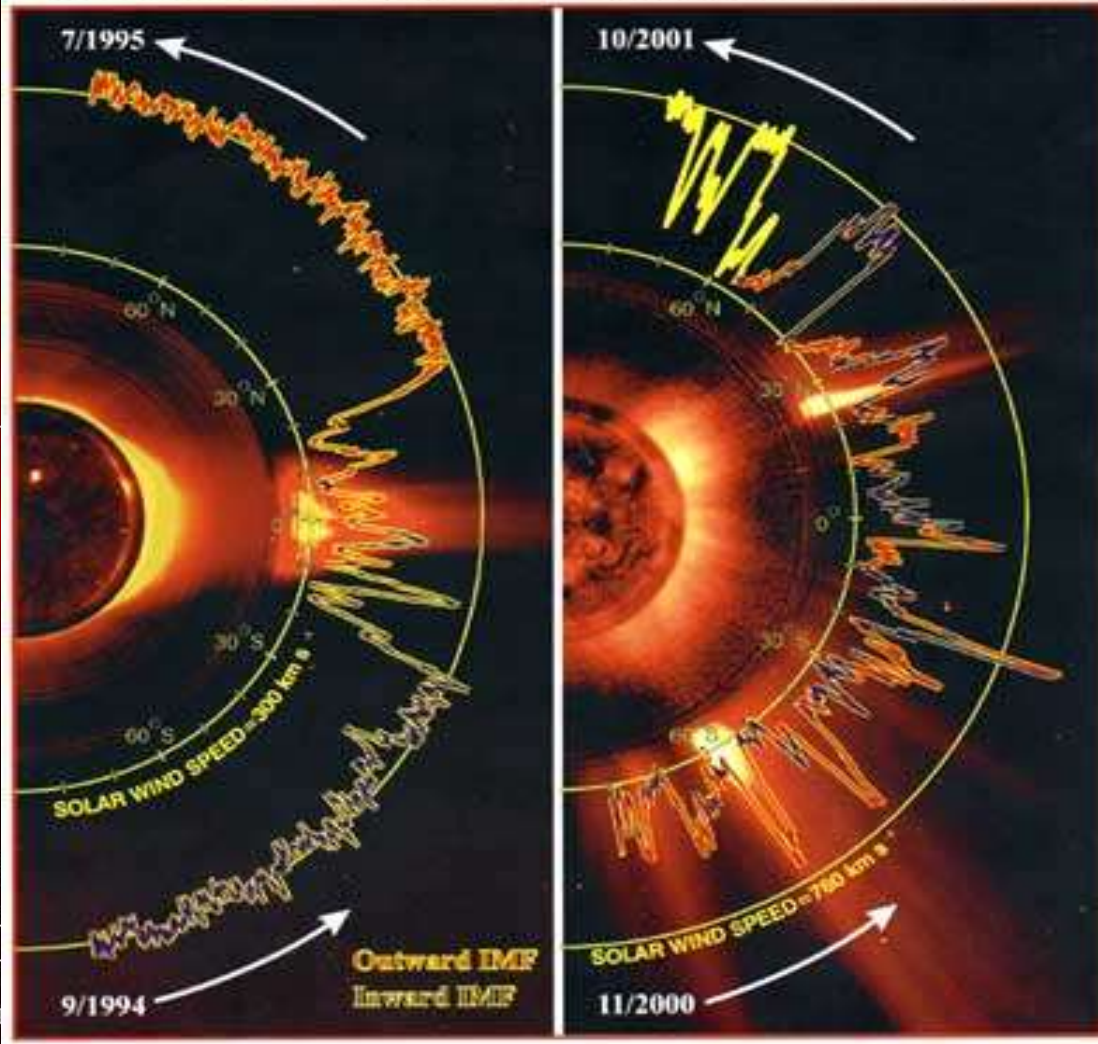
1000

Speed (km s^{-1})

ULYSSES FAST-LATITUDE SCANS

NEARING SOLAR MINIMUM

AROUND SOLAR MAXIMUM



1000

1000

ULYSSES
Imperial
● Outw
● Inwa

Outward IMF
Inward IMF

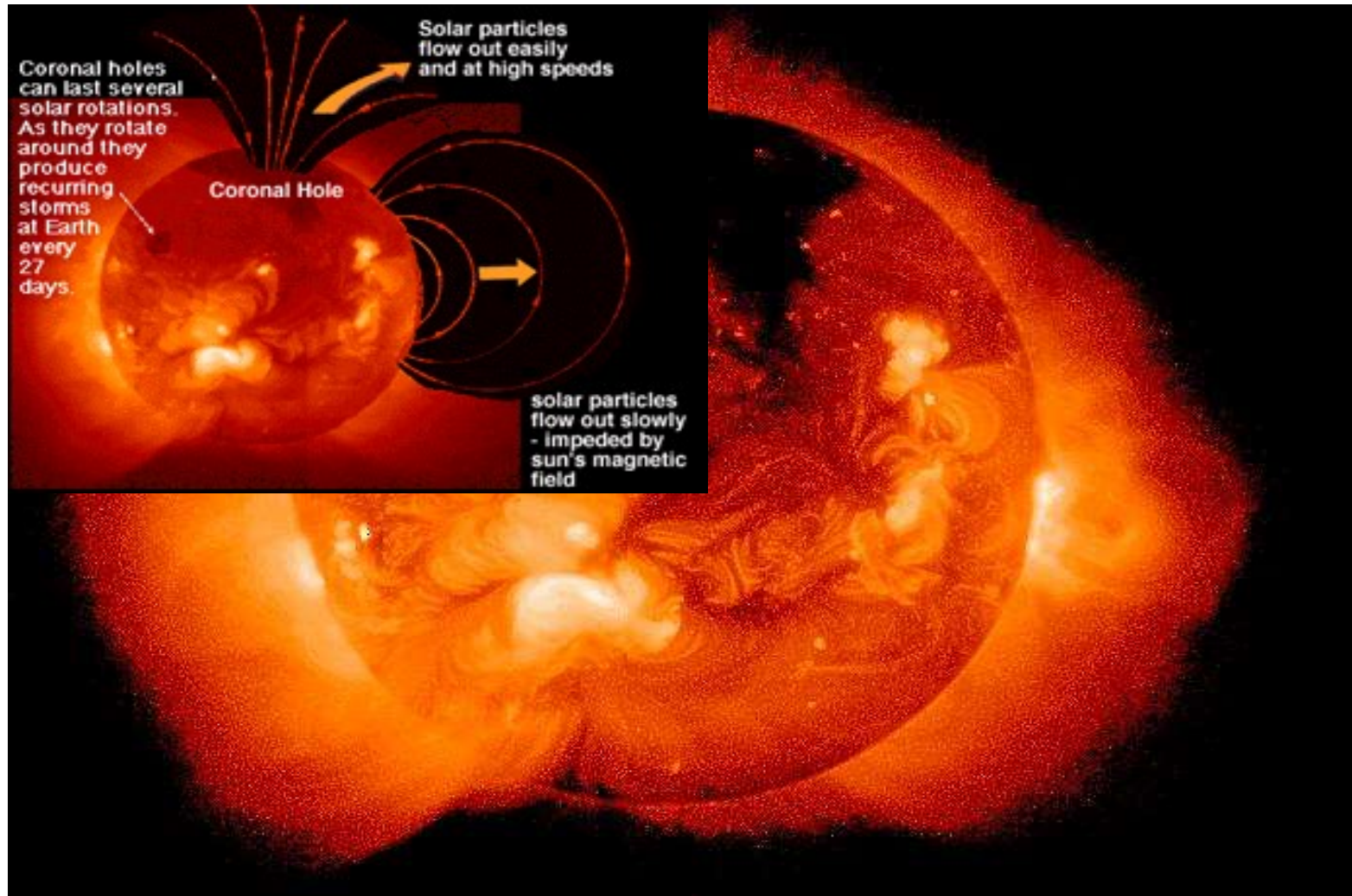
GSFC)
MK3 (HAO)
NRL)

1000

polar wind:
fast and thin

equatorial wind:
slow and dense

The solar wind – coronal holes



fast wind:
over coronal holes
(dark corona, “open”
field lines, e.g., in
polar regions)

coronal X-ray
emission

⇒

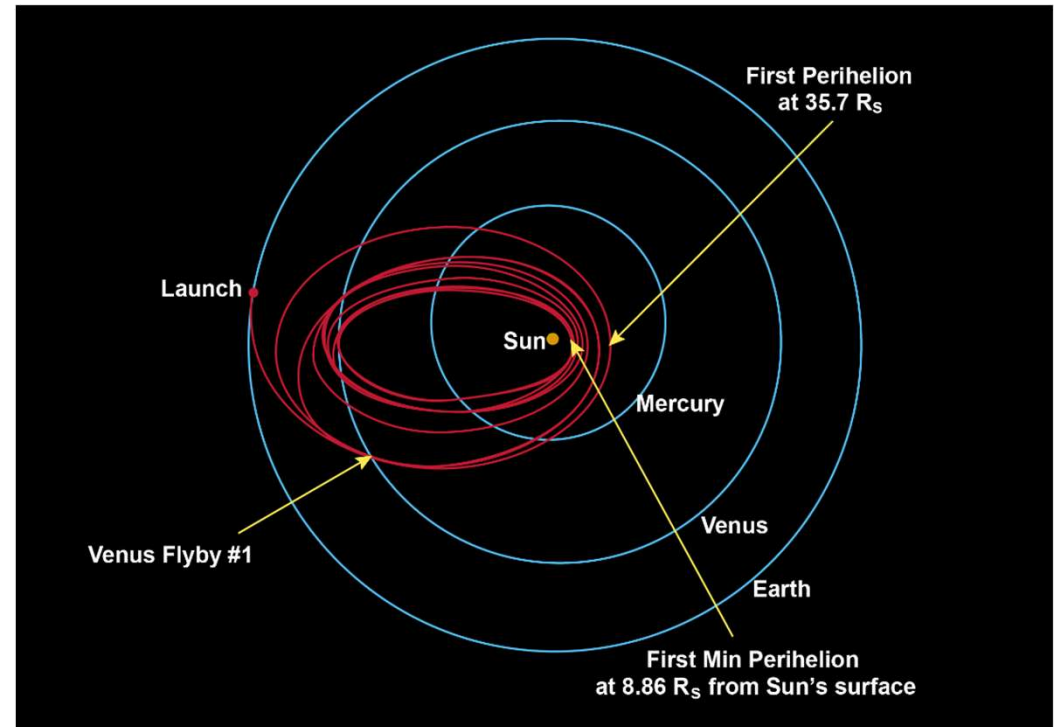
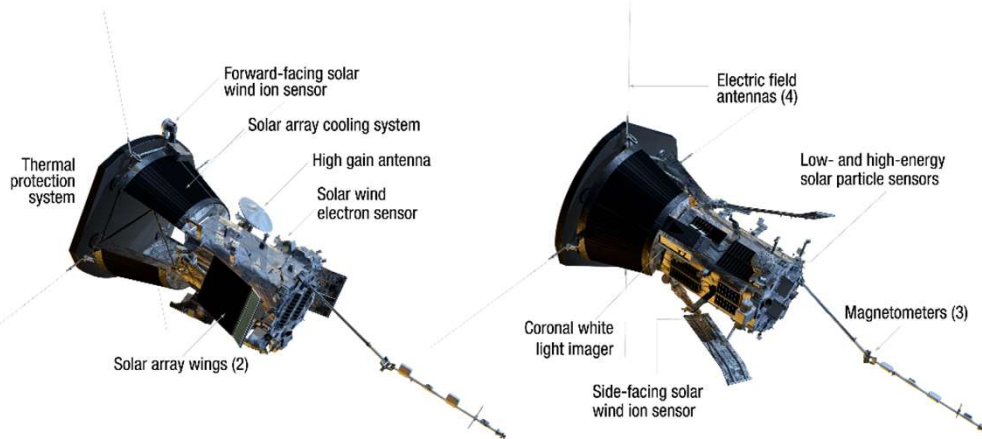
**very high
temperatures**

(Yohkoh Mission)

Parker Solar Probe

Primary objectives for the mission

- trace the energy flow, understand heating of the solar corona, study the outer corona.
- determine the structure and dynamics of the plasma and magnetic fields
- explore solar wind driving, and mechanisms that accelerate and transport energetic particles.

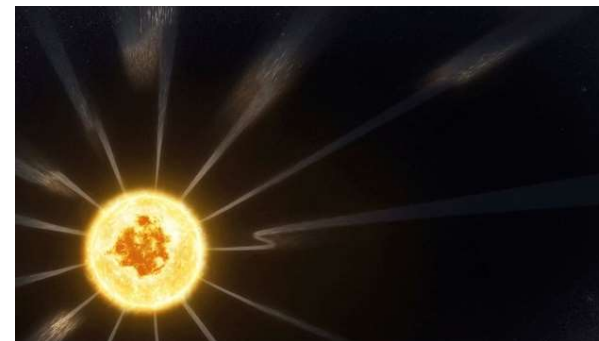


planned: 24 orbits, first perihelion on Nov. 5, 2018; seven Venus-flybys over 7 years, to decrease perihelion distance from 36 to $8.9 R_{\text{sun}}$ (6 Millionen km, with $T \sim 1100 \text{ K}$)

First results (Nov. 2019)

- wind rotates, but up to 10 times faster than expected
- high speed plasma waves, up to $c/6$, can revert direction of B-field → “switchbacks”: coherent (wind) structures
- coronal mass ejections much more irregular than expected
- dust cleared by solar wind

all material from: parkersolarprobe.jhuapl.edu



Credit: NASA's Goddard Space Flight Center/Conceptual Image Lab/Adriana Manrique Gutierrez

The sun

radius = 695,990 km = 109 terrestrial radii

mass = $1.989 \cdot 10^{30}$ kg = 333,000 terrestrial masses

luminosity = $3.85 \cdot 10^{33}$ erg/s = $3.85 \cdot 10^{20}$ MW $\approx 10^{18}$ nuclear power plants

effective temperature = 5770 °K

central temperature = 15,600,000 °K

life time approx. $10 \cdot 10^9$ years

age = $4.57 \cdot 10^9$ years

distance sun earth approx. $150 \cdot 10^6$ km ≈ 400 times earth-moon

The solar wind

temperature when leaving the corona: approx. $1 \cdot 10^6$ K

average speed approx. 400-500 km/s (travel time sun-earth approx. 4 days)

particle density close to earth: approx. 6 cm^{-3}

temperature close to earth: $\lesssim 10^5$ K

mass-loss rate: approx 10^{12} g/s (1 Megaton/s) $\approx 10^{-14}$ solar masses/year

\approx one Great-Salt-Lake-mass/day \approx one Baltic-sea-mass/year

\Rightarrow no consequence for solar evolution, since only 0.01% of total mass lost over total life time

Need mechanism which accelerates material beyond **escape velocity**:

- ✿ pressure driven winds
- ✿ radiation driven winds

Note: red giant winds still not understood, only scaling relations available (“Reimers-formula”)

remember equation of motion (conservation of momentum + stationarity, cf. Chap. 6, page 90)

$$v \frac{dv}{dr} = -\frac{1}{\rho} \frac{dp}{dr} + g^{ext} \quad (\text{in spherical symmetry}), \quad \text{and } p = \rho a^2 \quad (\text{equation of state, with isothermal sound-speed } a)$$

⇒ with mass-loss rate \dot{M} , radius r , density ρ and velocity v

$$\dot{M} = 4\pi r^2 \rho v,$$

equation of continuity:
conservation of mass

$$\left(1 - \frac{a^2}{v^2}\right) v \frac{dv}{dr} = -\frac{GM}{r^2} + g_{rad} + \frac{2a^2}{r} - \frac{da^2}{dr}$$

equation of motion:
from conservation of momentum

vel. field	grav. accel.	radiative accel.	(part of) accel. by pressure gradient
positive for $v > a$	inwards	outwards	outwards
negative for $v < a$			

$$\left(1 - \frac{a^2}{v^2}\right) v \frac{dv}{dr} = -\frac{GM}{r^2} + \cancel{g_{rad}} + \frac{2a^2}{r} - \cancel{\frac{da^2}{dr}}$$

vel. field
grav. accel.
radiative accel.
“pressure”

The solar wind as a proto-type for pressure driven winds

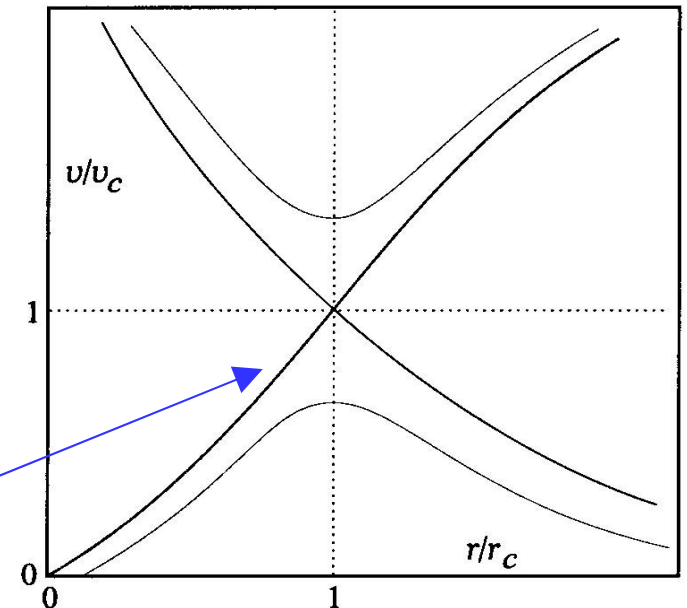
- present in stars which have an (extremely) hot corona ($T \approx 10^6$ K)
- with $g_{rad} \approx 0$ and $T \approx \text{const}$, the rhs of the equation of motion changes sign at

$$r_c = \frac{GM}{2a^2}; \quad \text{with } a (T=1.5 \cdot 10^6 \text{ K}) \approx 160 \text{ km/s,}$$

we find for the sun $r_c \approx 3.9 R_{sun}$

and obtain four possible solutions for v/v_c ("c" = critical point)

- only one (the "transonic") solution compatible with observations
- pressure driven winds as described here rely on the presence of a hot corona (large value of a !)
- Mass-loss rate $\dot{M} \approx 10^{-14} M_{sun} / \text{yr}$, terminal velocity $v_\infty \approx 500 \text{ km/s}$
- has to be heated (dissipation of acoustic and magneto-hydrodynamic waves)
- not completely understood so far



accelerated by radiation pressure:

$$\left(1 - \frac{a^2}{v^2}\right) v \frac{dv}{dr} = -\frac{GM}{r^2} + g_{rad} + \underbrace{\frac{2a^2}{r} - \frac{da^2}{dr}}_{\text{important only in lowest wind}}$$

pressure terms only of secondary order
($a \approx 20$ km/s for hot stars,
 ≈ 3 km/s for cool stars)

- ★ cool stars (AGB): major contribution from **dust** absorption; coupling to “gas” by viscous drag force (gas - grain collisions)

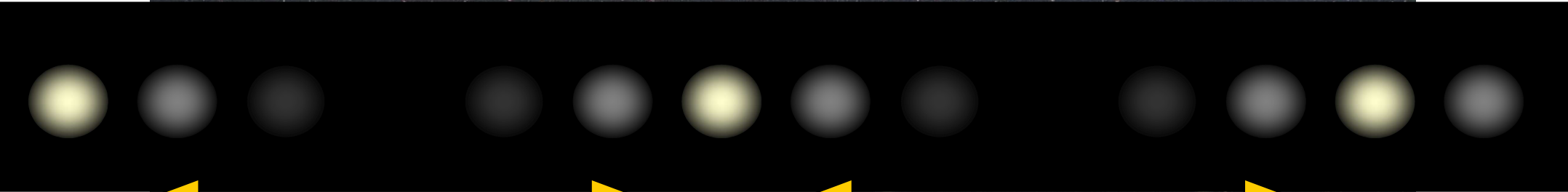
$$\dot{M} \approx 10^{-6} M_{\text{sun}} / \text{yr}, v_{\infty} \approx 20 \text{ km/s}$$

- ★ hot stars: major contribution from **metal line** absorption; coupling to bulk matter (H/He) by Coulomb collisions

$$\dot{M} \approx 10^{-6} \dots 10^{-5} M_{\text{sun}} / \text{yr}, v_{\infty} \approx 2,000 \text{ km/s}$$



dusty
winds

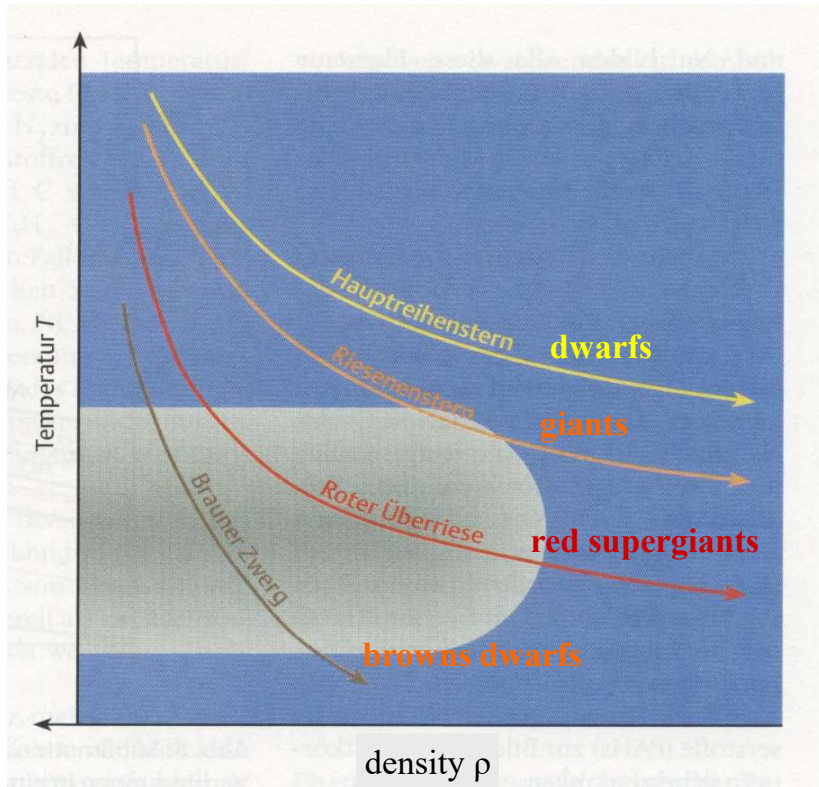


(David Fabricius, 1596)

- brightness variations by 5.5 mag (from 3.5 to 9), corresponding to a factor of 160

Eckhardt Slawik





Material on this and following pages from
Chr. Helling, *Sterne und Weltraum*,
Feb/March 2002

dust: approx. 1% of ISM, 70% of this fraction formed in the winds of AGB-stars (cool, low-mass supergiants)

Red supergiants are located in dust-forming “window”

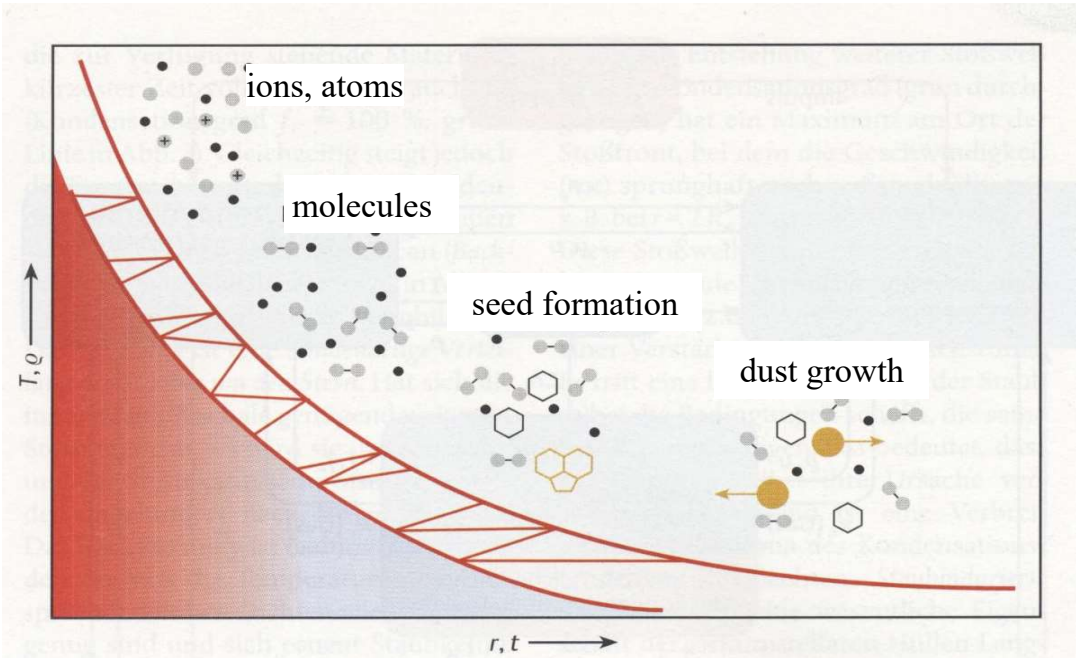
transition from gaseous phase to solid state possible only in **narrow range of temperature and density:**

gas density must be high enough and temperature low enough to allow for the chemical reactions:

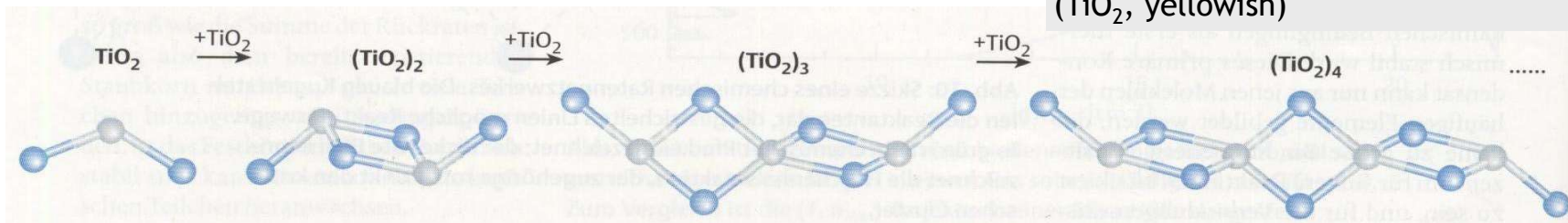
- sufficient number of dust forming molecules required
- the dust particles formed have to be thermally stable

Growth of dust in matter outflow

- decrease of density and temperature
- more and more complex structures are forming
- dust: macroscopic, solid state body, approx. 10^{-7} m (1000 Angstrom), 10^9 atoms



terrestrial, macroscopic rutile crystal (TiO_2 , yellowish)

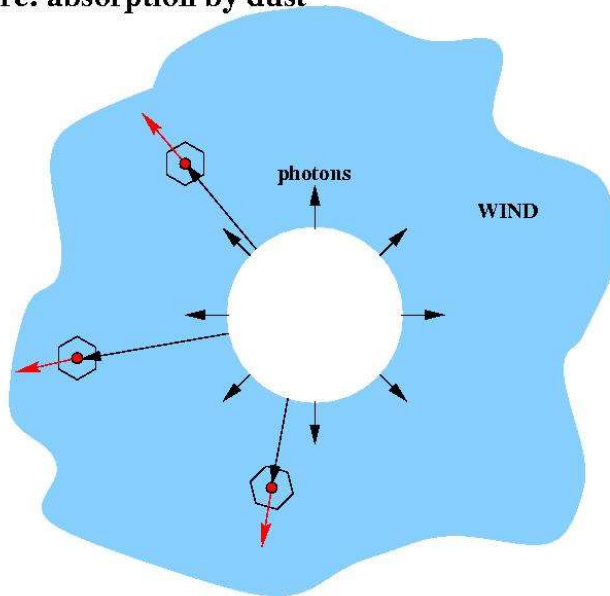


first steps of a linear reaction chain, forming the seed of $(\text{TiO}_2)_N$

Dust-driven winds: the principle

The principle of radiation driven winds

here: absorption by dust



- star emits photons
- photons absorbed by dust
- momentum transfer accelerates dust
- gas accelerated by viscous drag force due to gas-dust collisions

acceleration

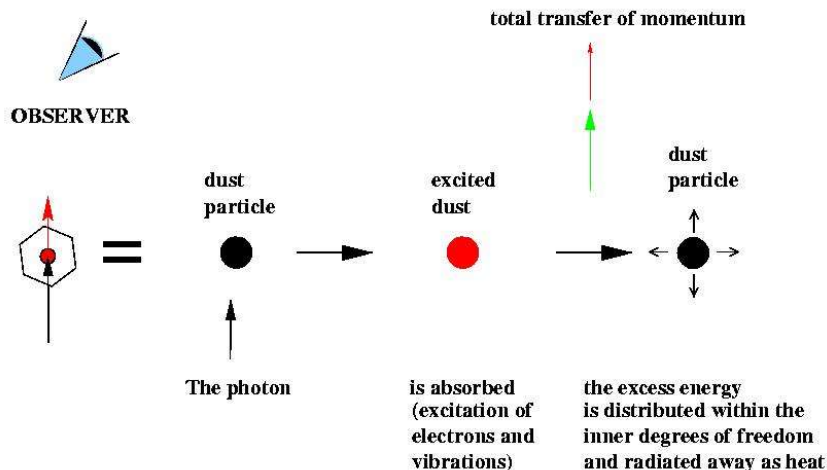
proportional to number of photons, i.e.,
proportional to *stellar luminosity* L

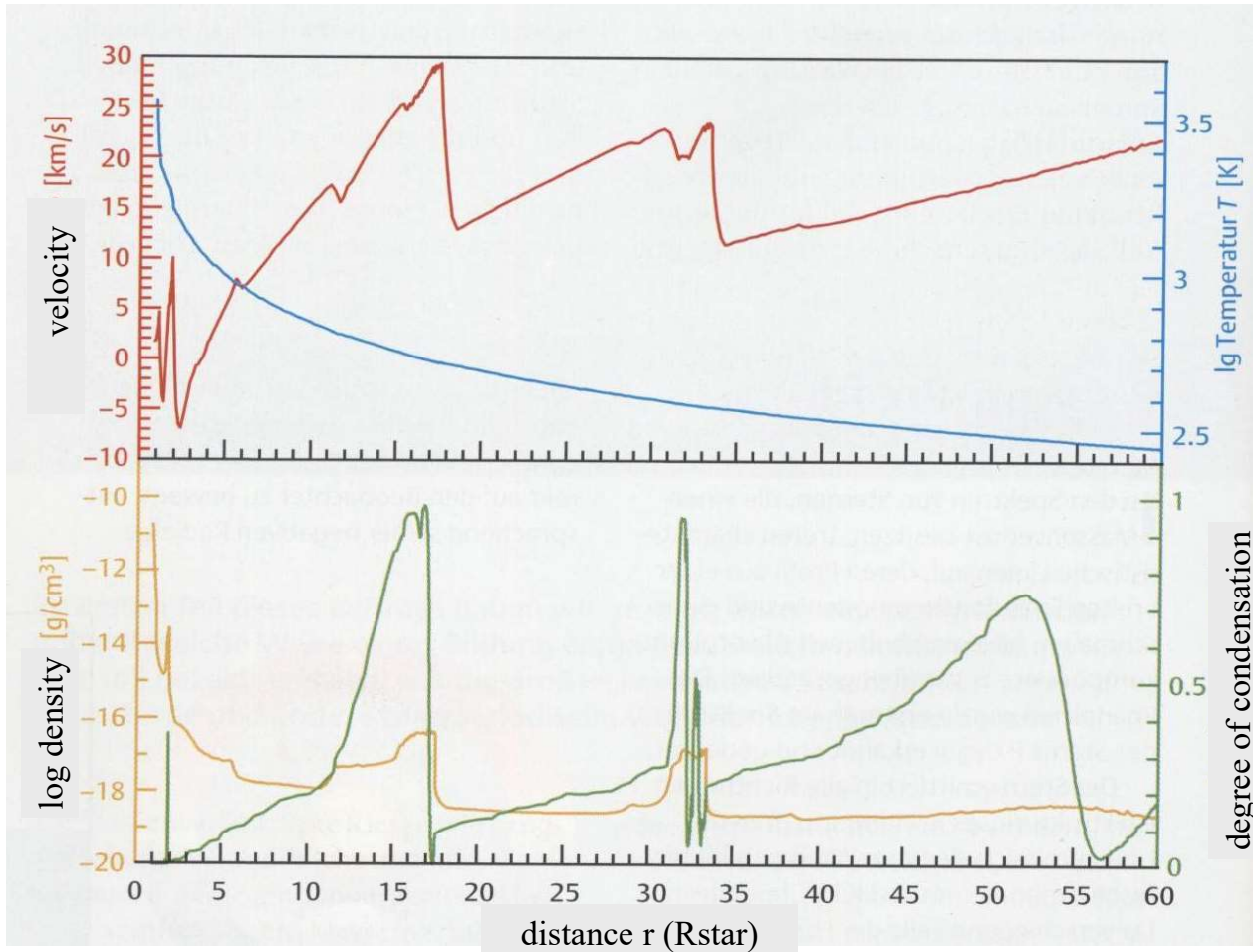
⇒ mass-loss rate $\propto L$

dust driven winds at tip of AGB responsible
for ejection of envelope

⇒ Planetary Nebulae

winds from **massive red supergiants** still
not explained, but probably similar mechanism



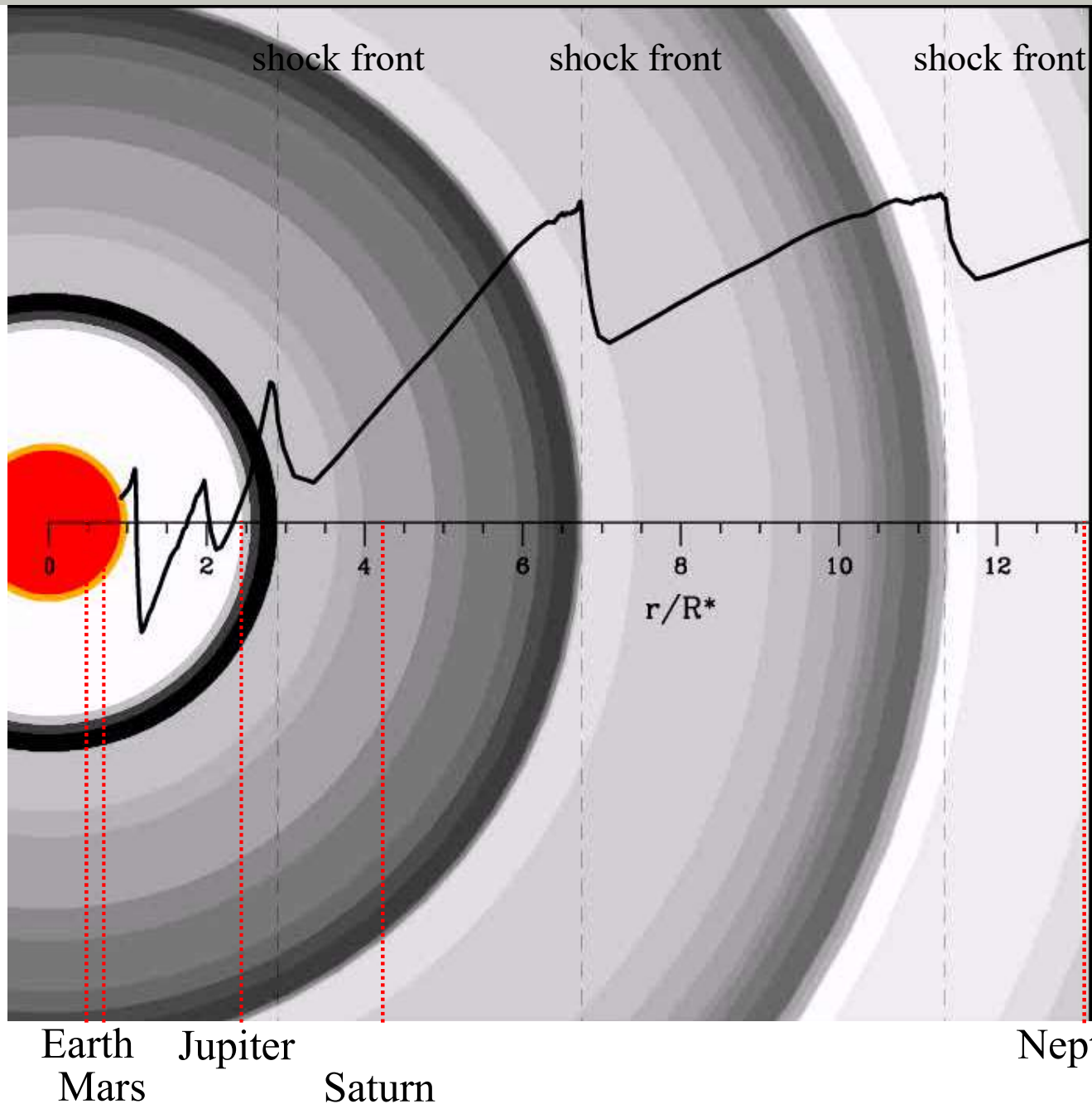


snapshot of a time-dependent hydro-simulation of a carbon-rich circumstellar envelope of an AGB-star. Model parameters similar to next slide.

- star (“surface”) pulsates,
- sound waves are created,
- steepen into shocks;
- matter is compressed,
- dust is formed
- and accelerated by radiation pressure

dust shells are blown away, following the pulsational cycle

- ⇒ periodic darkening of stellar disc
- ⇒ **brightness variations**



dark colors: dust shells

velocity

simulation of a
dust-driven wind
(previous working group
E. Sedlmayr, TU Berlin)

$$T = 2600 \text{ K}, L = 10^4 L_{\text{sun}},$$

$$M = 1 M_{\text{sun}}, \Delta v = 2 \text{ km/s}$$

	The sun	Red AGB-stars	Blue supergiants
mass [M_{\odot}]	1	1 ... 3	10...100
luminosity [L_{\odot}]	1	10^4	10^5 ... 10^6
stellar radius [R_{\odot}]	1	400	10...200
effective temperature [K]	5570	2500	10^4 ... $5 \cdot 10^4$
wind temperature [K]	10^6	1000	8000...40000
mass loss rate [M_{\odot} /yr]	10^{-14}	10^{-6} ... 10^{-4}	10^{-6} ... few 10^{-5}
terminal velocity [km/s]	500	30	200...3000
life time [yr]	10^{10}	10^5	10^7
total mass loss [M_{\odot}]	10^{-4}	$\gtrsim 0.5$	up to 90% of total mass

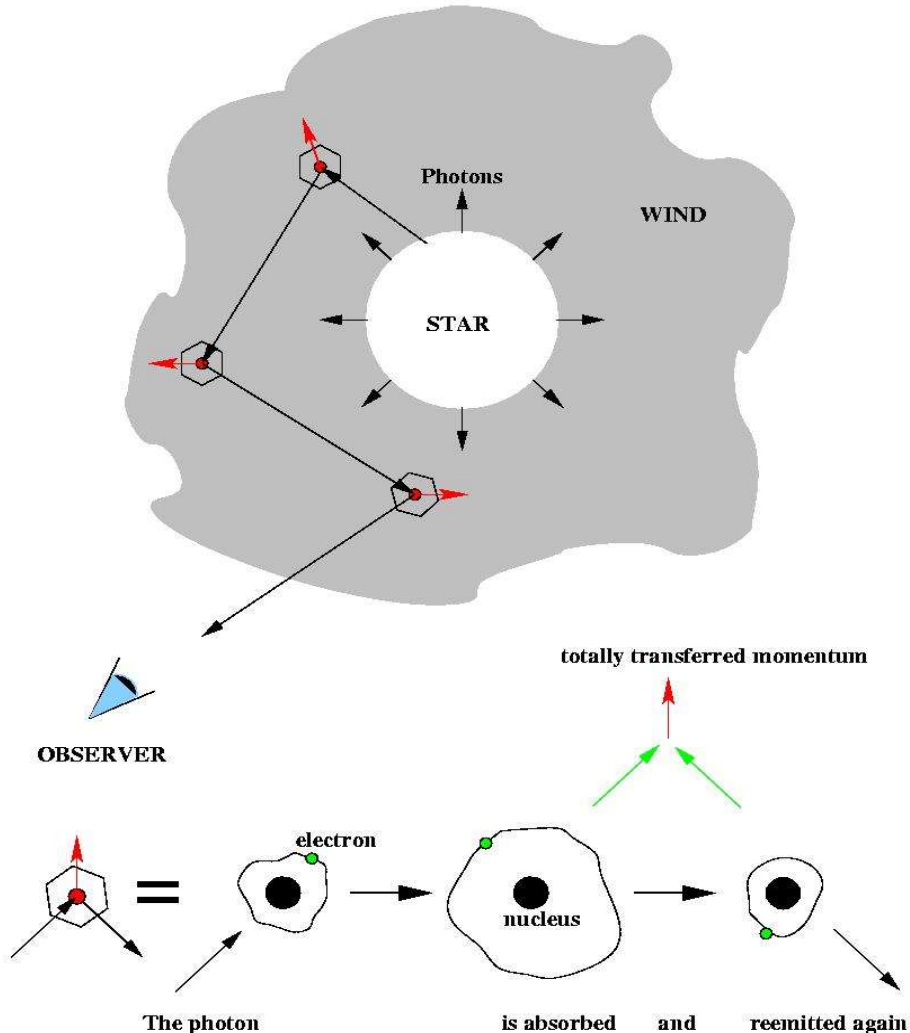
Massive stars determine energy (kinetic and radiation)
and momentum budget of surrounding ISM



Bubble Nebula
(NGC 7635)
in Cassiopeia

wind-blown
bubble around
BD+602522
(O6.5III(f))

The principle of radiatively driven winds



- accelerated by radiation pressure in lines
 $M \approx 10^{-7} \dots 10^{-5} M_{\text{sun}} / \text{yr}$, $v_{\infty} \approx 200 \dots 3,000 \text{ km/s}$
- momentum transfer from accelerated species (ions) to bulk matter (H/He) via Coulomb collisions

Prerequisites for radiative driving

- large number of photons => high luminosity
 $L \propto R_*^2 T_{\text{eff}}^4$ => supergiants or hot dwarfs
- line driving:
 large number of lines close to flux maximum (typically some $10^4 \dots 10^5$ lines relevant) with high interaction probability
 (=> mass-loss dependent on metal abundances)
- line driven winds important for chemical evolution of (spiral) Galaxies, in particular for starbursts
- transfer of momentum (=> can induce *star formation*, hot stars mostly in *associations*), energy and nuclear processed material to surrounding environment
- dramatic impact on stellar evolution of massive stars (mass-loss rate vs. life time!)

pioneering investigations by

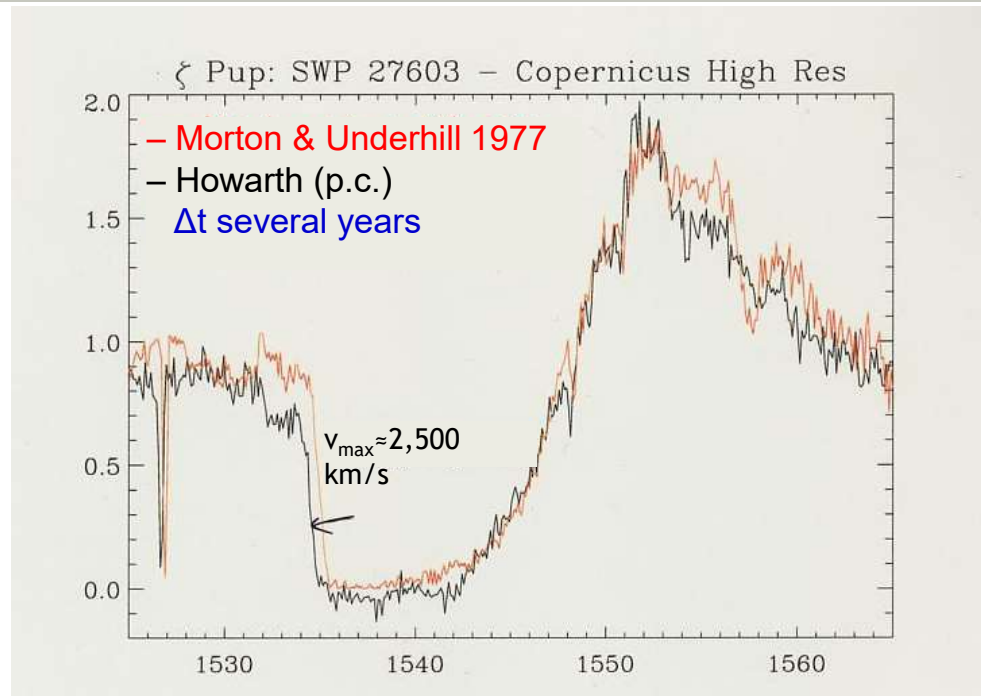
Lucy & Solomon, 1970, ApJ 159

Castor, Abbott & Klein, 1975, ApJ 195 (CAK)

reviews by Kudritzki & Puls, 2000, ARAA 38

Puls et al. 2008 A&Arv 16, issue 3

9.1 Radiative line driving and line-statistics



- **Observational findings:**
massive star have outflows, at least quasi-stationary
- only small, in NO WAY dominant variability of global quantities (\dot{M} , v_{∞})
- \dot{M} , v_{∞} , $v(r)$ have to be explained
- diagnostic tools have to be developed
- predictions have to be given

Equation of motion in the standard model

Hydro-equations

$$\frac{\partial}{\partial t} \rho + \nabla \cdot (\rho \mathbf{v}) = 0 \quad \text{continuity equation}$$

$$\frac{\partial}{\partial t} (\rho \mathbf{v}) + \nabla \cdot (\rho \mathbf{v} \mathbf{v}) = -\nabla p + \rho \mathbf{a}^{\text{ext}} \quad \text{momentum equation}$$

⇒ (use continuity equation)

$$\frac{\partial}{\partial t} \mathbf{v} + (\mathbf{v} \cdot \nabla) \mathbf{v} = -\frac{1}{\rho} \nabla p + \mathbf{a}^{\text{ext}} \quad \text{equation of motion}$$

⇒ (with $\frac{\partial}{\partial t} = 0$, 1-D spherically symmetric)

$$4\pi r^2 \rho(r) v(r) = \text{const} = \dot{M} \quad \text{mass-loss rate}$$

$$v \frac{dv}{dr} = -\frac{1}{\rho(r)} \frac{dp}{dr} + a^{\text{ext}}(r)$$

$$p = NkT \quad (\text{equation of state}) = \frac{kT}{\mu m_{\text{H}}} \rho = v_s^2 \rho$$

v_s isothermal sound speed, μ mean molecular weight

$$\Rightarrow v \left(1 - \frac{v_s^2}{v^2} \right) \frac{dv}{dr} = \frac{2v_s^2}{r} - \frac{dv_s^2}{dr} + a^{\text{ext}}$$

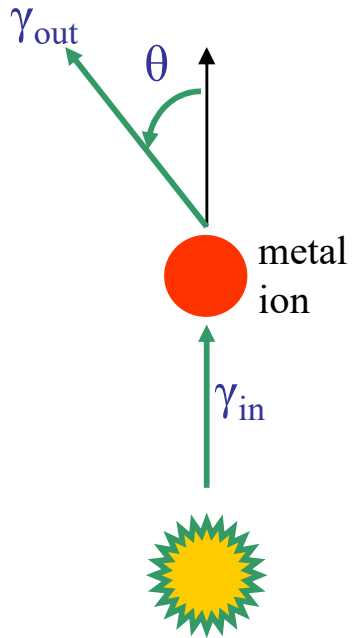
(assumption here: $v_s^2 \sim T$ known)

$$a^{\text{ext}}(r) = -\frac{GM}{r^2} (1 - \Gamma) + g_{\text{Rad}}^{\text{true cont}}(r) + g_{\text{Rad}}^{\text{line}}(r)$$

$$\Gamma = \frac{g_{\text{Rad}}^{\text{Thomson}}(r)}{g_{\text{grav}}(r)} = \text{const} \text{ is Eddington factor,}$$

corrects for radiative acceleration due to Thomson scattering

Principle idea of line acceleration



$$\left. \begin{array}{l} \cos \theta_{in} \approx 1 \\ \text{isotropic reemission} \\ \langle \cos \theta_{out} \rangle = 0 \end{array} \right\} \langle \Delta P \rangle = \frac{h\nu_{in}}{c}$$

$$\Rightarrow g_{rad} = \frac{\langle \Delta P \rangle_{tot}}{\Delta t \Delta m} = \frac{\sum_{\text{all lines}} \langle \Delta P \rangle_i}{\Delta t \Delta m}$$

a) scattering of continuum light in resonance lines

$$\begin{aligned} \Delta P_{radial} &= P_{in} - P_{out} \\ &= \frac{h}{c} (\underbrace{\nu_{in} \cos \theta_{in}}_{\text{absorption}} - \underbrace{\nu_{out} \cos \theta_{out}}_{\text{reemission}}) \end{aligned}$$

b) momentum transfer from metal ions (fraction 10^{-3}) to bulk plasma (H/He) via Coulomb collisions (see Springmann & Pauldrach 1992)

- velocity drift of ions w.r.t. H/He is compensated by frictional force as long as $v_D/v_{th} < 1$ (linear regime, “Stokes” law)

$$R_{ij}^{\text{fric}} \sim G(x_{ij}) \quad x_{ij} = \sqrt{A_{ij}} \frac{|v_i - v_j|}{v_{\text{th}}(\text{prot})} \quad A_{ij} \text{ is reduced mass}$$

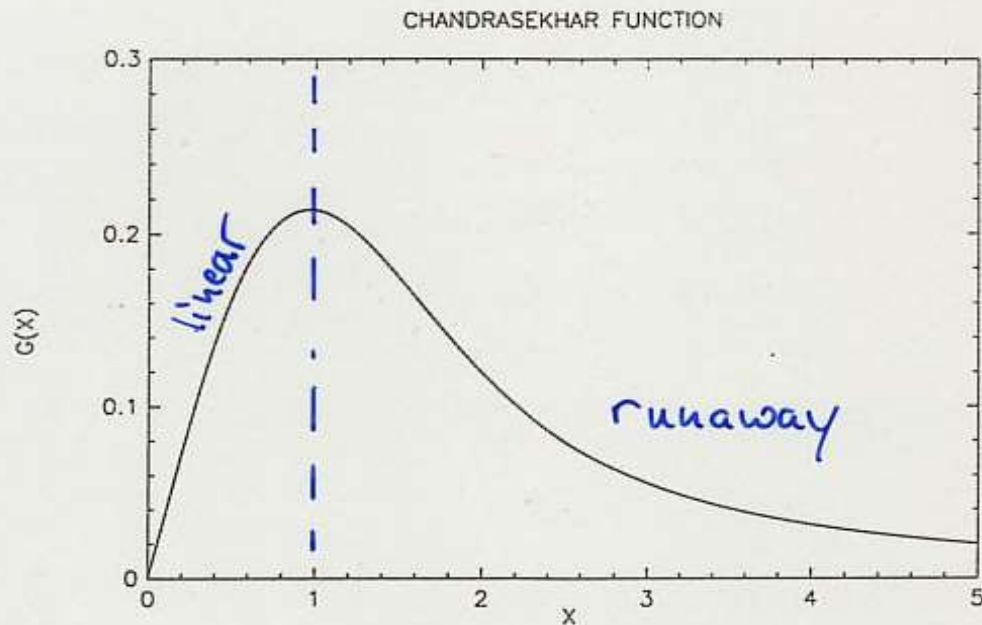


Fig. 1. The Chandrasekhar function $G(x)$ which gives the frictional force on test particles by field particles of unit density for an inverse square law of Coulomb interaction. The variable x is essentially the ratio of the velocity of the test particles in the rest frame of the field particles to the thermal velocity of the field particles (see text). The limiting cases are $G(x) \sim x$ for $x \ll 1$ and $G(x) \sim x^{-2}$ for $x \gg 1$

approximate description (supersonic regime)
by linear diffusion equation

$$v_{\text{ion}} \frac{d}{dr} v_{\text{ion}} = g_{\text{Rad}}^{\text{ion}} - \frac{GM}{r^2} - \frac{w}{\tau_{ib}} \quad w \text{ drift velocity}$$

$$v_{\text{bulk}} \frac{d}{dr} v_{\text{bulk}} = -\frac{GM}{r^2} + \frac{w}{\tau_{bi}} \quad \text{bulk} \approx \text{H/He,}$$

τ relaxation time between collisions

in order to obtain one-component fluid,

$$v_{\text{ion}} \frac{dv_{\text{ion}}}{dr} = v_{\text{bulk}} \frac{dv_{\text{bulk}}}{dr}$$

$$\Rightarrow w = g_{\text{Rad}}^{\text{ion}} \left(\frac{1}{\tau_{ib}} + \frac{1}{\tau_{bi}} \right)^{-1} \approx g_{\text{Rad}}^{\text{tot}} \frac{\rho_{\text{tot}}}{\rho_{\text{ion}}} \cdot \tau \sim g_{\text{Rad}}^{\text{tot}} \frac{1}{Z} \frac{1}{\rho}$$

tot = bulk + ion, Z is metallicity

for low $\rho \sim \frac{\dot{M}}{V}$ and/or low $Z \rightarrow$ drift large \rightarrow runaway

e.g., winds of A-dwarfs, [Babel et al. 1995, A&A 301](#)

The photon-tiring limit

What is the maximum mass-loss rate that can be accelerated???

- mechanical luminosity in wind at infinity is

$$L_{\text{wind}} = \dot{M} \left(\frac{v_{\infty}^2}{2} + \frac{GM}{R} \right) = \dot{M} \left(\frac{v_{\infty}^2}{2} + \frac{v_{\text{esc}}^2}{2} \right) \quad \text{with } v_{\text{esc}} = \sqrt{\frac{2GM}{R}}$$

- maximum mass loss, if $L_{\text{wind}} = L_*$ $\Rightarrow L(\infty) = 0$, star becomes invisible

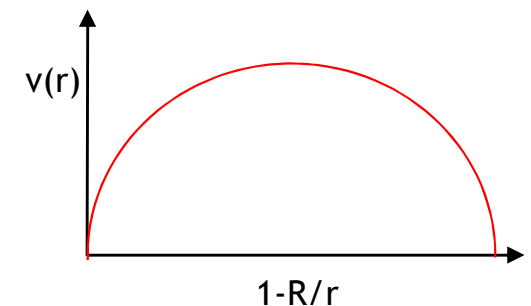
$$\dot{M}_{\text{max}} = \frac{2L_*}{v_{\infty}^2 + v_{\text{esc}}^2}$$

$$\Rightarrow \eta_{\text{max}} = \frac{\dot{M}_{\text{max}} v_{\infty}}{L/c} = \frac{2c}{v_{\infty} \left(1 + \left(\frac{v_{\text{esc}}}{v_{\infty}} \right)^2 \right)}$$

typical values: $v_{\infty} \approx 2000 \dots 3000 \text{ km/s} \approx 0.01c$, $v_{\text{esc}}/v_{\infty} \approx 1/3 \rightarrow \eta_{\text{max}} \approx 200$

\dot{M}_{tir} (Owocki & Gayley 1997) is maximum mass-loss rate when wind just escapes the gravitational potential, with $v_{\infty} \rightarrow 0$

$$\dot{M}_{\text{tir}} = \frac{2L_*}{v_{\text{esc}}^2} = 0.032 \frac{M_{\odot}}{\text{yr}} \frac{L_*}{10^6 L_{\odot}} \frac{R}{R_{\odot}} \frac{M_{\odot}}{M} = 0.0012 \frac{M_{\odot}}{\text{yr}} \Gamma_c \frac{R}{R_{\odot}}$$



Calculation of the line force

crucial point of the problem

$$g_{\text{Rad}}^{\text{line}} = \frac{4\pi}{c\rho} \frac{1}{2} \int_0^\infty d\nu \int_{-1}^1 \mu d\mu \left[\chi_\nu^{\text{line}}(r, \mu) I_\nu(r, \mu) - \eta_\nu^{\text{line}}(r, \mu) \right]$$

absorbed emitted

→ (in single-line approximation: no interaction of different lines)

$$g_{\text{Rad}}^{\text{line}} = \frac{2\pi}{c\rho} \sum_{\text{lines } i} \int_{\text{line}} \int_{-1}^1 d\nu \mu d\mu \chi_\nu^i(r, \mu) I_\nu^i(r, \mu)$$

- two quantities to be known
 - force/line in response to χ_ν
 - distribution of lines with χ_ν and ν

The force per line

- super-simplified
- simplified: “Sobolev approximation” :
 - assume that opacities and source functions are constant inside τ -integral,
 - i.e., over Doppler-shifted profile function
 - analytic solution possible, purely local
- “exact”:
 - comoving frame, special cases
 - observer’s frame, instability

Super-simplified theory

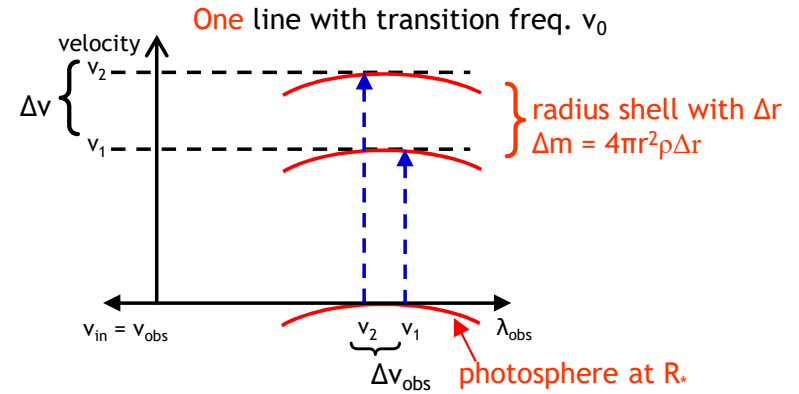
interaction with line at ν_0 , when comoving frame frequency of photon starting at R_* with ν_{obs} is equal to ν_0

(finite profile width neglected, interaction probability = 1)

$$\nu_{\text{CMF}} = \nu_{\text{obs}} - \frac{\nu_0 v(r)}{c} =: \nu_0 \quad (\text{Doppler shift, radial photons, } \mu=1, \text{ assumed})$$

$$\left. \begin{aligned} \nu_0 &= \nu_1^{\text{obs}} - \frac{\nu_0}{c} v_1(r) \\ \nu_0 &= \nu_2^{\text{obs}} - \frac{\nu_0}{c} v_2(r) \end{aligned} \right\} \text{scattering at larger } v \text{ requires 'bluer' photons}$$

$$\Rightarrow \Delta \nu_{\text{obs}} = \frac{\nu_0}{c} \Delta v$$



Number of photons in interval $[\nu_1^{\text{obs}}, \nu_2^{\text{obs}} = \nu_1^{\text{obs}} + \Delta \nu_{\text{obs}}]$ per unit time

$$\frac{N_\nu \Delta \nu}{\Delta t} = \frac{L_\nu \Delta \nu}{h \nu_{\text{obs}}} \Rightarrow (g_{\text{Rad}} = \frac{\Delta P}{\Delta t \Delta m})$$

$$g_{\text{Rad}} = \frac{h \nu_{\text{obs}}}{c} \cdot \frac{L_\nu \Delta \nu}{h \nu_{\text{obs}}} \cdot \frac{1}{\Delta m} = (\Delta \nu = \frac{\nu_0}{c} \Delta v)$$

$$= \frac{L_\nu \nu_0}{c^2} \frac{\Delta v}{\Delta r} \frac{1}{4 \pi r^2 \rho} \propto \frac{d\nu}{dr} \frac{1}{r^2 \rho}$$

Why $g_{\text{rad}} \propto dv/dr$?

shell of matter with spatial extent Δr ,

and velocity $v_0 + \left(\frac{dv}{dr}\right)_1 \Delta r$

absorption of photons at $\nu_0 \pm \delta\nu$

in frame of matter

photons must start at higher (stellar)

frequencies, are "seen" at $\nu_0 \pm \delta\nu$

in frame of matter because of Doppler-effect.

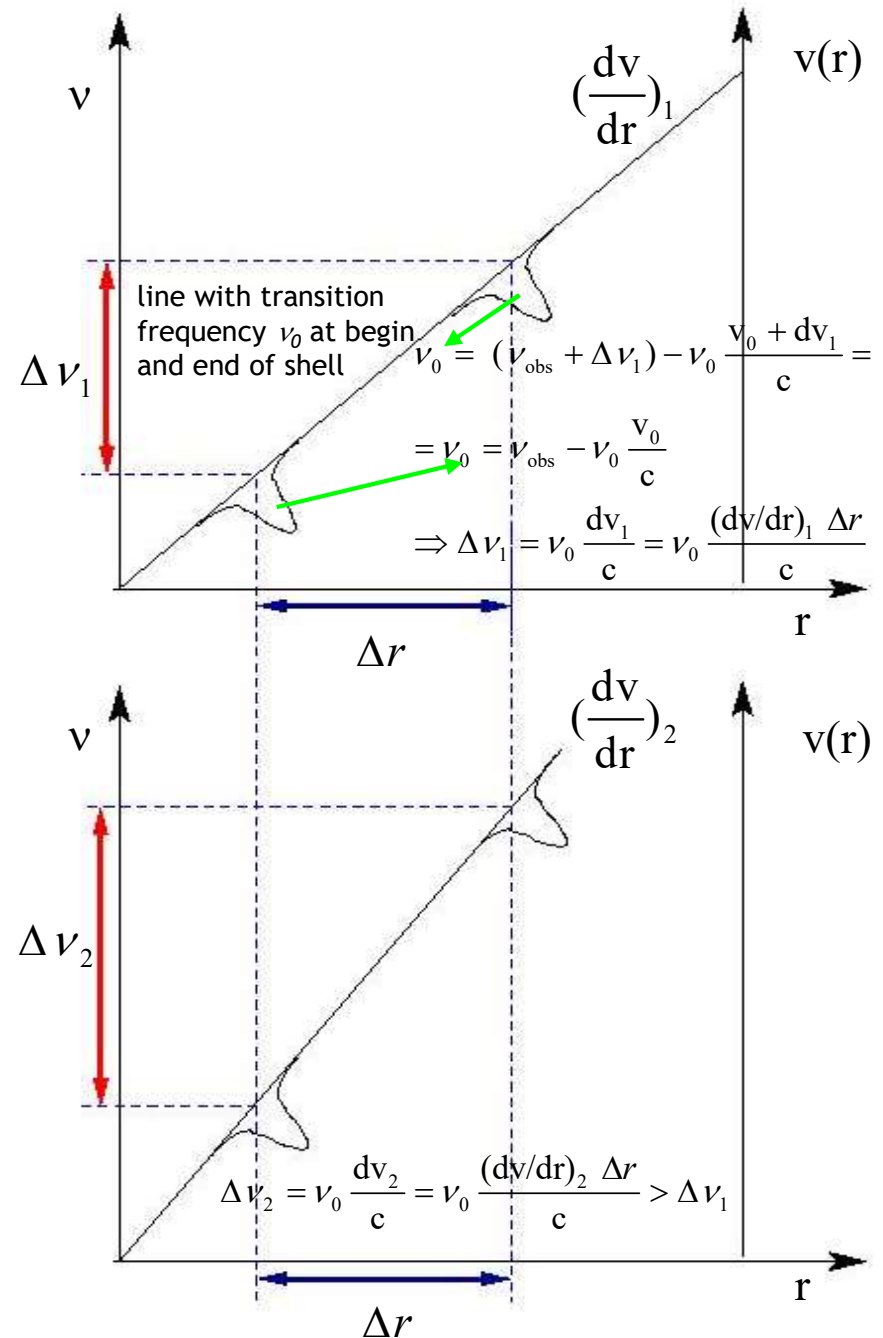
Let $\Delta\nu$ be frequency band contributing to acceleration of matter in Δr

The larger $\frac{dv}{dr}$,

- the larger $\Delta\nu$
- the more photons can be absorbed
- the larger the acceleration

$$g_{\text{rad}} \propto \frac{dv}{dr}$$

(assuming that each photon is absorbed, i.e., acceleration from optically **thick** lines)



Accounting for finite interaction probability

$$g_{\text{rad}}(\text{one line at } \nu_0) = \frac{L_\nu \nu_0}{c^2} \frac{\Delta \nu}{\Delta r} \frac{1}{4\pi r^2}$$

Assumption was: **each photon** is scattered

Then: g_{rad} independent of cross-sections, occupation numbers etc.
only dependent on hydro-structure and flux distribution

What happens if interaction probability < 1 ?

interaction probability = $1 - e^{-\tau}$, with optical depth τ

$$\tau \gg 1 \quad \text{prob} = 1$$

$$\tau \ll 1 \quad \text{prob} = \tau$$

Now: division in two classes

optically thick lines, $\tau \geq 1$ $\xrightarrow{\approx}$ prob = 1 (saturation, independent of τ)

optically thin lines $\tau < 1$ $\xrightarrow{\approx}$ prob = τ

$$\Rightarrow g_{\text{rad}}(\text{optically thin line}) = \tau \cdot g_{\text{rad}}(\text{optically thick line})$$

Line acceleration from a line ensemble

$$g_{\text{Rad}}^{\text{tot}}(r) = \sum_{\text{thick}} g_{\text{Rad}}^{\text{i}}(r) + \sum_{\text{thin}} g_{\text{Rad}}^{\text{j}}(r) =$$

$$= \frac{1}{4\pi r^2 c^2} \left(\sum_{\text{thick}} L_v v_i \underbrace{\frac{dv}{dr} \frac{1}{\rho}}_{k_1} + \sum_{\text{thin}} L_v v_i \underbrace{\frac{dv}{dr} \frac{\tau_i}{\rho}}_{k_i} \right)$$

$$\tau_i = \frac{\bar{\chi}_{\text{Li}} \lambda_i}{dv/dr} =: \frac{k_i \rho(r)}{dv/dr} \quad \left(\text{precisely: } k_i = \frac{\bar{\chi}_{\text{Li}} \lambda_i}{\rho s_c v_{\text{th}}} \right)$$

↑ optical depth of line in "Sobolev theory"

k_i is line strength $\sim \frac{\sigma_i n_i(r) \lambda_i}{\rho(r)}$ σ_i cross section,

n_i lower occup. number of line transition

k_i roughly constant in wind!!!

Which line strength corresponds to 'border' $\tau_i = 1$?

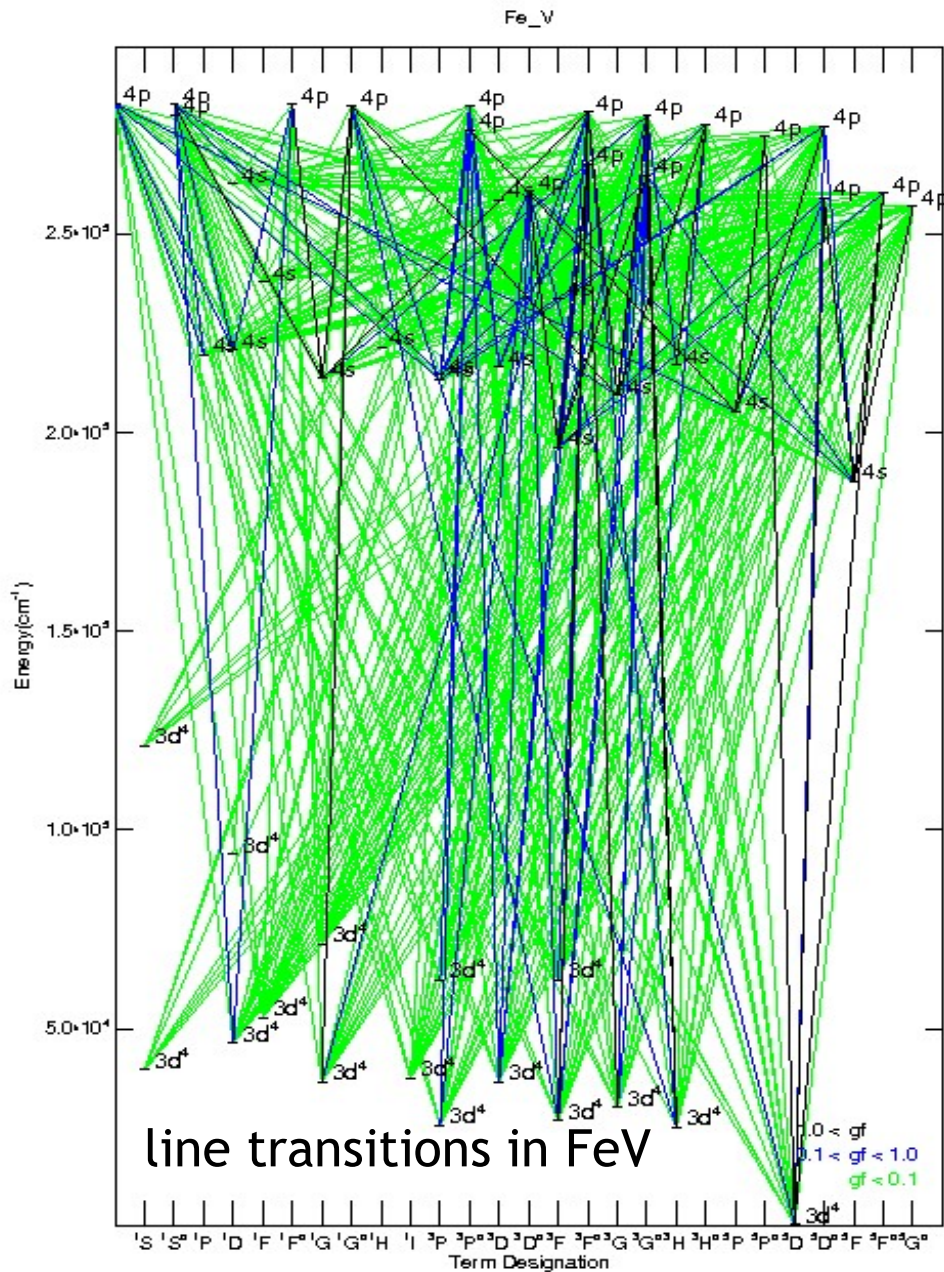
$$1 = \frac{k_1 \rho}{dv/dr} \quad \Rightarrow \quad k_1 = \frac{dv/dr}{\rho}$$

$$\Rightarrow g_{\text{Rad}}^{\text{tot}}(r) = \frac{1}{4\pi r^2 c^2} \left(k_1 \sum_{k_i > k_1} L_v v_i + \sum_{k_i < k_1} L_v v_i k_i \right)$$

optically thick optically thin

depends on hydrostruct. depends on line-strength

Millions of lines



... are present
... and needed!

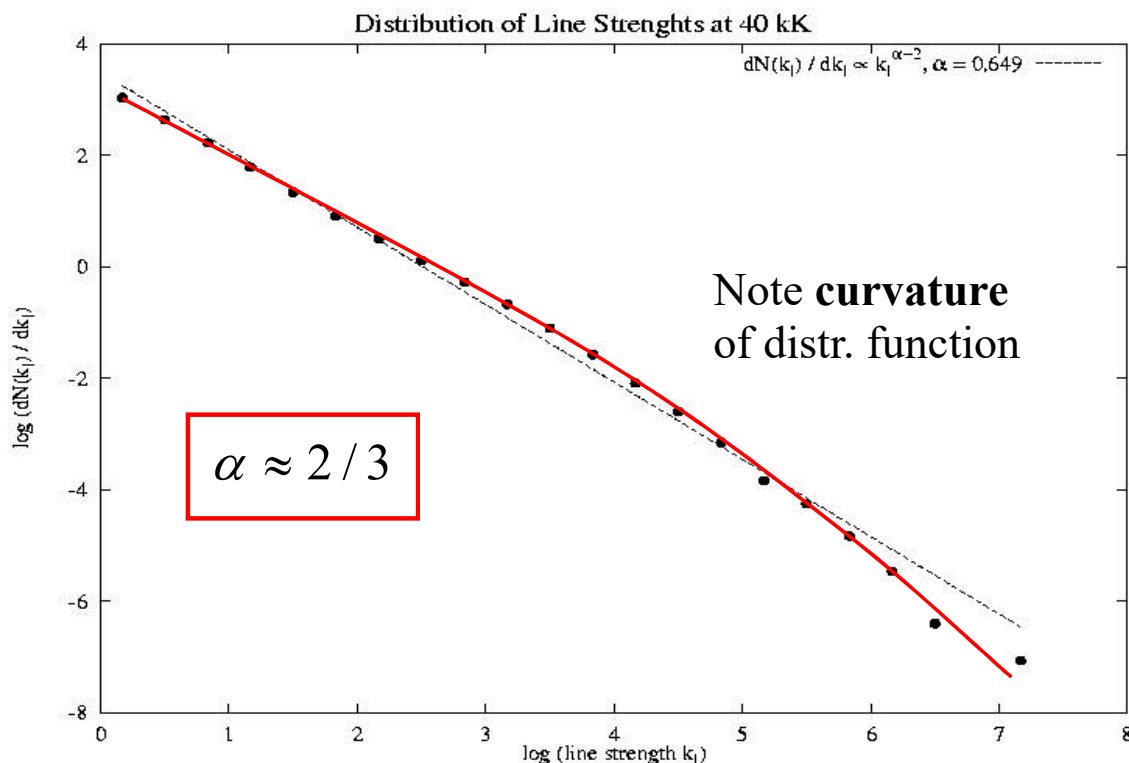
$$g_{\text{Rad}}^{\text{tot}} = \sum_{\text{all lines}} g_{\text{Rad}}^i$$

$$g_{\text{Rad}}^{\text{thin}} = L_v^i v_i k_i, \quad k_i \propto \frac{\bar{\chi}_i \lambda_i}{\rho} \quad (\text{line-strength})$$

$$g_{\text{Rad}}^{\text{thick}} = L_v^i v_i \frac{dv/dr}{\rho} \propto L_v^i v_i k_i$$

The line distribution function

- pioneering work by **Castor, Abbott & Klein** (CAK, 1975):
 - from glance at CIII atom in LTE, they suggested that ALL line-strengths follow a power-law distribution
- first realistic line-strength distribution function by Kudritzki et al. (1988)
- NOW: couple of Ml (Mega lines), 150 ionization stages (H – Zn), NLTE



$$\frac{dN(k)}{dk} = k^{\alpha-2}, \quad \alpha \approx 0.6...0.7$$

+ 2nd empirical finding:
valid in *each* frequential subinterval

$$dN(k, \nu) = -N_0 f(\nu) d\nu k^{\alpha-2} dk$$

Logarithmic plot of line-strength distribution function for an O-type wind at 40,000 K and corresponding power-law fit (see Puls et al. 2000, A&AS 141)

Force/line + line-strength distribution

$$\begin{aligned} \Rightarrow g_{\text{Rad}}^{\text{tot}}(r) &= \frac{1}{4\pi r^2 c^2} \left(k_1 \sum_{k_i > k_1} L_\nu \nu_i + \sum_{k_i < k_1} L_\nu \nu_i k_i \right) \rightarrow \\ &\rightarrow \frac{1}{4\pi r^2 c^2} \left(\int_0^\infty k_1 \int_{k_{\text{max}}}^{k_1} L(\nu) \nu dN(k, \nu) + \int_0^\infty \int_{k_1}^0 L(\nu) \nu k dN(k, \nu) \right) = \\ &= \frac{N_0 \int L(\nu) \nu f(\nu) d\nu}{4\pi r^2 c^2} \left(\underbrace{k_1 \int_{k_1}^{k_{\text{max}}} k^{\alpha-2} dk}_{k_1 \frac{1}{1-\alpha} k_1^{\alpha-1}} + \underbrace{\int_0^{k_1} k \cdot k^{\alpha-2} dk}_{\frac{1}{\alpha} k_1^\alpha} \right) \\ &= \frac{N_0 \int L(\nu) \nu f(\nu) d\nu}{4\pi r^2 c^2} \left(\frac{1}{\alpha(1-\alpha)} k_1^\alpha \right) \end{aligned}$$

⇒ final result

$$g_{\text{Rad}}^{\text{tot}}(r) = \frac{\text{const}}{4\pi r^2} k_1^\alpha$$

very 'strange' acceleration,
non-linear in dv/dr

$$k_1 = \frac{dv/dr}{\rho} = \frac{4\pi}{\dot{M}} r^2 v \frac{dv}{dr}; \quad \text{const} = \frac{N_0 \int L(\nu) \nu f(\nu) d\nu}{c^2 \alpha(1-\alpha)}$$

9.2 Theoretical predictions for line-driven winds

first hydro-solution developed by CAK 1975, ApJ 195,
improved for non-radial photons and ionization effects
by Pauldrach, Puls & Kudritzki 1986, A&A 164 and Friend
& Abbott 1986, ApJ 311

had equation of motion

$$v \left(1 - \frac{v_s^2}{v^2} \right) \frac{dv}{dr} = \frac{2v_s^2}{r} - \frac{dv_s^2}{dr} + a^{\text{ext}}(r)$$

$$a^{\text{ext}}(r) = -\frac{GM}{r^2}(1 - \Gamma) + \cancel{g_{\text{Rad}}^{\text{true}}(r)} + g_{\text{Rad}}^{\text{line}}(r)$$

$$g_{\text{Rad}}^{\text{line}}(r) = f \cdot \frac{L}{r^2} k_1^\alpha \quad \text{for 'normal' winds}$$

$$k_1 = \frac{r^2 v dv / dr}{\dot{M} / (4\pi)} \quad f = f\left(r, v, \frac{dv}{dr}, \dot{M}\right) \text{ if all subtleties included}$$

All together

$$v \left(1 - \frac{v_s^2}{v^2} \right) \frac{dv}{dr} = -\frac{GM}{r^2}(1 - \Gamma) + \frac{2v_s^2}{r} - \frac{dv_s^2}{dr} + \frac{f \cdot L}{r^2} \left(\frac{\dot{M}}{4\pi} \right)^{-\alpha} \left(r^2 v \frac{dv}{dr} \right)^\alpha$$

- non-linear differential equation
- has 'singular point' in analogy to solar wind
- $v_{\text{crit}} \gg v_s$ (100... 200 km/s)
- solution: iteration of singular point location/velocity, integration inwards and outwards

Approximate solution

(see also Kudritzki et al., 1989, A&A 219)

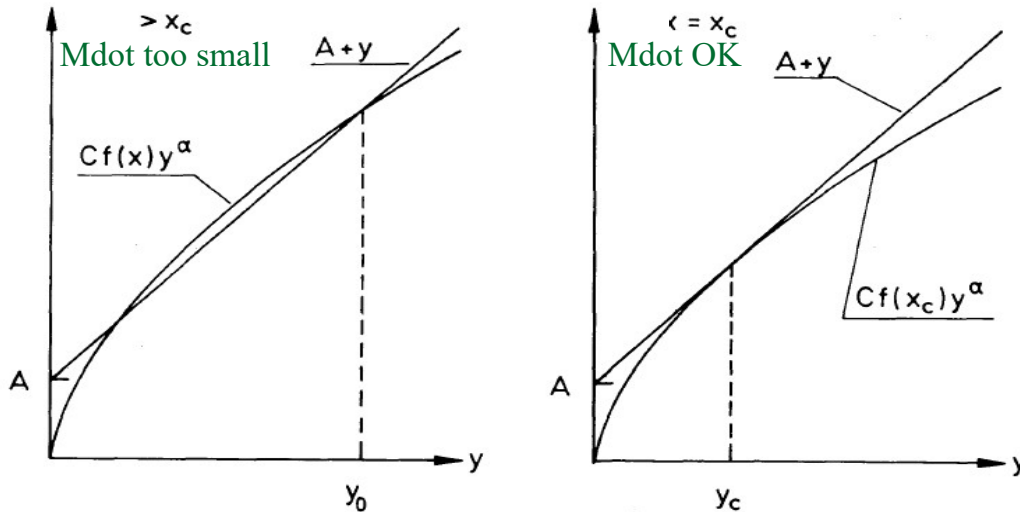
- supersonic \rightarrow pressure terms vanish
- radially streaming photons $\rightarrow f(4\pi)^\alpha \rightarrow \text{const}$

$$v \frac{dv}{dr} = -\frac{GM}{r^2}(1-\Gamma) + \frac{\text{const} \cdot L}{r^2} \dot{M}^{-\alpha} (r^2 v \frac{dv}{dr})^\alpha$$

$$\Rightarrow y + A = \text{const} \cdot L \cdot \dot{M}^{-\alpha} y^\alpha \Rightarrow y \text{ is constant}$$

$$\text{with } A = GM(1-\Gamma), \quad y = r^2 v \frac{dv}{dr}$$

graphical solution (Cassinelli et al. 1979, ARAA 17, Kudritzki et al. 1989)



$y + A = \text{const} \cdot L \cdot \dot{M}^{-\alpha} y^\alpha$ equation of motion
and equality of derivatives

$$1 = \text{const} \cdot L \cdot \dot{M}^{-\alpha} \alpha y^{\alpha-1} \text{ at critical point } y_c$$

$$\dot{M}^{-\alpha} = \frac{1}{\text{const} \cdot L \cdot \alpha} y_c^{1-\alpha}$$

in equation of motion at critical point

$$y_c + A = \frac{1}{\alpha} y_c, \quad \text{i.e., } y_c \left(1 - \frac{1}{\alpha}\right) = -GM(1-\Gamma)$$

$$y_c = \frac{\alpha}{1-\alpha} GM(1-\Gamma) = y$$

finally ...

for unique solution, derivatives have to be EQUAL!

Scaling relations for line-driven winds (without rotation)

- $\dot{M} \propto N_{\text{eff}}^{\frac{1}{\alpha'}} L^{\frac{1}{\alpha'}} (M(1-\Gamma))^{1-\frac{1}{\alpha'}}$ scaling law for \dot{M}
- $r^2 v \frac{dv}{dr} = \frac{\alpha}{1-\alpha} GM(1-\Gamma)$
 → Integration between ∞ and R_*
- $v(r) = v_{\infty} \left(1 - \frac{R_*}{r}\right)^{\beta}$, $\beta = \begin{cases} 0.5 \text{ for approx. solution, "CAK-velocity law"} \\ 0.8 \text{ (O-stars) ... 2 (BA-SG), see next slide} \end{cases}$
- $v_{\infty} = \left(\frac{\alpha}{1-\alpha}\right)^{\frac{1}{2}} \left(\frac{2GM(1-\Gamma)}{R_*}\right)^{\frac{1}{2}}$ scaling law for v_{∞}
- → $v_{\infty} \approx 2.25 \frac{\alpha}{1-\alpha} v_{\text{esc}}$, if all subtleties included

Γ Eddington factor, accounting for acceleration by Thomson-scattering, diminishes effective gravity

N_{eff} number of lines effectively driving the wind, dependent on metallicity and spectral type

α exponent of line-strength distribution function, $0 < \alpha < 1$

large value: more optically thick lines

$\alpha' = \alpha - \delta$, with δ ionization parameter, typical value for O-stars: $\alpha' \approx 0.6$

The wind-momentum luminosity relation (WLR)

- use scaling relations for \dot{M} and v_∞ , calculate **modified wind-momentum rate**

$$\dot{M} v_\infty \propto N_{\text{eff}}^{1/\alpha'} L^{1/\alpha'} (M(1-\Gamma))^{1-1/\alpha'} \frac{(M(1-\Gamma))^{1/2}}{R_*^{1/2}}$$

$$\dot{M} v_\infty R_*^{1/2} \propto N_{\text{eff}}^{1/\alpha'} L^{1/\alpha'} \cancel{(M(1-\Gamma))}^{3/2-1/\alpha'}$$

The wind-momentum luminosity relation (WLR)

- use scaling relations for \dot{M} and v_∞ , calculate **modified wind-momentum rate**

$$\dot{M} v_\infty R_*^{1/2} \propto N_{\text{eff}}^{1/\alpha'} L^{1/\alpha'} \quad \text{since } (\alpha' \approx \frac{2}{3})$$

independent of M and Γ !!!!

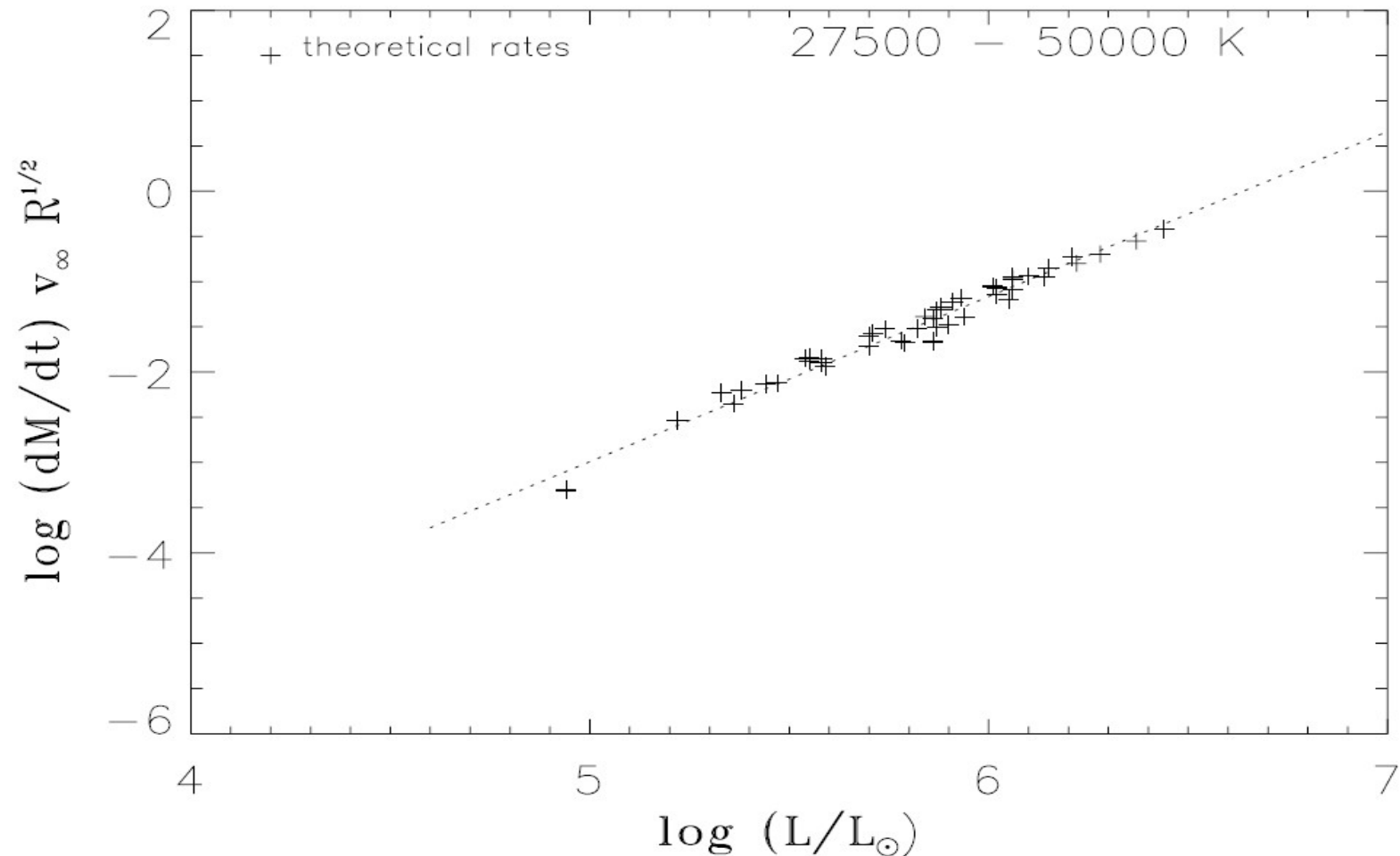
$$\log (\dot{M} v_\infty R_*^{1/2}) \approx \frac{1}{\alpha'} \log L + \text{const}(z, \text{sp.type})$$

► **stellar winds contain info about stellar radius!!!**

(Kudritzki, Lennon & Puls 1995)

- (at least) two applications
 - construct **observed** WLR, calibrate as a function of spectral type and metallicity (N_{eff} and α' depend on both parameter)
 - independent tool to measure extragalactic distances**
from *wind-properties*, T_{eff} and metallicity
 - compare with **theoretical** WLR to test validity of radiation driven wind theory

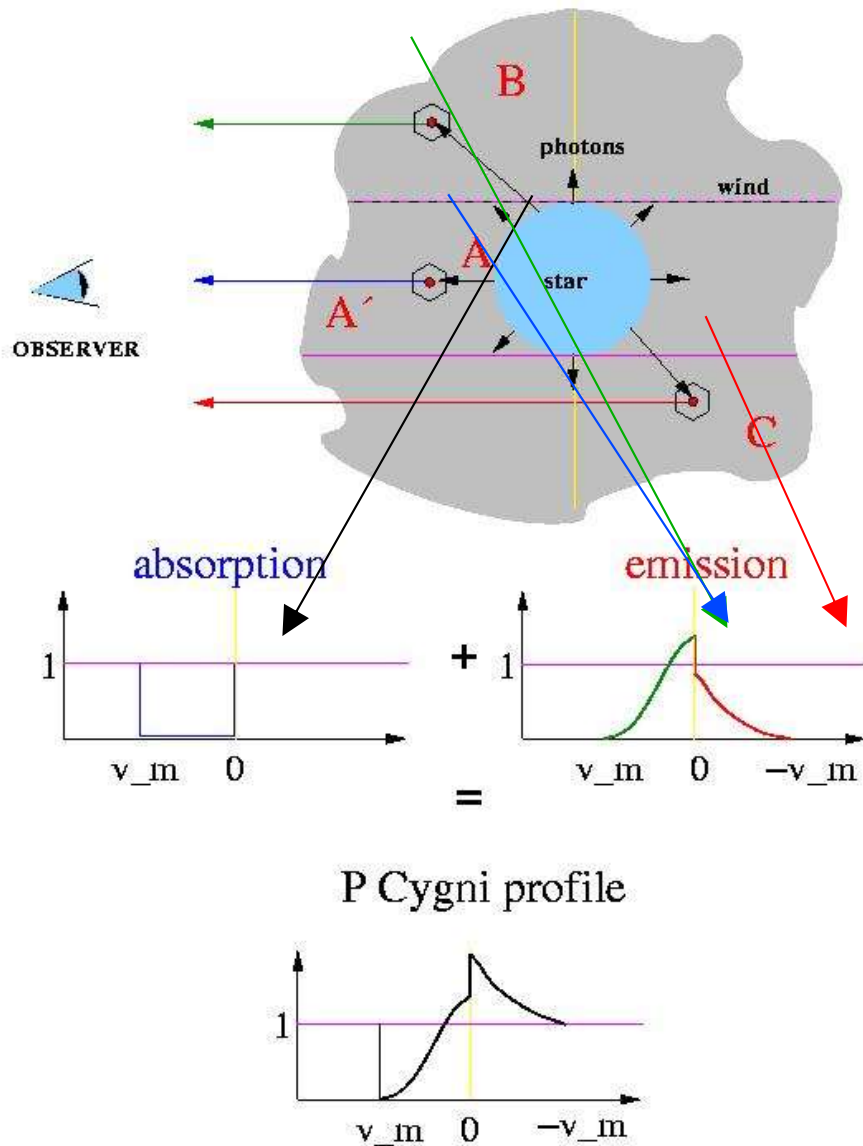
Validity of WLR concept



Theoretical wind-momentum rates as a function of luminosity, as calculated by Vink et al. (2000). Though multi-line effects (line overlaps) are included, the WLR concept (derived from simplified arguments) holds!

Determination of wind-parameters: v_∞

P Cygni profile formation



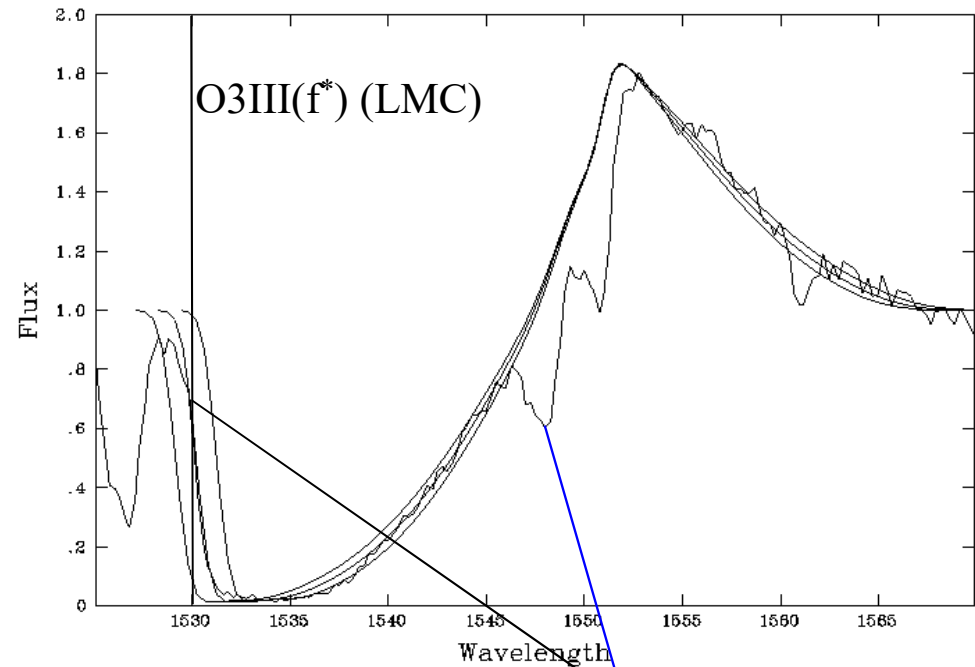
$$v_{\text{obs}} = v_0 \left(1 + \frac{\mu v(r)}{c} \right); \quad v_0 \text{ line frequency in CMF}$$

$$\mu v(r) > 0: \quad v_{\text{obs}} > v_0 \quad \text{blue side}$$

$$\mu v(r) < 0: \quad v_{\text{obs}} < v_0 \quad \text{red side}$$

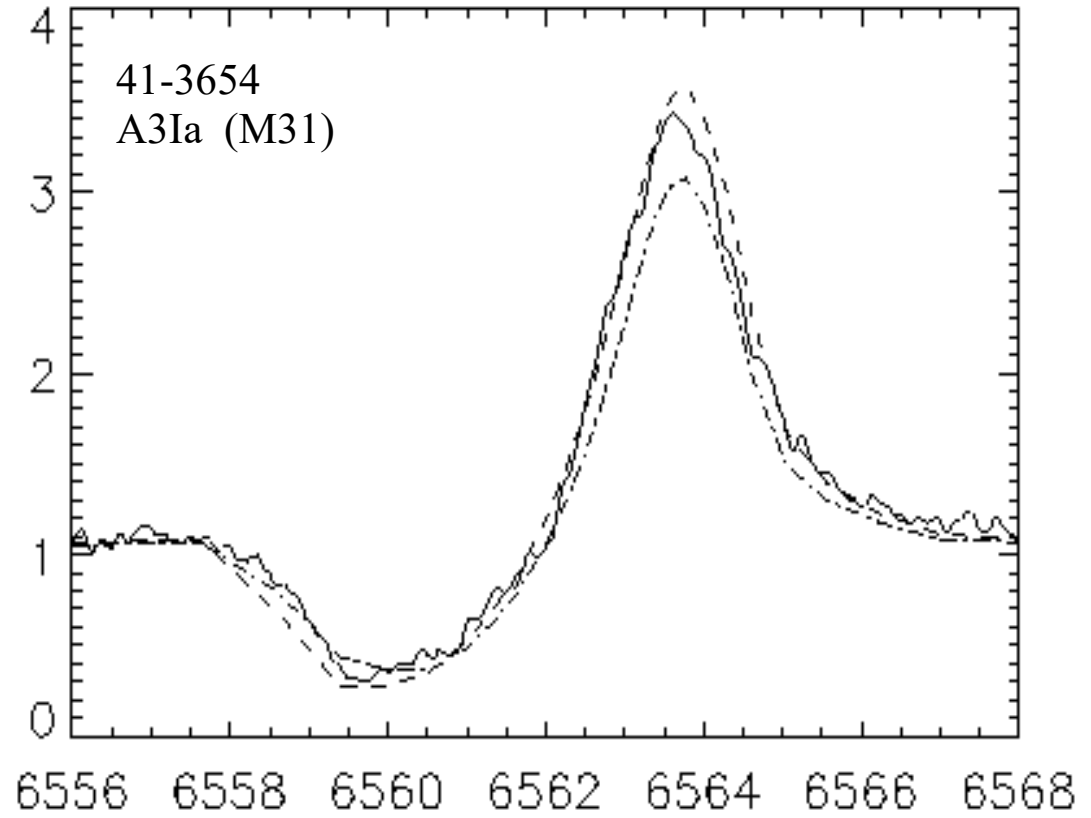
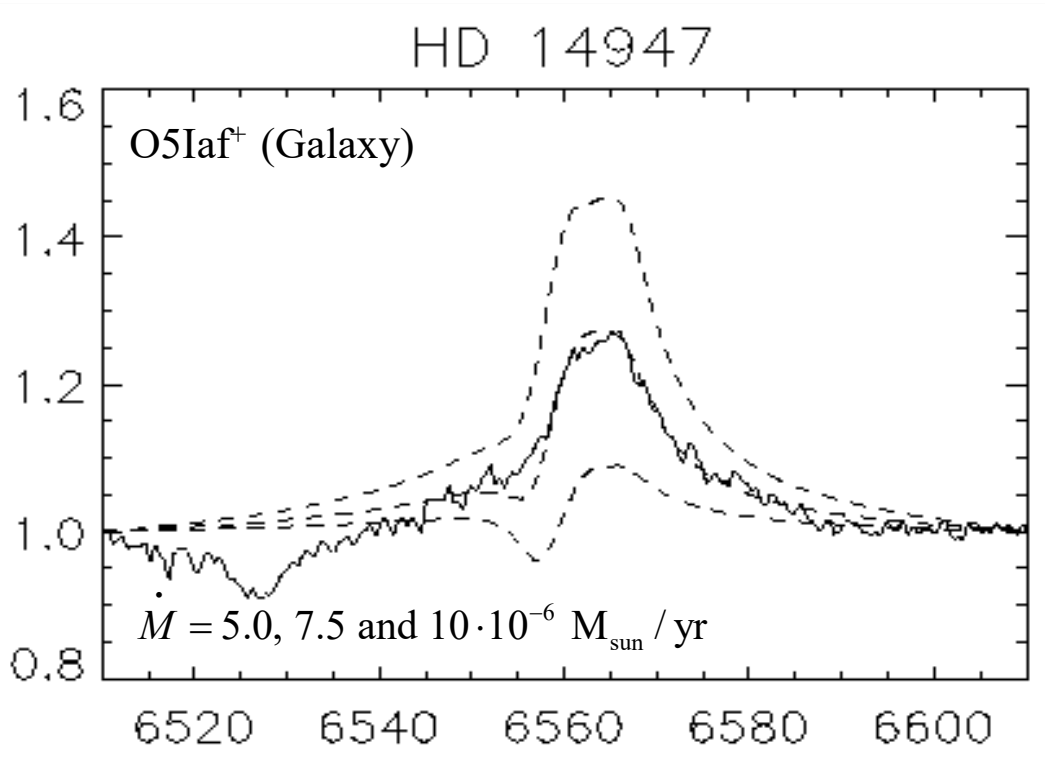
$$\frac{v_m}{c} = \frac{v_{\text{max}} - v_0}{v_0} = 1 - \frac{\lambda_{\text{min}}}{\lambda_0}$$

Sk -68 137 CIV $v_{\text{inf}}=3200/3400/3600$ km/s



$$v_m \approx 2.998 \cdot 10^5 \left(1 - \frac{1530}{1548} \right) \approx 3,480 \text{ km/s}$$

Determination of mass-loss rate from H_α



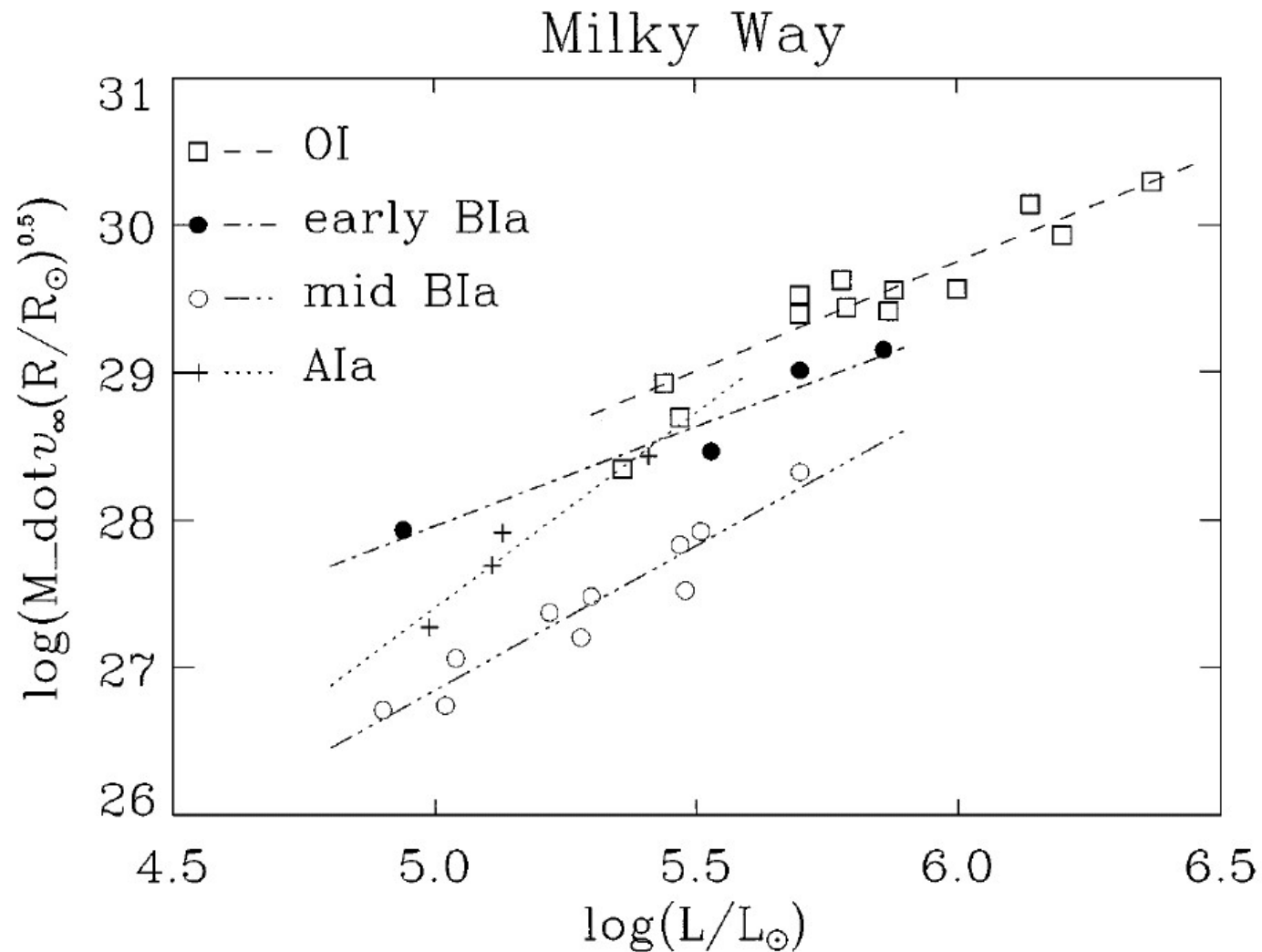
Note: Wind parameters can be cast into one quantity

$$Q = \frac{\dot{M}}{(R_* v_\infty)^{1.5}} \quad \text{or} \quad Q' = \frac{\dot{M}}{R_*^{1.5}}$$

For same values of $Q^{(\prime)}$ (albeit different combinations of \dot{M} , v_∞ and R_*), profiles look almost identical!

H_α taken with the Keck HIRES spectrograph, compared with two model calculations adopting $\beta = 3$, $v_\infty = 200 \text{ km/s}$ and $\dot{M} = 1.7 \text{ and } 2.1 \times 10^{-6} M_{\text{sun}}/\text{yr}$.

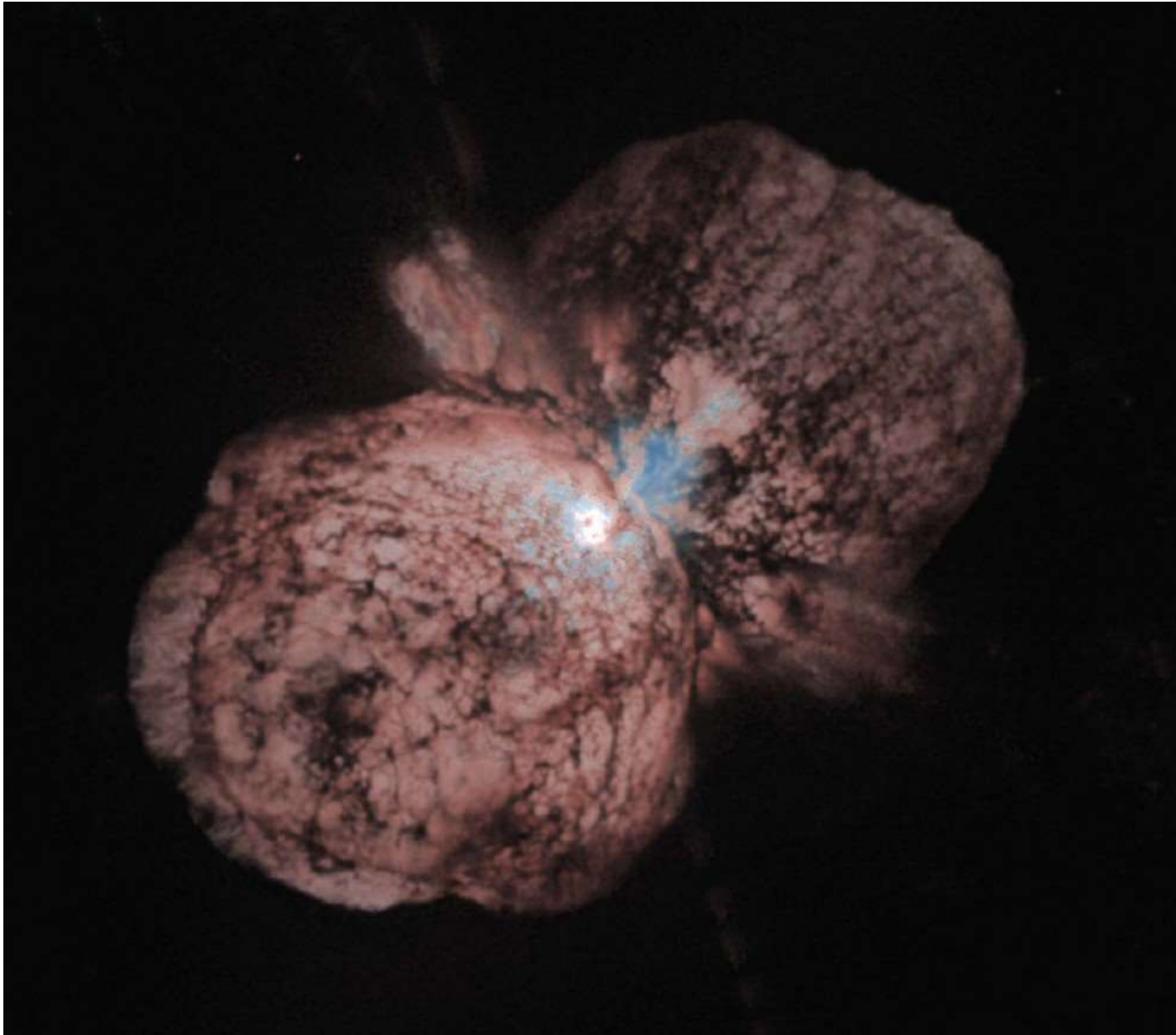
Observed WLR



Modified wind momenta of Galactic O-, early B-, mid B- and A-supergiants as a function of luminosity, together with specific WLR obtained from linear regression. (From Kudritzki & Puls, 2000, ARAA 38).

η Car: Aspherical ejecta

image by HST

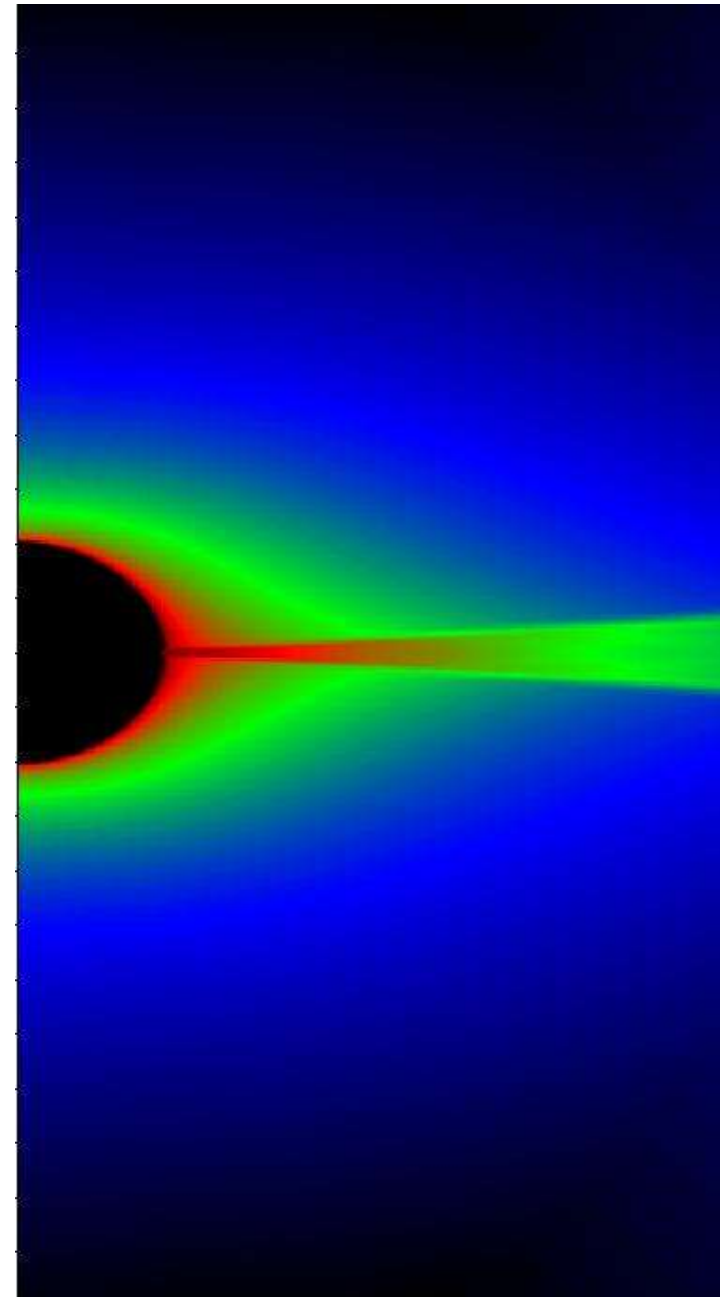


hot, massive stars = **young stars**

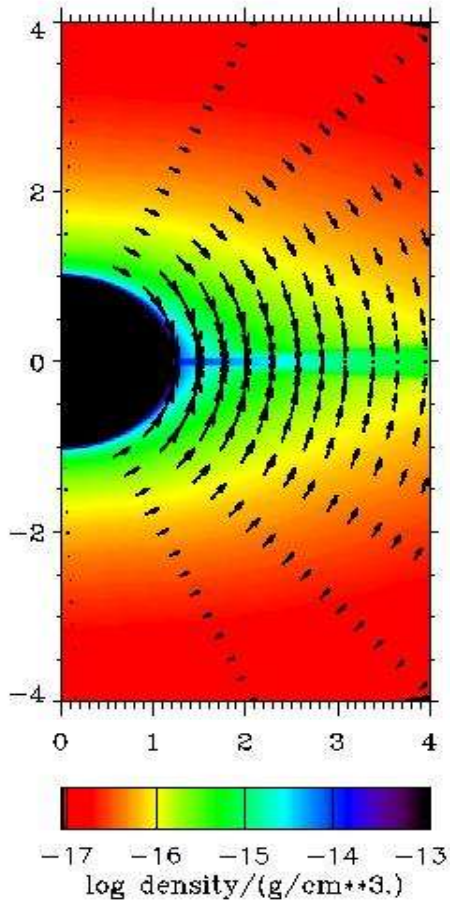
rapidly rotating (up to several 100 km/s)

twofold effect

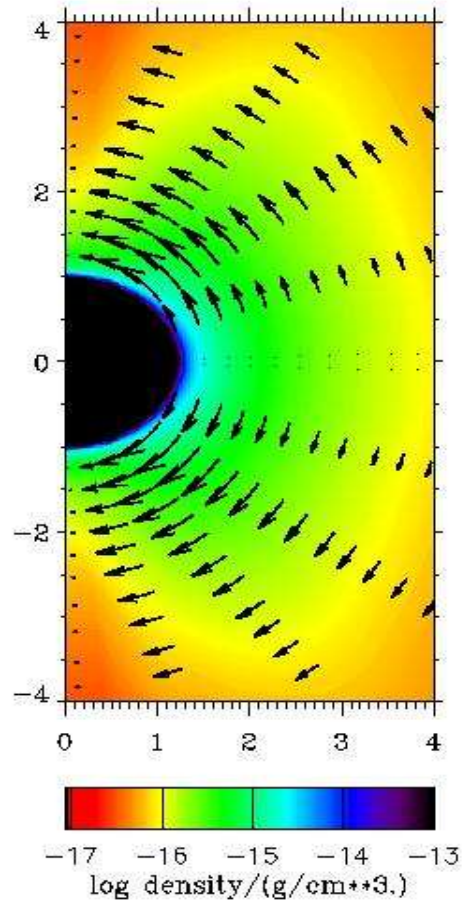
- star becomes “oblate”
- wind has to react on additional **centrifugal acceleration**,
large in equatorial, small in polar regions



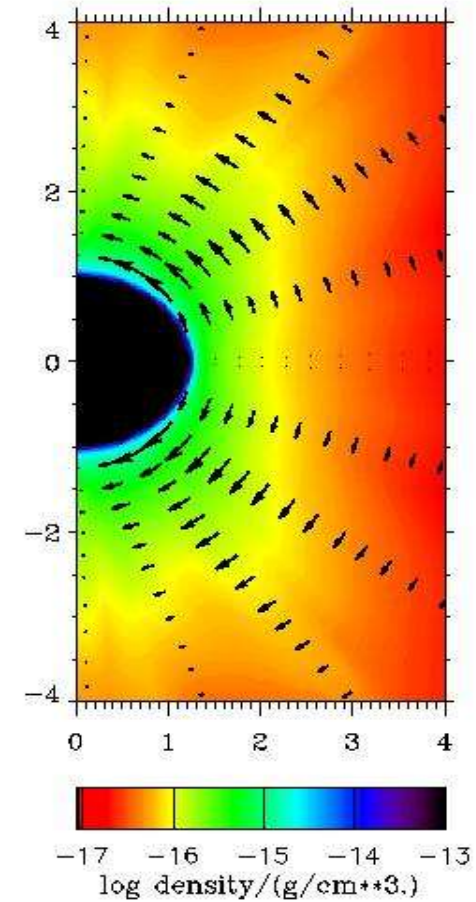
Prolate or oblate wind structure?



purely radial radiative
acceleration:
wind-compressed disk

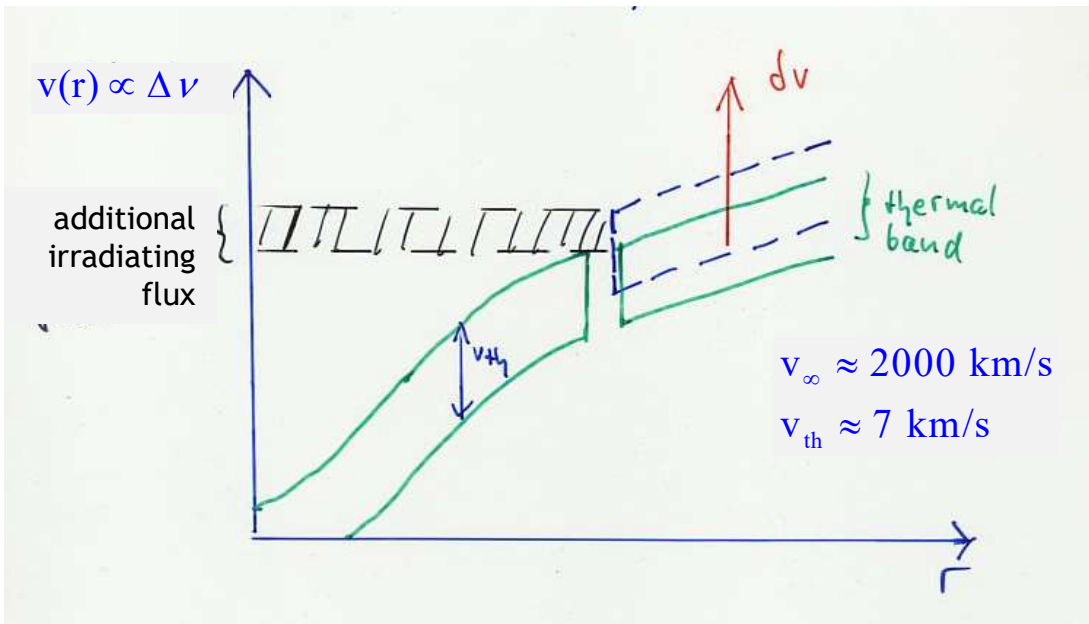


inclusion of non-
radial component
of line-acceleration
(rotation breaks
symmetry)



non-radial line-acceleration
plus „gravity darkening“:
prolate geometry

The line-driven instability



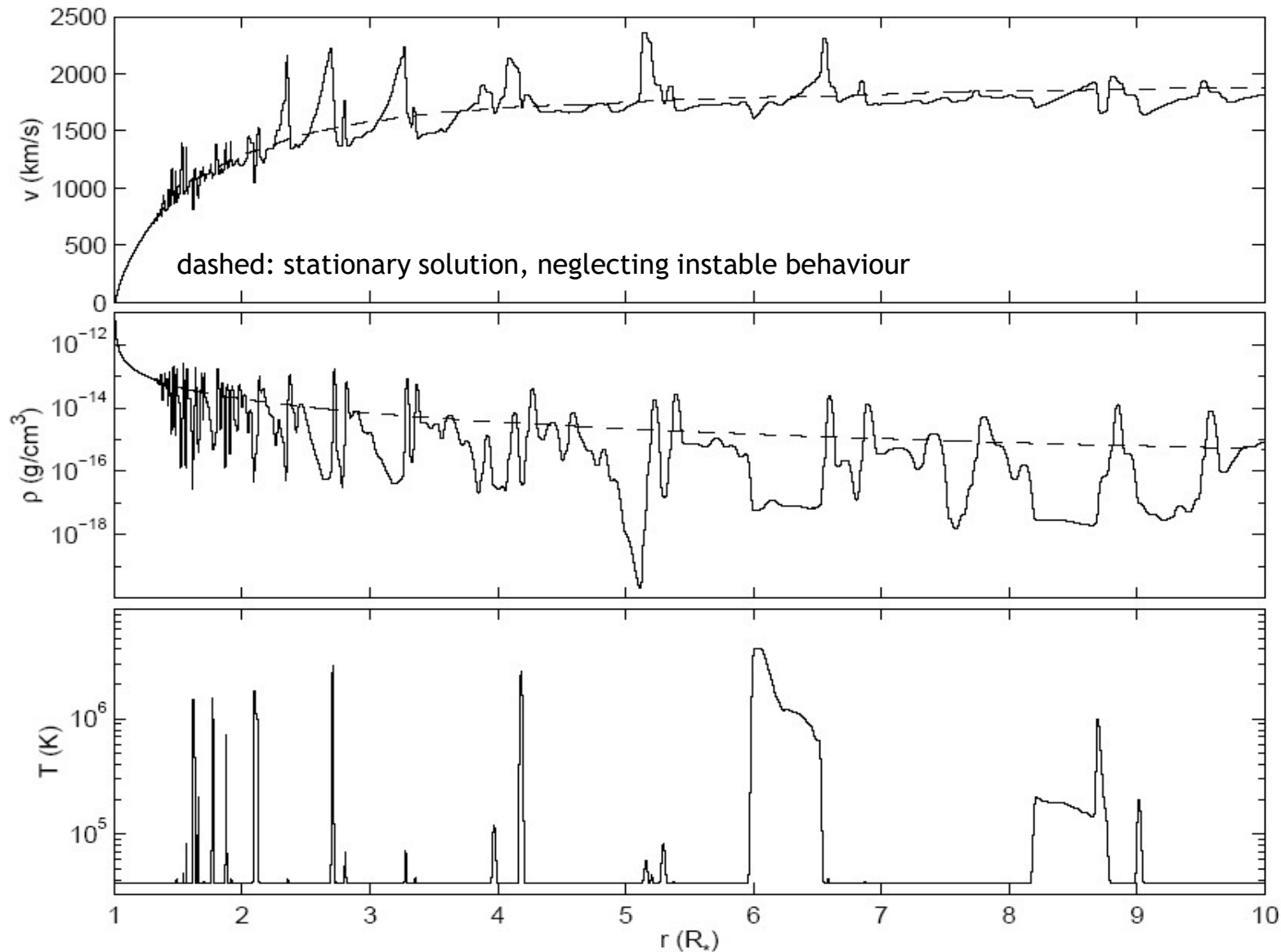
- perturbation $\delta \nu \uparrow$
- profile shifted to **higher freq.**
- line 'sees' more stellar flux
- line force **grows** $\delta g \uparrow$
- additional acceleration $\delta \nu \uparrow$

exponential growth of perturbation

$$\delta g_{\text{Rad}} \propto \delta \nu$$

[for details, see MacGregor et al. 1979 and Carlberg 1980]

Time dependent hydro-simulations of line-driven winds: Snapshot of density, velocity and temperature structure



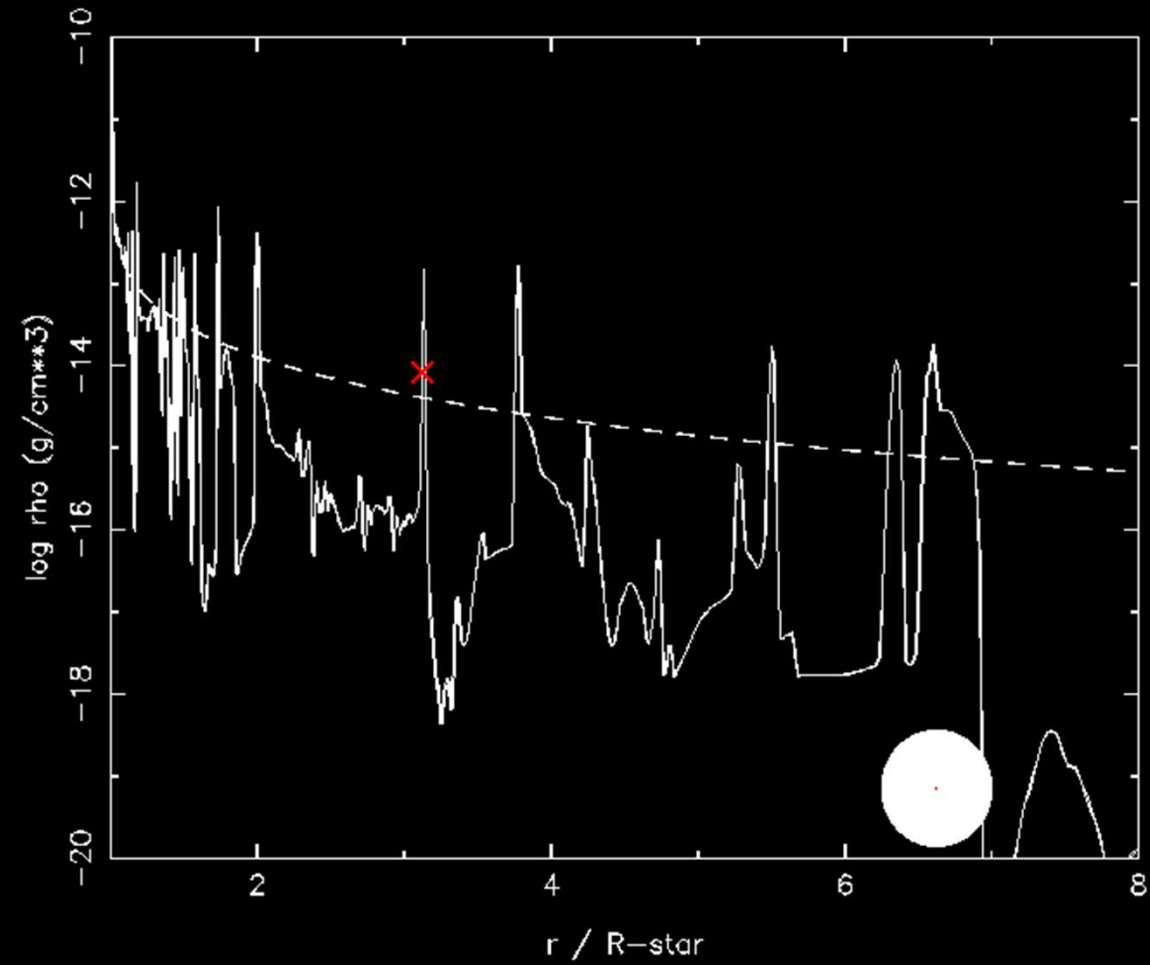
average hydro-structure
 not too different from
 stationary approx.:
 Most line profiles fairly
 similar, but effect
 (“clumping”)
 needs to be accounted
 for in analysis

(very) hot gas
 → X-ray emission
 (observed!)

From Runacres & Owocki, 2002, A&A 381

Density evolution in an unstable wind

X
X-ray
“flash”



Determine atmospheric parameters from observed spectrum

Required

T_{eff} , $\log g$, R , Y_{He} , \dot{M} , v_{∞} , β (+ metal abundances)
(R stellar radius at $\tau_R = 2/3$)

also necessary

v_{rad} (radial velocity)
 $v \sin i$ (projected rotational velocity)

Given

- *reduced* optical spectra (eventually +UV, +IR, +X-ray)
- $\lambda/\Delta\lambda$, resolution of observed spectrum
- Visual brightness V
- distance d (from cluster/association membership), partly rather insecure
- NLTE-code(s), "model grid"

1. Rectify spectrum, i.e. divide by continuum (**experience required**)

2. Shift observed spectrum to lab wavelengths (use narrow **stellar** lines as reference):

$$\lambda_{\text{lab}} \approx \lambda_{\text{obs}} \left(1 - \frac{v_{\text{rad}}}{c} \right), \quad v_{\text{rad}} \text{ assumed as positive if object moves away from observer}$$

• Alternative set of parameters

L , M , R *or*

L , M , T_{eff} *or*

T_{eff} , $\log g$, R ...

• interrelations

$$L = 4\pi R_*^2 \sigma_B T_{\text{eff}}^4$$

$$g = \frac{GM}{R_*^2}$$

• Useful scaling relations

If L , M , R in *solar units*, then

$$R_* = \frac{L^{0.5}}{T_{\text{eff}}^2} \cdot 3.327 \cdot 10^7$$

$$\log g = \log \left(\frac{M}{R_*^2} \cdot 2.74 \cdot 10^4 \right)$$

$$v_{\text{esc}} = \sqrt{R_* g (1 - \Gamma)} \cdot 1.392 \cdot 10^{11}$$

$$\Gamma = s_e T_{\text{eff}}^4 / g \cdot 1.8913 \cdot 10^{-15}$$

$$s_e = 0.4 \frac{1 + I_{\text{He}} Y_{\text{He}}}{1 + 4Y_{\text{He}}}$$

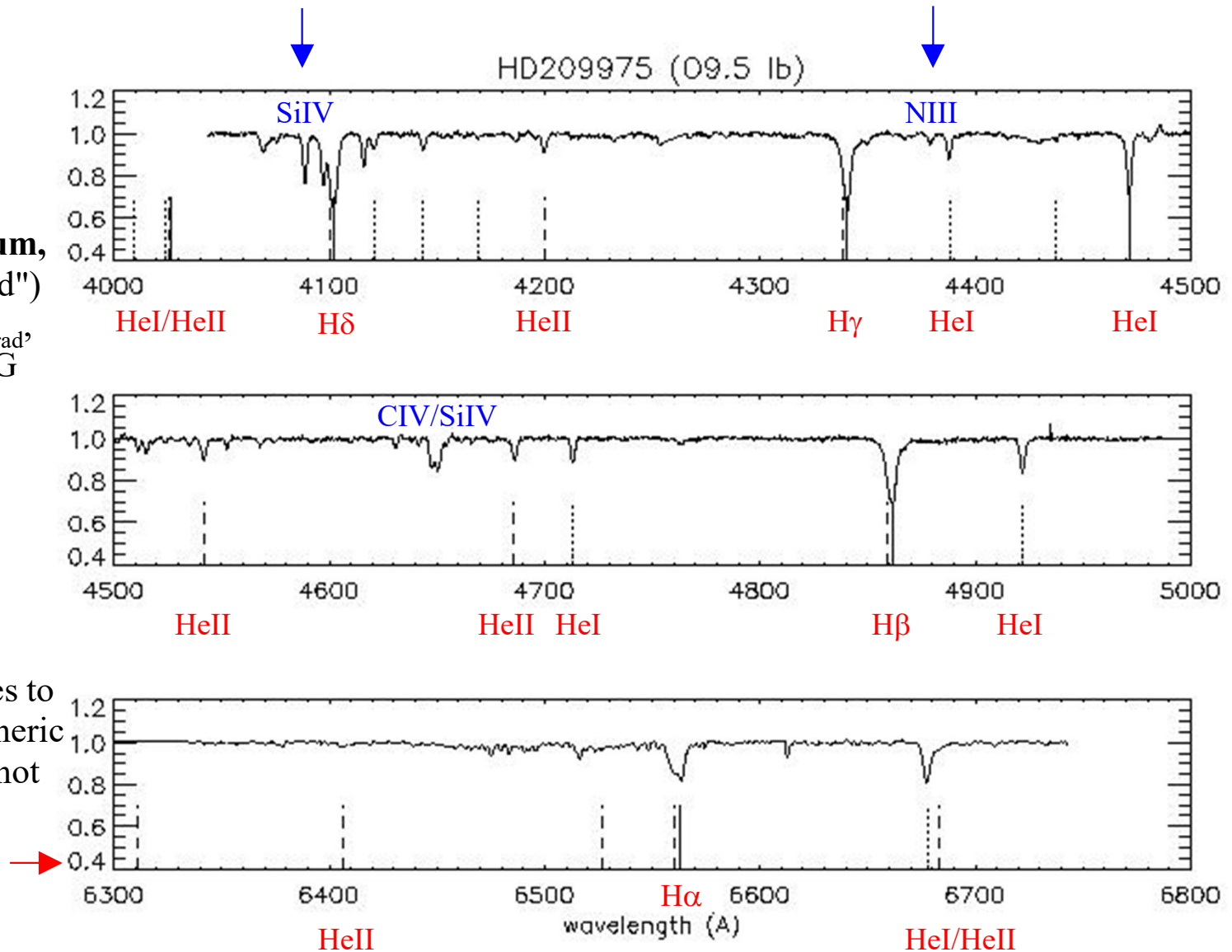
with I_{He} number of free electrons per Helium atom

(e.g., =2, if completely ionized)

rectified
optical spectrum,
 ("blue" and "red")
 corrected for v_{rad}
 of the late O-SG
19 Cep

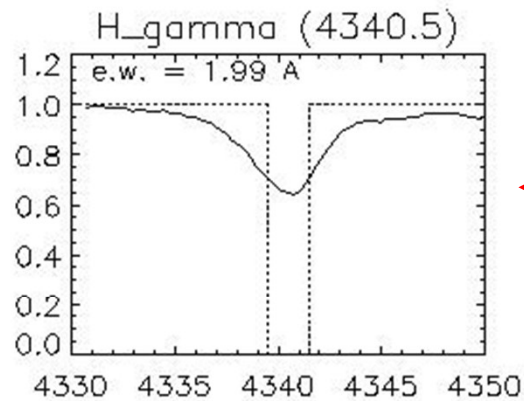
— Hydrogen
 Helium I
 - - - Helium II

in "red":
 "strategic" lines to
 derive atmospheric
 parameters in hot
 stars

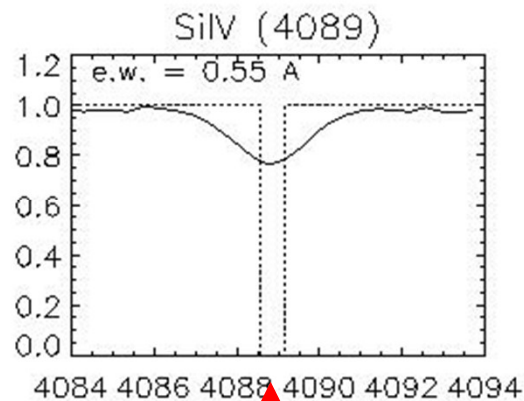


$$\text{equivalent width } W_\lambda = \int_{\text{line}} \frac{H_{\text{cont}} - H_{\text{line}}(\lambda)}{H_{\text{cont}}} d\lambda = \int_{\text{line}} (1 - R(\lambda)) d\lambda,$$

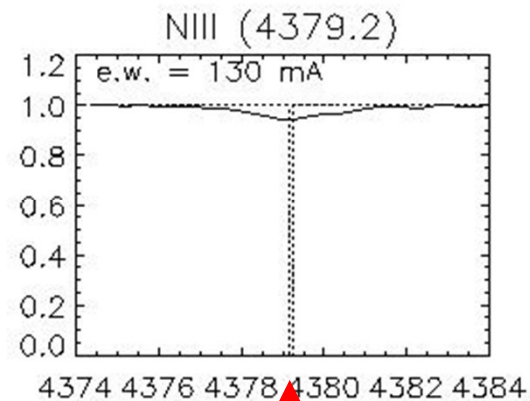
area of profile under continuum, $\text{dim}[W_\lambda] = \text{Angstrom or milliAngstrom, m}\text{\AA}$
 corresponds to width of saturated profile ($R(\lambda) = 0$) with same area



← strong line



↑ intermediate line

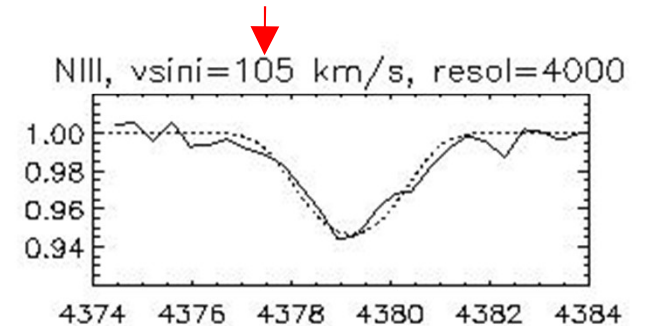
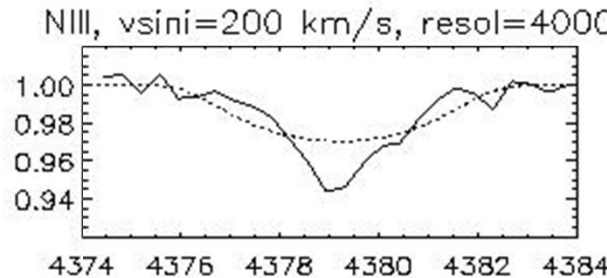
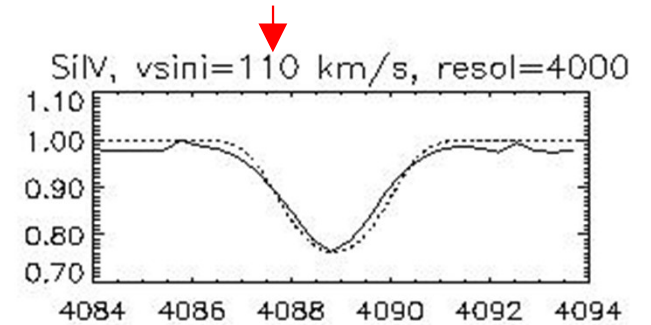
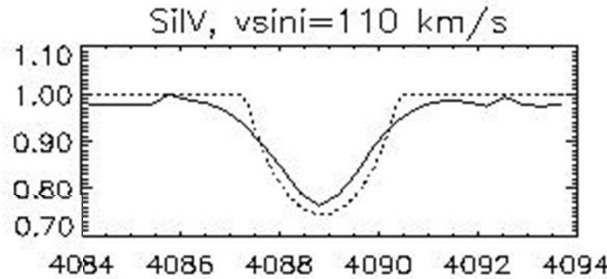
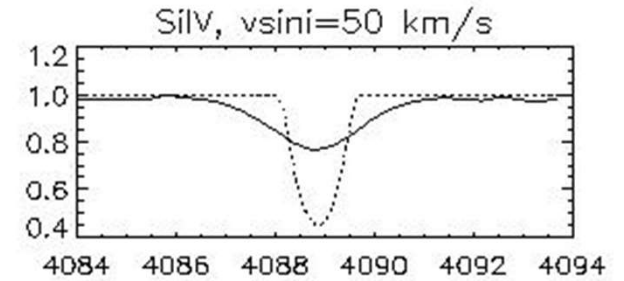
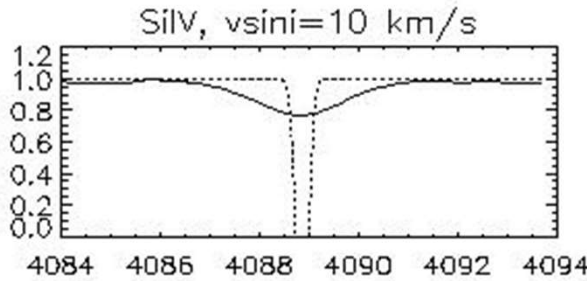
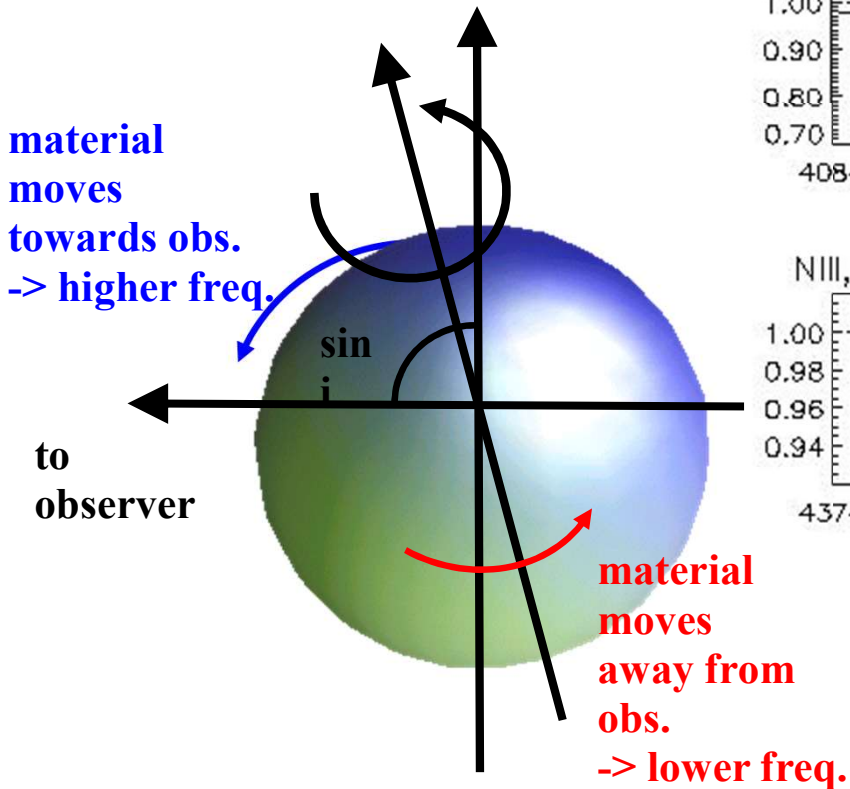


↑ weak line

Determine projected rotational speed $v \sin i$

Use **weak metal lines** to derive $v \sin i$:
Convolve theoretical line with rotational profile.

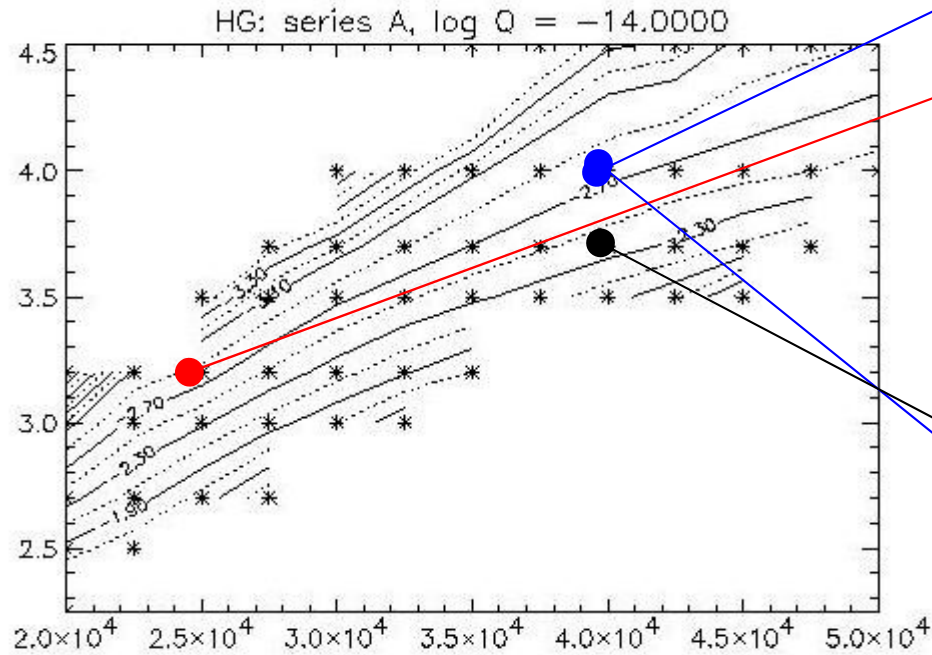
Convolve finally with instrumental profile (~ Gauss) according to **spectral resolution**



Convolution with rotational and instrumental profile conserves equivalent width!!!

Recent methods use a Fourier technique to infer $v \sin i$

H γ - log g and T $_{\text{eff}}$

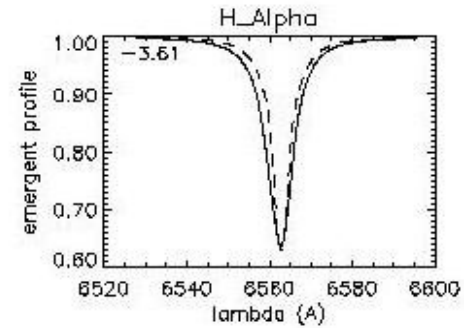
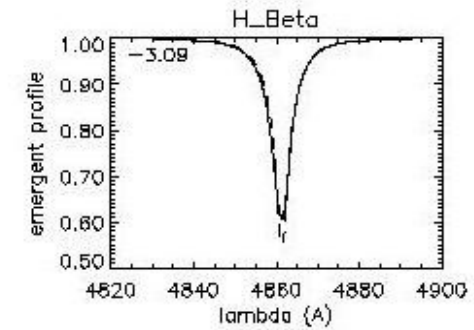
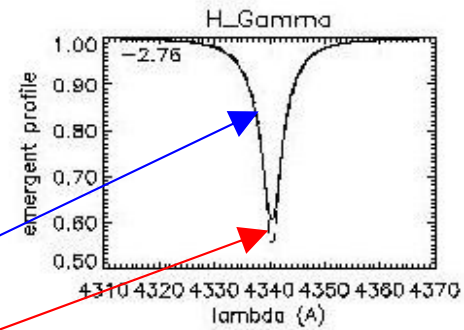


Iso-contours of equiv. widths for H γ (from model grid), for solar Helium abundance and (very) thin winds

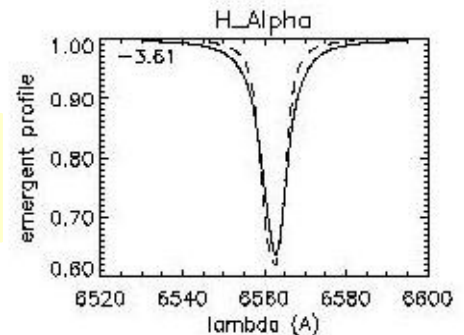
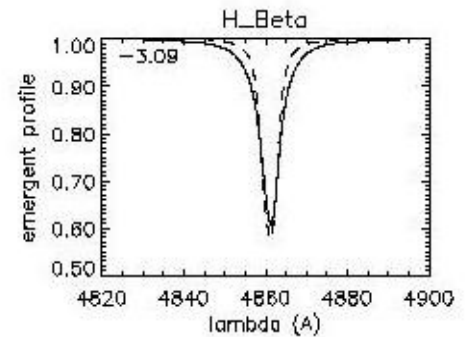
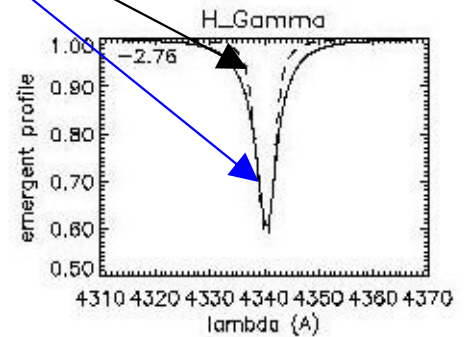
to derive T $_{\text{eff}}$, log g and Y $_{\text{He}}$, at least 3 lines have to be fitted in parallel (if no wind is present):

H γ defines log g (for given T $_{\text{eff}}$)
 HeII/HeI define T $_{\text{eff}}$ (for given log g)
 absolute strength of He lines define Y $_{\text{He}}$

usually, wind emission has to be accounted for (profiles shallower)

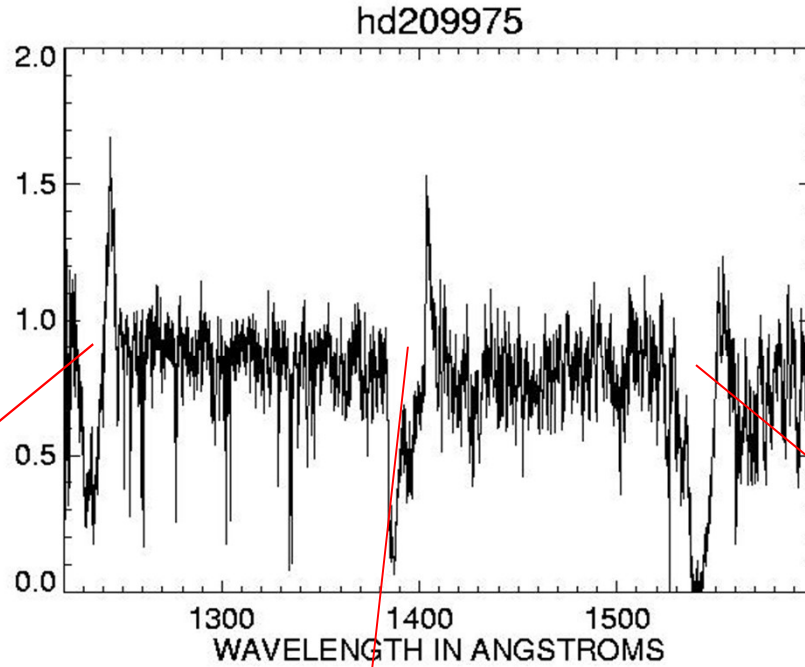


degeneracy of profiles: (almost) identical lines for T $_{\text{eff}}$ = 40,000 and log g = 4.0 and T $_{\text{eff}}$ = 25,000 and log g = 3.2



wings of Balmer lines (Stark-broadened) react strongly on electron-density (as a function of τ) => perfect gravity indicator

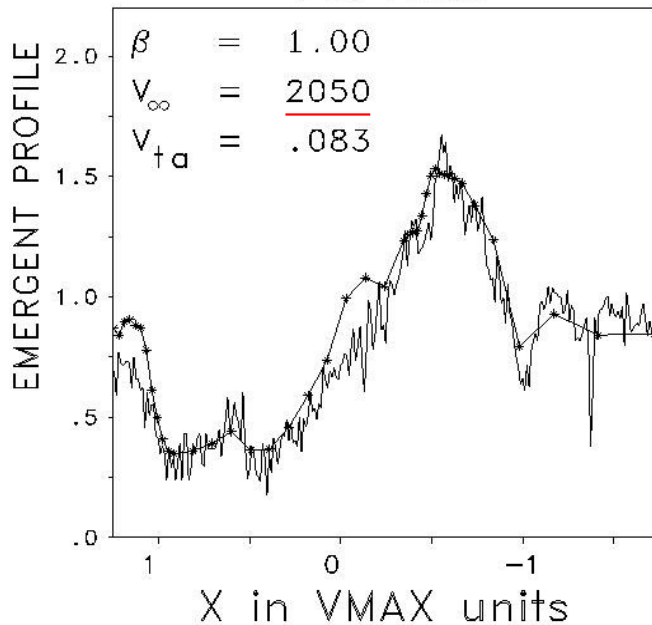
Determination of terminal velocity from UV-P Cygni profiles



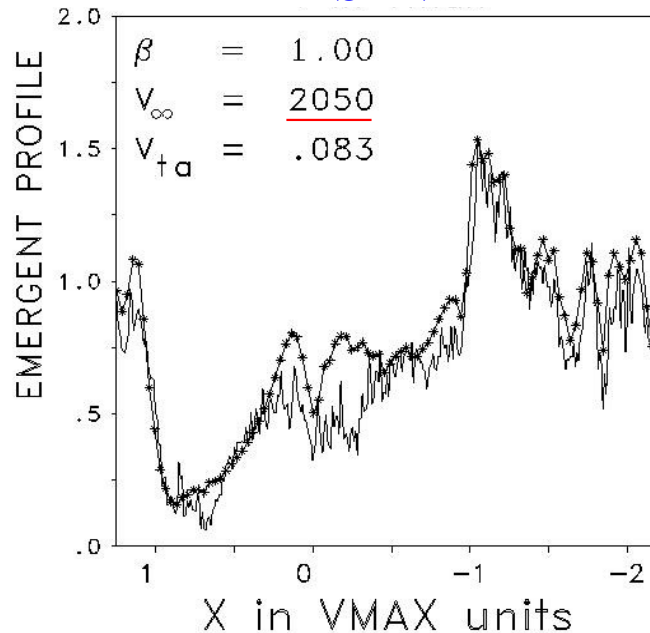
observation with IUE
(International Ultra-
violet Explorer)
no longer active

recent data (archive!)
from HST ($\lambda > 1200 \text{ \AA}$)
and FUSE ($\lambda > 911 \text{ \AA}$)

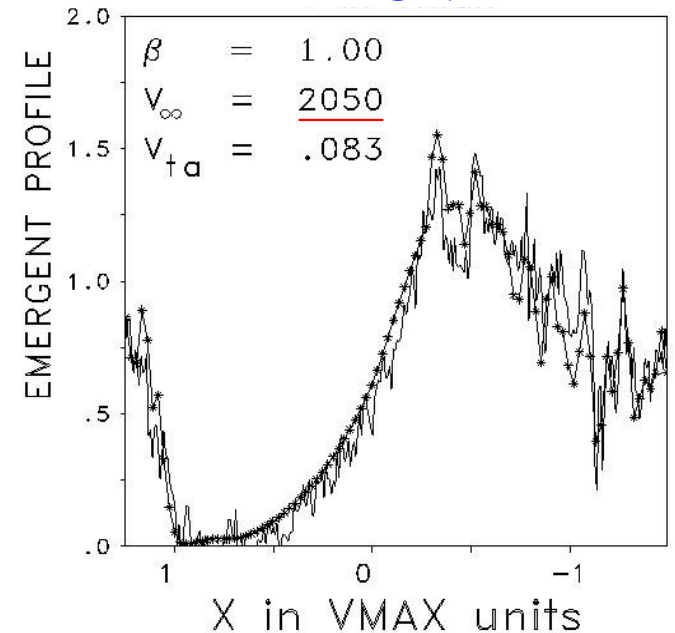
NV



Si IV



CIV



Line fitting = detailed comparison of observed and synthetic line profiles based on atmospheric models

____ Hydrogen
 Helium I
 - - - Helium II

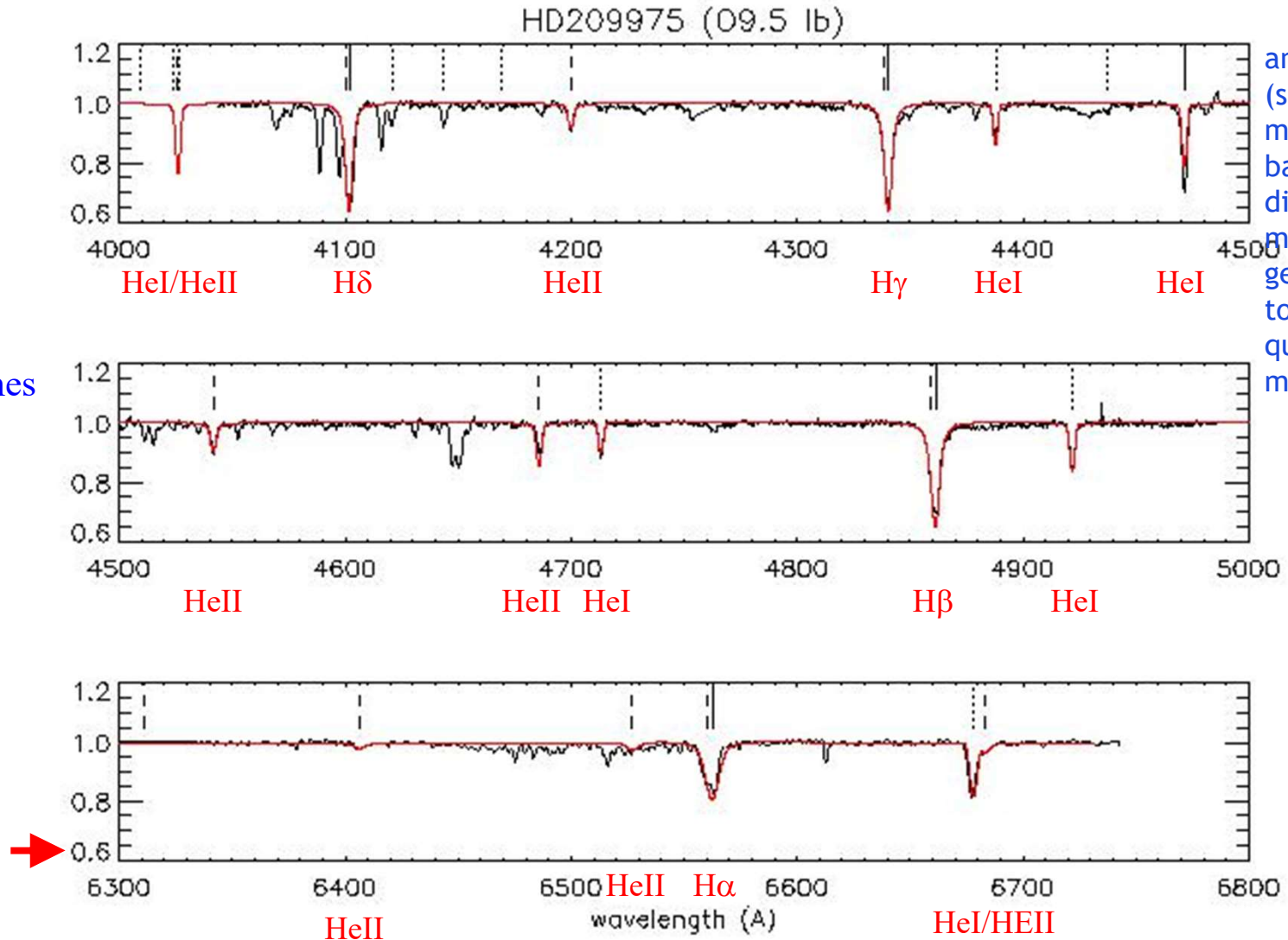
indicated lines used for fits

derived parameters

$T_{\text{eff}} = 31,000 \text{ K}$
 $\log g = 3.17$
 $\log Q = -12.87$
 $Y_{\text{He}} = 0.10$
 $\beta = 1.0$

with $v_{\infty} = 2050 \text{ km/s}$
we have

$$\log(M/R_*^{1.5}) = -7.9$$



analysis via (semi-) automatic methods, based on high-dimensional model grids or genetic algorithms, to optimize the fit quality for a multitude of lines

Determination of stellar radius – if it cannot be resolved

● **IF you believe in stellar evolution models**

- ★ use **evolutionary tracks** to derive M from (measured) T_{eff} and $\log g \Rightarrow R$
- ★ transformation of conventional HRD into $\log T_{\text{eff}} - \log g$ diagram required
- ★ problematic for evolved massive objects, "mass discrepancy":
spectroscopic masses (derived from spectroscopic analysis) and evolutionary masses often not consistent

● **IF you know the distance and have theoretical fluxes** (from model atmospheres), proceed as follows

$$V = -2.5 \log \int_{\text{filter}} \mathcal{F}_\lambda S_\lambda d\lambda + \text{const}$$

S_λ spectral response of photometric system

absolute flux calibration

$V = 0$ corresponds to $\mathcal{F}_\lambda = 3.66 \cdot 10^{-9} \text{ erg s}^{-1} \text{ cm}^{-2} \text{ \AA}^{-1}$ at $\lambda_0 = 5,500 \text{ \AA}$ outside earth's atmosphere

λ_0 *isophotal* wavelength such that $\int_{\text{filter}} \mathcal{F}_\lambda S_\lambda d\lambda \approx \mathcal{F}(\lambda_0) \int_{\text{filter}} S_\lambda d\lambda$, $\int_{\text{filter}} S_\lambda d\lambda \approx 2895$ for Johnson V-filter

\Rightarrow

$$\text{const} = -2.5 \log(3.66 \cdot 10^{-9} \cdot 2895) = -12.437$$

$$M_V = -2.5 \log \left[\left(\frac{R_* R_{\text{sun}}}{10 \text{ pc}} \right)^2 \int_{\text{filter}} \mathcal{F}_\lambda S_\lambda d\lambda \right] + \text{const}$$

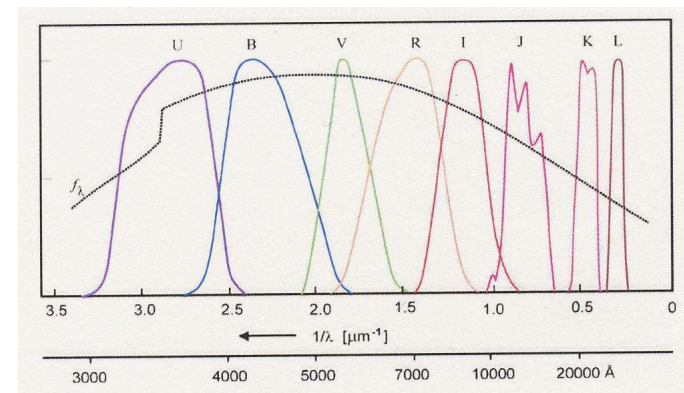
$$5 \log R_* = 29.553 + (V_{\text{theo}} - M_V)$$

if R_* in solar units, M_V the absolute visual brightness (dereddened!) and

$$V_{\text{theo}} = -2.5 \log \int_{\text{filter}} 4H_\lambda S_\lambda d\lambda \text{ with } H_\lambda \text{ the theoretical Eddington flux in units of } [\text{erg s}^{-1} \text{ cm}^{-2} \text{ \AA}^{-1}]$$

● **IF you believe in radiation driven wind theory**

- ★ use **wind-momentum luminosity relation**



• **Alternatively, use bolometric correction (BC)**

Calibration **for Galactic O-stars:**

$$BC = M_{\text{Bol}} - M_V \approx 27.58 - 6.8 \log(T_{\text{eff}}) \quad (\text{see Martins et al. 2005, A\&A 436})$$

and definition of M_{Bol}

$$\log \frac{L}{L_{\odot}} = 4 \log \frac{T_{\text{eff}}}{T_{\text{eff}, \odot}} + 2 \log \frac{R_*}{R_{\odot}} = 0.4(M_{\text{Bol}, \odot} - M_{\text{Bol}})$$

$$\log \frac{R_*}{R_{\odot}} = 0.2(4.74 - M_{\text{Bol}}) - 2 \log \frac{T_{\text{eff}}}{5770} =$$

$$= 0.2(4.74 - M_V - 27.58 + 6.8 \log(T_{\text{eff}})) - 2 \log \frac{T_{\text{eff}}}{5770} =$$

$$= 2.954 - 0.2M_V - 0.64 \log(T_{\text{eff}}) \quad [\text{valid only for O-stars with } Z \approx Z_{\odot}]$$

remember relation between M_V and V (distance modulus)

$$M_V = V + 5(1 - \log d) - A_V, \quad d \text{ distance in pc, } A_V \text{ reddening}$$

d from parallaxes (if close) or cluster/ association/ galaxy membership (hot stars)
(note: clusters/ assoc. radially extended!)

For Galactic objects, use GAIA (if you believe DR2 parallaxes), or compilation by
Roberta Humphreys, 1978, ApJS 38, 309 *and/or*
Ian Howarth & Raman Prinja, 1989, ApJS 69, 527

Back to our example

HD 209975 (19 Cep): $M_V = -5.7$

check: belongs to Cep OB2 Assoc., $d \approx 0.83$ kpc (Gaia parallax: 1.165 ± 0.15 mas = 0.85 ± 0.11 kpc)

$$V = 5.11, A_V = 1.17 \Rightarrow M_V = -5.65, \text{ OK}$$

From our final model, we calculate $V_{\text{theo}} = -29.08 \Rightarrow R = 17.4 R_{\text{sun}}$
(Alternatively, by using BC, M_V and $T_{\text{eff}} = 31\text{kK}$, we would obtain $R = 16.6 R_{\text{sun}}$)

Finally, from the result of our fine fit, $\log(\dot{M} / R_*^{1.5}) = -7.9$, we find $\dot{M} = 0.91 \cdot 10^{-6} M_{\text{sun}} / \text{yr}$

Finished, determine metal abundances if required,
next star but end of lecture ...